A GRID FEEDBACK INCORPORATED ECONOMIC POWER DISPATCH MODEL FOR A COGENERATION FERROCHROME PLANT

by

Michael Chennells

Submitted in partial fulfilment of the requirements for the degree
Master of Engineering (Electrical Engineering)

in the

Department of Electrical, Electronic and Computer Engineering
Faculty of Engineering, Built Environment and Information Technology

UNIVERSITY OF PRETORIA

December 2014

SUMMARY

A GRID FEEDBACK INCORPORATED ECONOMIC POWER DISPATCH MODEL FOR A COGENERATION FERROCHROME PLANT

by

Michael Chennells

Supervisor: Prof. X. Xia
Co-Supervisor: Mr L. Zhang
Department: Electrical, Electronic and Computer Engineering
University: University of Pretoria
Degree: Master of Engineering (Electrical Engineering)
Keywords: Waste heat recovery, organic rankine cycle, bottoming cycle cogeneration, economic power dispatch, optimal power flow and optimisation

An energy saving opportunity exists in mining and smelting industries such as the Ferrochrome industry, in the form of waste heat extraction and recovery. The mining and smelting of metals requires the use of high-power, AC or DC electric-arc furnaces that melt raw feed material in order to separate and produce useful metals from the feed. The smelting of raw materials into metals inside arc furnaces produces large quantities of hot gas as by-products, according to specific process-controlled chemical reactions. These hot gases combined with small feed dust particles thrown up from the feed process must be extracted from the smelting process and therefore from the furnaces themselves. The furnaces operate at internal temperatures around 1 500 ^{o}C and therefore the extracted hot material, referred to as the smelting process off-gas, is extracted at extremely high temperatures and thermal energy levels.

The implementation of a bottoming cycle cogeneration system allows for the extraction and recovery of thermal energy from the furnace off-gases which can then be used to generate additional useful electrical energy via the heat exchanger and electrical energy

generation components of the proposed cogeneration system. This additional energy improves the energy savings of the smelting process and the entire plant since thermal energy that was previously dissipated into the atmosphere and wasted is now used to generate additional and useful electricity. This additional electricity can either be used to power the furnace loads associated with the smelting of the raw materials into metals, thereby supplementing the utility grid electrical supply to the plant, or it can be fed back to or wheeled through the utility grid to be supplied to third party customers and consumers. This however creates a power dispatch and optimal power flow problem.

The power dispatch and optimal power flow problem is solved and controlled through the implementation of an Economic Power Dispatch (EPD) model. The model considers the operating conditions of the furnaces in order to determine how much additional electrical energy can be generated from the available thermal energy, recovered from the smelting process via the proposed cogeneration system. The model then utilises information regarding all costs associated with the consumption and generation of electrical energy as a result of the smelting and heat recovery cogeneration system operation. With these considerations the model then determines the optimal manner in which to dispatch the cogeneration generated electrical energy between the furnace loads and the utility grid so as to achieve the maximum possible overall system associated energy savings. The model is implemented as a half-hourly cogeneration-generated optimal power dispatch schedule.

The consideration of a bottoming cycle cogeneration system for heat recovery and additional electrical energy generation, and the development and implementation of an Economic Power Dispatch (EPD) model for the control of the dispatch of cogeneration generated power between the furnace loads and the utility grid, allow for considerable system associated energy savings. These savings are obtained due to the reduced net electrical energy required from the utility grid, and the financial incentives and rebates obtained due to the feed of electrical energy back to and through the utility grid to third party consumers.

OPSOMMING

'N EKONOMIESE KRAGVERSENDINGSMODEL VIR DIE KRAGKOPPELING VAN 'N FERROCHROOMAANLEG MET NETWERKTERUGVOER.

deur

Michael Chennells

Studieleier: Prof. X. Xia
Medestudieleier: Mnr L. Zhang
Departement: Elektriese, Elektroniese en Rekenaaringenieurswese
Universiteit: Universiteit van Pretoria
Graad: Magister in Ingenieurswese (Elektriese Ingenieurswese)
Sleutelwoorde: Afvalhitte herstel, organiese rankine-siklus, bodemsiklus kragkoppelingsisteem, ekonomiese kragversendings, optimale krag vloei en optimalisering.

Die ontginning en hergebruik van afvalhitte verteenwoordig 'n energiebesparingsgeleentheid bestaan in die mynbou- en smelterindustrieë, spesifiek die Ferrocrhoom industrie. Die smelterye gebruik hoë-krag WS of GS elektriese boogoonde wat roumateriaal smelt om nuttige metale te ontgin. Hierdie proses skei groot hoeveelhede warm gas as 'n byproduk af, volgens prosesbeheerde chemiese reaksies. Hierdie warm gasse en stofdeeltjies van die voerproses moet uit die boogoond verwyder word. Die interne temperatuur van die boogoond is sowat 1 500 °C, en dus bevat die afvalgasse 'n groot hoeveelheid termiese energie.

'n Bodemsiklus kragkoppelingsisteem gebruik die boogoondafvalgasse om elektriese energie te genereer deur middel van 'n hitteruiler en verskeie generatorkomponente. Hierdie aanvullende elektrisiteit verbeter die energiedoeltreffendheid van die aanleg deur termiese energie wat vantevore na die atmosfeer ontsnap het, te hergebruik. Dit kan gebruik word om die boogoond se elektrisiteitsverbruik te verminder, of dit kan terug in die elektrisiteitsnetwerk gevoer word. As die tweede moontlikheid gebruik word, is daar 'n elektrisiteitsvloei- en kragversending optimeringsprobleem.

Hierdie problem word opgelos en beheer deur ‘n ekonomiese kragversendingsopteringsmodel. Die model oorweeg die werkstoestande van die oonde ten einde die aanvullende energie wat gegenereer kan word deur middel van die kragkoppelingsiklus, te bepaal. Die model gebruik dan die inligting die genererings- en verbruikskostes van die elektrisiteit, en bepaal die optimale versendingsregime. Die model is geïmplimenteer op ‘n halfuurlikse kragkoppelings-gegenereerde kragversendingskedule.

Die oorweging van die die bodemsiklus kragkoppelingsisteem vir hitteherwinning en aanvullende elektrisiteitdsgenerering deur ekonomiese kragversending tussen die boogoond en elektrisiteitsnetwerk verteenwoordig ‘n noemenswaardige energiebesparingsgeleentheid. Hierdie besparing word verwerklik deur die netto elektrisiteitsverbruik van die aanleg te verminder, en insentiewe en kortings te gebruik om elektriseit aan derdepartyverbruikers te verkoop.

ACKNOLEDGEMENTS

I would like to acknowledge the following contributors in the development of this research and the preparation of this dissertation:

1. Stephane Senechal from Turboden s.r.l, for the assistance provided with regards to the cogeneration and power generation unit to be considered for this research from which crucial system operational and capacity information was obtained.
2. Aly Noorani from Voltas Technologies, for the assistance provided with regards to all cooling aspects of this research and a potential cooling or chiller unit that could be implemented in the proposed system.
3. Rudolf Krynauw, Don Smit and the rest of Glencore Ferrochrome in Rustenburg, for the provision of real system and facility operational data that was essential in the development of the EPD model.
4. Rodney Jones from Mintek and Peter Chennells, for all assistance provided with regards to smelting processes, furnace technologies and the chemical and internal smelting process aspects of this research.

This work is supported by the Centre for New Energy Systems and the National Hub for the Post-graduate Programme in Energy Efficiency and Demand Side Management at the University of Pretoria.

LIST OF ABBREVIATIONS

AC	Alternating Current
DC	Direct Current
EPD	Economic Power Dispatch
T.O.U	Time-of-use
MW	Mega-Watt, unit of real power
MVA	Mega-Volt-Ampere, unit of apparent power
ORC	Organic Rankine Cycle
DG	Distributed Generation
FeCr	Ferrochrome
CHP	Combined Heat and Power
MSMP	Multi-Source Multi-Product
CHPED	Combined Heat and Power Economic Dispatch
SED	Single Extraction Duct
ID fan	Induced Draft fan
COP	Coefficient of Performance
U.o.S	Use-of-System
WEPS	Wholesale Electricity Pricing System

TABLE OF CONTENTS

CHAPTER 1 INTRODUCTION

1.1 PROBLEM STATEMENT

1.1.1 Research Problem Formulation

Glencore Ferrochrome in Rustenburg is a ferrochrome smelting plant that utilises 3-phase AC submerged-electrode arc furnaces for the smelting of raw materials to form a molten bath. The bath is tapped off from the furnaces at regular intervals throughout the day, and separated into waste slag and molten ferrochrome using a density separator. After cooling, crushing and treatment processes, the ferrochrome is stored in a range of rock sizes for dispatch. Ferrochrome is used in the manufacture of stainless steels.

The furnaces operate at internal temperatures around 1 500 ^{o}C in order to maintain the molten characteristic of the furnace bath. Hot dust and gas is extracted from the furnaces via extraction vents and stacks, at trend-based temperatures between 250 and 600 ^{o}C as determined by the operation of the furnaces. The hot material is then transferred via the extraction ducts to the bagplant, where it is compressed into a fine powder and mixed with water to produce sludge. This sludge is pumped to slimes dams around the facility where it is treated. However, the bags used at the bagplant, for the housing of the compressed hot material fines, have maximum temperature ratings significantly less than the temperatures of the extracted hot material. Therefore an intermediate cooling process is implemented between the furnaces and the bagplant.

The facility utilises large trombone coolers for the intermediate cooling process. The hot material flows through the coolers which use vast surface areas to transmit heat to the surrounding atmosphere thereby cooling the hot material. This process however, demonstrates an extremely significant waste of thermal energy.

A bottoming cycle cogeneration system, comprising of a heat exchanger for thermal energy recovery and a turbine generator for electrical energy generation, implemented in place of the current cooling process, will have the potential to utilise the heat from the

extracted hot material to generate additional useful electricity, while still performing the required cooling of the extracted hot material. This electricity must then be dispatched in an economically optimal manner between the furnace loads and the utility grid, resulting in energy and economic savings.

1.1.2 Research Problem Statement

The purpose of this study is the consideration of a simplified theoretical bottoming cycle cogeneration system, as described above, and the development of an Economic Power Dispatch (EPD) model that determines the optimal half-hourly cogeneration output power dispatch schedule between the furnace loads and the utility grid, so as to achieve the maximum possible system associated energy savings.

1.1.3 Research gap

Most EPD and optimal power flow problems involve the economic dispatch of power and heat from and between various power and heat generators and loads within a certain facility or site. The main considerations for these problems are fuel and maintenance costs that form the bulk of the cost of energy generation, as well as ensuring that all electrical and thermal energy demands are met.

The model developed in this research will add value to the current body of knowledge concerning the economic dispatch of power from power-only and combined heat and power units, as specific utility contractual-based power costs and incentives will be considered and implemented. In addition to this, the developed optimal power dispatch model will determine the optimal dispatch schedule of power to on-site loads as well as back onto the utility grid for utilisation by the grid itself or third party grid-connected consumers. Therefore the system proposed is a grid-feedback incorporated system.

1.2 RESEARCH OBJECTIVE AND QUESTIONS

The proposed research involves the consideration of the implementation of a simplified theoretical bottoming cycle cogeneration system at the Glencore Ferrochrome furnaces in Rustenburg, in order to utilise waste heat from the furnaces for the generation of additional

useful electricity for the facility. The additionally generated electricity can either be used to substitute some of the utility grid supply by feeding the furnace loads, or it can be wheeled back to and through the utility grid to be sold to third party customers and even the utility itself. The implementation of the cogeneration system and an EPD model for the development of the optimal cogeneration output power dispatch schedule between the furnace loads and the utility grid will result in energy and corresponding cost savings for the facility.

The two questions posed by this research are as follows:

- How can the waste heat be extracted from the furnaces and used to generate additional useful electricity?
- How must this additionally generated electricity be dispatched between the furnace loads and the utility grid in order to ensure the maximum possible system associated energy savings are obtained?

1.3 RESEARCH HYPOTHESIS

The implementation of a bottoming cycle cogeneration system allows for the generation of additional useful electricity using thermal energy from the extracted hot material. The EPD model ensures that this generated electrical energy is dispatched optimally between the furnace loads and the utility grid. It is expected in the research that this system will introduce significant energy and associated cost savings for the facility, as less electricity will be consumed directly from the utility grid, and electricity sold back to the utility grid or to third party customers, during high demand and peak time-of-use (T.O.U) periods, will allow for additional financial incentives for the facility through the utilisation of energy that was previously wasted.

1.4 PROPOSED RESEARCH OVERVIEW AND METHODOLOGY

1.4.1 Research Overview

For this research, the model boundary is set so that only the furnace and bagplant sections of the facility are considered. Therefore other sections of the plant such as the final

material dispatch section, the pelletizing plant, the recovery plant and the water cooling section, are not considered. All final energy savings and costs are therefore based only on and within the established model boundary.

The simplified theoretical cogeneration system and dispatched energy flow diagram is shown in Figure 1.1. Figure 1.1 shows how extracted thermal energy is recovered by a heat exchanger and expanded through a turbine generator to produce electrical energy. It is this generated electrical energy that must be dispatched between the furnace loads and the utility grid as depicted by the EPD model which considers the overall system operation and the electrical consumption and feed-in (generation) tariff structures.

The purpose of the EPD model is therefore to generate a half-hourly power dispatch schedule that will depict and control the dispatch of the cogeneration generated electricity in an economically optimal manner, between the furnace loads and the utility grid. The main research associated issues and difficulties are:

- The varying furnace operating conditions, i.e. when the furnaces are tapped and when the furnaces are in idle conditions, as well as the varying furnace sizes, generates varying extracted furnace off gas temperatures and chemical compositions.
- The extraction of the off gas is performed via three extraction stacks per furnace that fuse into a single large extraction duct. The flow of the extracted material is controlled via large extraction fans. Therefore the flow rate of the extracted hot material and the combined extracted hot material chemical composition and temperature must be considered.
- The determination of the overall combined extracted available thermal energy requires information regarding the chemical composition, temperature and flow rate of the extracted hot material for each furnace. Therefore information regarding the raw material feed composition and feed rate, the internal smelting process chemical reactions as well as the method of off gas extraction for each furnace must be obtained.

- The conversion of thermal energy to electrical energy via the implemented bottoming cycle cogeneration process must be considered in order to determine the cogeneration output power profile from the extracted hot material temperature, flow rate and chemical composition profiles according to the operating schedule of the furnaces.
- Contractual based energy consumption tariffs and rates must also be considered. This information can be sensitive to many companies and therefore certain company protocols need to be followed in order to obtain this information.
- Lastly, the energy feed-in or generation tariff structure must be considered, even though the energy feed-in tariff structure, for the feed of energy back onto the utility grid, is not currently widely implemented and operational.

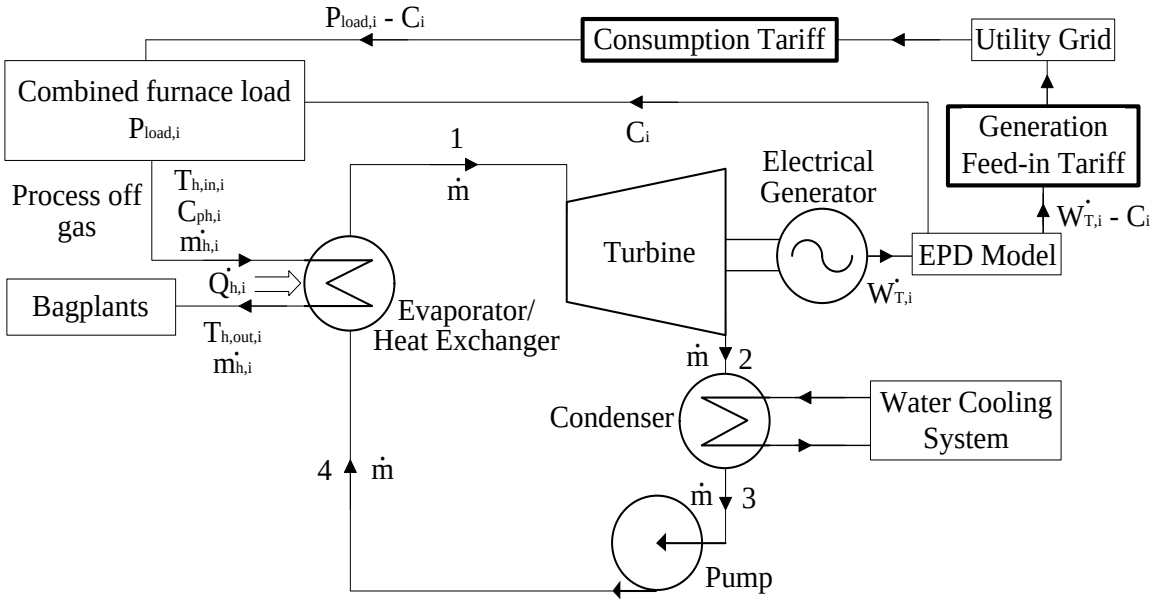

Figure 1.1: Waste heat recovery cogeneration system and EPD model energy flow diagram

To overcome these difficulties, specific information and facility operational data must be obtained from Glencore Ferrochrome and the utility grid supplier, Eskom. The time interval characteristic of the data (half-hourly, hourly or daily), must coincide with the EPD schedule time interval characteristic. The power dispatch schedule time interval is chosen as half-hourly and therefore all time-dependent information and operational data must be acquired on the same time interval, half-hourly. Therefore the information that must be obtained from the facility and the utility is as follows:

- The extraction stack temperatures for all 4 furnaces, used in order to calculate the temperatures at which the hot material is extracted via the single output extraction duct for each furnace,
- The bagplant inlet temperatures for all 4 furnaces, used in order to calculate the change in temperature values that are essential in determining the enthalpy or heat available from the heat extraction component (heat exchanger) of the cogeneration system,
- The furnace operation schedule (when the tapping and idle operations occurred),
- The composition, quantity and feed rate of the raw feed material as well as the furnace internal process chemical reactions, used in order to determine the chemical composition and volume of the extracted off gases from the internal smelting process.
- The mass flow rate at which the furnace off gases are extracted,
- All furnace load profiles (MW and MVA) for at least a single month,
- All furnace maximum demands or capacities for the same month,
- The electricity consumption tariff structure on which Glencore Ferrochrome is billed by Eskom, and
- A feed-in or generation tariff structure as determined by the utility, Eskom.

1.4.2 Research Methodology

Using the gathered time-dependent information regarding the temperature, chemical composition and mass flow rate of the extracted furnace off gas, as well as gathered knowledge and information concerning the smelting process chemical reactions and the thermodynamic and enthalpy properties of the off gas constituents, an overall available heat in MW can be obtained from the extracted hot material. The available energy in heat must then be converted into available electrical energy through considerations and research concerning heat recovery power generation cycles and units. Once an electrical energy output is obtained the EPD model must be developed with the purpose of dispatching this electrical energy optimally between the furnace loads and the utility grid so as to obtain the maximum possible system associated energy and associated cost savings, whilst ensuring that all the plant load demands and requirements are still met.

Therefore the time-dependent and independent information gathered from the facility and the utility, is used to determine the amount of electrical energy that can be obtained from the extracted thermal energy through the implementation of a bottoming cycle cogeneration system that performs both the heat recovery and electrical energy generation processes, while still performing the required cooling of the extracted hot material. The EPD model must then dispatch this cogeneration-generated electrical energy in an economically optimal manner between the furnace loads and the utility grid. The procedures and calculations that are used as well as the EPD model development procedures and explanations will be further discussed in Chapter 3.

1.5 RESEARCH GOAL

The main goal associated with this research is the development of an EPD model for a cogeneration ferrochrome plant that will introduce significant energy and associated cost savings for the facility. Not only will originally wasted energy be effectively utilised, but a grid feedback connection will be in place so as to allow for the support of the utility grid when it is under strain during high demand seasons and peak demand time of use (T.O.U) periods.

CHAPTER 2 LITERATURE STUDY

2.1 CHAPTER OBJECTIVES

This research deals with the consideration of a bottoming cycle heat recovery cogeneration system that can be implemented in a chrome smelting industry with the purpose of recovering and utilising waste heat extracted from the smelting process to generate additional useful electricity. Once a theoretical electrical energy output is obtained, an EPD model must be developed that will dispatch this electrical energy in an economically optimal manner between the facility loads and the utility grid, resulting in the maximum possible system associated energy and cost savings. Therefore, the literature that surrounds this research includes the following themes:

- The chrome smelting industry,
- The abundance of chromite ore and chrome smelting in South Africa and the energy consumption capacities of the chrome smelting industry,
- Current methods and techniques for improved energy efficiency and reduced system associated costs in the chrome smelting industry,
- The introduction of cogeneration and refrigeration as viable heat recovery and utilisation systems,
- The Organic Rankine Cycle (ORC) and cogeneration system working fluids,
- The Organic Rankine Cycle (ORC) and how it relates to heat recovery and cogeneration systems, and
- Cogeneration as an example of Distributed Generation (DG) and the modelling of the resulting optimal power flow and power dispatch problem.

Each of these themes will be discussed in the detailed literature study themes that follow.

2.2 CHROME SMELTING IN LITERATURE

The smelting of chrome is the metallurgical process of extracting chrome metal from chromite ore by exposing the ore to extremely high temperatures [1]. Chromite ore is smelted to produce ferrochrome (FeCr), which is a vital component in the production of stainless steels. The smelting of metals requires extremely high temperatures and is

achieved through the use of AC and DC arc furnaces. Arc furnaces utilise furnace conductors and the resistance of the metal ore and charge material to generate an electrical arc with sufficient thermal energy to melt the furnace feed material and form a molten bath inside the furnace. The smelting of metals not only deals with the melting processes but the chemical reactions and fusion of materials inside the molten bath as well. The chemical reactions and fusion of materials inside the molten bath all follow specific process chemical reactions that only occur at temperatures greater than 1 400 or 1 500 ^{o}C [2], according to the type of metal that is being smelted, and results in the separation and production of the desired metal or metal alloy.

In 2005, the worldwide production of high carbon FeCr was estimated at six million tons. Most of this FeCr was produced using submerged arc furnaces which are, due to the limited role of DC arc furnace technologies, predominantly AC arc furnaces [2]. The smelting of metals requires the carbothermic reduction of the metal ore in order to extract the metal. Therefore, for a smelting process of chrome to occur the following feed or charge materials are required [2], [3]:

- Chromite ore,
- Carbonaceous reductant material and
- Fluxing material.

Chromite ore is raw mined rock that contains the essential FeCr oxides, Chrome Oxide (Cr_2O_3) and Iron Oxide (FeO), as well as other waste oxides that separate from the ore and end up in the slag material after the smelting process has occurred. These oxides include Silicon Oxide (SiO_2), Magnesium Oxide (MgO), Aluminium Oxide (Al_2O_3) and small amounts of Calcium Oxide (CaO) [3]. Chromite ore can be fed into the furnace as lumps, pellets or chips depending on the type of feed material the furnace can handle as well as the chemical composition of feed material the furnace requires. The chemical composition of chromite ore varies with the type of ore mined, but is in the range of the following [3]:

- Cr_2O_3 – Between 29% and 43%,
- FeO – Between 18% and 24%,

- Al_2O_3 – Between 10% and 15%,
- MgO – Between 10% and 17%,
- SiO_2 – Between 3% and 20%, and
- CaO – Between 0.5% and 2%.

From this it is clear that the most varying component of chromite ore is Silicon Oxide. The quality of ore is therefore often graded according to the amount of Silicon in the ore material. The most desirable ore according to this is ore with about 7% Silicon. Another constituent of chromite ore is moisture (H_2O), about 3% [3]. The amount of energy required to remove moisture from the feed material inside the furnace is very high in comparison to other constituents and therefore the ore usually undergoes drying and pre-heating processes to remove some of this moisture before the material is fed into the furnace.

The carbonaceous reductant is the material fed into the furnace with the purpose of reducing the metal oxides from the chromite ore, thereby extracting the metal from the raw feed ore material. Common reductants are Coke, Anthracite and Coal, each with specific percentages of carbon content and therefore reducing ability [2], [3], [4]. The metal oxides are reduced by the carbonaceous reductants according to specific chemical reactions upon which furnaces are designed and operated. The production of FeCr is dependent on these reactions which are shown in equations (2.1) and (2.2) [2], [4]:

- At a furnace temperature of 1 400 °C:

$$FeO + C \rightarrow Fe + CO \quad (2.1)$$

- At a furnace temperature of 1 500 °C:

$$Cr_2O_3 + 3C \rightarrow 2Cr + 3CO \quad (2.2)$$

Furnaces can either be open or closed furnaces according to the furnace design. In closed furnaces, the Carbon Monoxide (CO) gas that is produced from the furnace internal chemical reactions moves up through the various charge material layers and can be extracted from the top of the furnace. This CO gas is highly flammable and can therefore

be directly burnt off and the heat either dissipated or used for additional energy requirements. In open furnaces, air is present at the top of the furnace and the chemical reaction-resulting CO gas once again passes up through the various charge material layers. This CO gas is at a temperature of between 800 and 1000 ^{o}C [2]. The autoignition temperature of CO gas is 609 ^{o}C. Therefore in open furnaces, once the CO gas exits the top of the charge material and comes into contact with the air, autoignition occurs, producing Carbon Dioxide gas (CO_2), according to the chemical reaction shown in equation (2.3) [4]:

- At temperatures of 609 ^{o}C and above:

$$2CO + O_2 \rightarrow 2CO_2 \quad (2.3)$$

This CO_2 gas is also extracted from the furnace, but cannot be immediately burnt off as in the case of closed furnaces and CO gas.

The final feed material required for the smelting of chrome is fluxing material. In order to obtain the reduced metals from the furnace, the molten bath must be tapped off from the furnace through the furnace tap hole at regular intervals, approximately every 2.5 hours [2]. During tapping conditions the furnace tap hole is drilled opened and oxygen is injected directly into the furnace in order to provide additional chemical energy to the molten bath. This additional energy allows the molten bath to flow smoothly out of the furnace tap hole.

When the molten furnace material flows out of the furnace tap hole, a density separator is used to separate the molten FeCr metal from the molten waste slag, since the molten metal sinks to the bottom of the tapped molten material due to a much higher density as opposed to slag. In order for this separation to occur effectively, the molten slag must be at an appropriate chemical composition, density and viscosity. Fluxing material is essential in controlling these slag conditions so that the molten metal can separate easily from the molten slag, and more molten material can be obtained per tap due to a higher tapped molten material flow rate. The most common fluxing materials include Quartzite, Bauxite, Dolomite and Lime [2], [3].

2.3 THE ROLE AND IMPACT OF CHROME SMELTING IN SOUTH AFRICA

2.3.1 The abundance of chromite ore and chrome smelting in South Africa

It has been estimated that 80% of the world's chromium deposits can be found in the Bushveld Complex in South Africa, and that there are sufficient platinum group element deposits in the Bushveld Complex to supply the world's demand for these elements for almost a century, using current mining and smelting techniques [5], [6]. The Bushveld Complex is an extremely large irruption of molten rock deep within the Earth, which spans an estimated cumulative diameter of approximately 300 km in South Africa. It is a combination of three or four separate deposits, one approximately 50 km west of Polokwane in Limpopo, one spanning the distance between Polokwane and Middelburg, also in Limpopo, and one made up of two deposits right next to each other, around Sun City and Rustenburg in the North West Province. After irruption the Bushveld Complex molten rock was cooled slowly allowing minerals to solidify in thin, parallel layers of mineral-rich rock. The maximum thickness of these layers was found to be approximately 8 km [6].

Due to the sheer size of the Bushveld Complex and the overwhelming deposits of platinum group elements and chromium in the complex rock, the mining and smelting of chrome ore forms an extremely vital and influential sector of South Africa's economy. It is for this reason that 24 active mines and 24 mine projects currently exist all around the Bushveld Complex with the purpose of extracting these precious elements from their rich deposit sites [6]. In conjunction with the mines, similar quantities of smelting plants operate continuously in order to process the mined rock and extract the precious metals for use or export. Companies involved in the mining and smelting of chrome and platinum group elements include Anglo, Glencore, Samancor, IFM, Mintek, and numerous others.

2.3.2 The energy consumption and capacity of chrome smelting in South Africa

The sheer abundance of chromium deposits, and therefore chrome mining and smelting plants in South Africa, has raised concerns with regards to the county's power generating capabilities and the need to supply these power-hungry industries. This is due to the

energy-intensive production process that is the smelting of FeCr and metals in general. The smelting of FeCr is an electrical process that consumes approximately 3.3 to 3.8 MWh of energy per ton of FeCr metal produced [3]. South Africa's current power generating capacity is approximately 40 GW. The mining and smelting industry utilises about 15% of this capacity (6 GW), with a smelting capacity alone of about 4 GW. Half of this is consumed in Ferro-Alloy furnaces only, about 2 GW of power required [1].

Since the country is currently faced with a major problem, that of electrical demand growth being higher than electrical supply growth, the country's complete and overall benefit from a rich and plentiful mineral supply has been prevented. This is primarily due to the enormity of the power that is required for the mining and smelting of these metals and the lack of power supply capacity in South Africa as a whole. It is because of this, and the urbanisation of China, that many Ferro-Alloy smelters and industries in South Africa have been shut down and are in fact paid by the country's utility, Eskom, not to use electricity to make it available to others. In addition to this much of the country's mined chromite ore is now sold to China for the smelting process and the production of FeCr. As of 2012 it was reported that China had overtaken South Africa as the world's leading FeCr producer [1].

FeCr industries in South Africa are therefore constrained by a lack of power supply and rising electrical consumption costs. It is because of this that these industries need to look to the future at improving the energy efficiency of FeCr smelting. This might involve updating smelting technologies, techniques and processes, or looking to utilise and reuse any energy or resources that are currently wasted through the smelting of metals as a whole. If the efficiency of the utilisation of energy for the mining and smelting of metals can be improved, the country can once again become more competitive in the production of FeCr worldwide, from which the country's economy and the country itself can only benefit.

2.4 METHODS AND TECHNIQUES FOR INCREASED ENERGY EFFICIECNY AND COST SAVINGS IN THE CHROME SMELTING INDUSTRY

There are various methods in which the Ferro-Alloy and FeCr smelting industries can improve their efficiency of energy utilisation. It is important to realise however that the efficient use of energy not only depends on the consumption of energy itself, but the pricing and tariff aspects that accompany this utilisation of energy. The South African electricity supply industry is on the verge of a process of restructure with aspects such as ownership, infrastructure and regulation of great concern. With the changes in these aspects imminent, it is expected that the electricity consumption tariff will become a lot more volatile and dynamic [7].

Therefore before even considering actual technological and process-related aspects of energy utilisation it has become just as important for industries to adjust to the dynamics of the electrical supply economics. That is why one of the most important facets of improving the energy efficiency of an industry has become the optimal utilisation of the electrical consumption tariff [7], [8]. The optimal utilisation of the tariff involves integrating energy cost management, implementing demand-side management, optimisation of energy consumption processes and maintenance scheduling, all in coordination with the electrical consumption tariff structure [7]. In essence if an industrial plant can synchronise the dynamics of the plant operation with the dynamics of the electrical consumption tariff, the plant can expect to achieve considerable cost and energy savings.

The main challenges that arise in the Ferro-Alloys industry include equipment and process technology limitations, the minimisation of operation and investment costs, the minimisation of waste gas and materials from industrial operations, and the improvement of the industry working conditions. In addition to this, it has also been found that these industries tend to be very traditional and difficult to change [9]. However, with the squeeze being provided by the electrical supply utility and the country's economic status, energy and cost-related changes are not only necessary, but vital. In this light, numerous energy and cost saving techniques have been identified for the Ferro-Alloys industry.

Regardless of the developments in smelting technologies the majority of FeCr smelting is performed using submerged arc furnaces. In terms of the cost of operation of theses FeCr smelting industries, 30% can be attributed to the consumption of electricity, whereas 50% of the cost of operation has been recognised as the cost of the raw feed materials, including the chromite ore and the reducing material [9]. Therefore by simply improving aspects regarding the utilisation of electrical energy, and optimising the desired product output based on the raw material feed, both energy and cost savings can be obtained. The main technologies that have been adopted with the purpose of increasing the efficient use of electricity in the FeCr industry revolve around the pre-treatment of the raw feed before it enters the submerged arc furnace for smelting. These pre-treatment methods include agglomeration, pre-heating and the pre-reduction of the raw materials [9]. The purpose of pre-treatment methods is to reduce the cumulative utilisation of electrical energy required to produce the same quantity of metal.

The energy consumption in FeCr smelting industries is also largely effected by the feed material. The feed recipe or composition is vital in firstly obtaining the appropriate slag characteristics for metal and slag separation, and secondly producing a furnace internal charge resistance that reduces the amount of current drawn in order to smelt the charge material. The addition of fine or lumpy materials affects the charge resistance and therefore energy consumed for smelting. If the addition of these materials is closely and continuously monitored, energy and cost savings can once again be achieved. It is clear from this that before even considering brand new technologies, processes and methods for waste energy recovery and utilisation, savings can already be achieved simply through optimising current technologies and processes.

With this in mind however, new technologies are essentially the way forward. The FeCr smelting technologies that have been introduced in the past 20 years that have become commercially successful in improving energy and cost savings include the utilisation of open or semi-closed furnaces, rotary kiln pre-heating and reduction, DC arc furnaces and advanced system automation [9]. Open and semi-closed furnaces allow for the use of fines materials in the furnace which require less energy for smelting. In conjunction with this,

open or semi-closed furnaces also allow for more efficient and effective ventilation and off-gas extraction. As mentioned previously, the pre-treatment of the feed material ensures that materials enter the furnace at a significantly reduced moisture level and in a pre-reduced state. Even though energy is required to perform pre-treatment operations, investigations have shown that the cumulative energy required for the entire smelting process is reduced through the utilisation of these operations, as compared to smelting processes without pre-treatment operations [9].

The most significant cost factor however is the availability of the furnace. This is due to the energy and costs required for furnace start-up and shut-down operations. If a furnace is allowed to operate continuously and without fault, the greatest cost and energy savings for that system will be achieved. DC arc furnaces have shown great promise in being more economical to operate than traditional AC arc furnaces. However, experts are still not confident of this, primarily due to a much lower availability. Other factors such as higher power consumption and shorter equipment life spans have also caused doubt on whether DC arc furnaces are indeed more economical than their AC counterparts [9].

Another important technological advancement in the smelting industry is the automation of the smelting process as a whole. It has been shown that the operation of smelting processes can be significantly improved by advanced automation systems that have centralised digital control units that facilitate the monitoring, control and the development of the entire smelting process. These automation systems include sophisticated control systems that incorporate fuzzy logic, neural calculations and genetic algorithms [9].

Additional operational and economical improvements in the FeCr industry have also been shown through actions taken at the No.1 Submerged Arc Furnace at the Kashima Works (KF-1) in Japan that produces high carbon FeCr. These actions include the improvement of the tapped material runners for increased tapping cycles per day, the utilisation of cold raw materials to increase the charge resistance when this resistance becomes too low due to unstable tapping conditions, and the installation of water-cooled copper pipes in the furnace tap holes in order to restore the furnace self-lining coating in the event that this

lining requires maintenance. With these improvements a power reduction from 24.7 MW to 22.8 MW was achieved [8].

2.5 COGENERATION AND REFRIGERATION SYSTEMS FOR VIABLE THERMAL ENERGY RECOVERY AND UTILISATION

Various methods and updated technologies for improving the efficient use of energy and reducing costs associated with the operations in a FeCr industry have so far been discussed. Even though significant energy and cost savings can be achieved from these methods and technologies, a more important topic has recently come under scrutiny. That is the utilisation of waste from mining and smelting industries to produce or generate additional useful energy. In the mining and smelting industries this can be in the form of re-using waste process materials, such as the utilisation of slag by civil engineering companies as building materials [2], or re-using physical waste energy, usually thermal energy. The use of waste thermal energy in the FeCr smelting industry has become of great interest due to the significant amount of heat that is rejected from the furnaces during smelting processes. It is due to this that cogeneration has become a promising technological solution.

Cogeneration is the generation of electrical and thermal energy simultaneously from a single energy source or fuel [10], [11]. There are various cogeneration system configurations based on two important aspects. These aspects include the sequence of energy use from the fuel or energy source to the final industrial load, in order to meet the electrical and thermal load requirements, and the nature and characteristics of the thermal and electrical demands of the facility. However, the two main types of cogeneration configurations are topping cycle and bottoming cycle cogeneration systems.

For a topping cycle cogeneration system, fuel is used to generate electrical power and heat. The heat, which is considered the by-product of the process, is recovered and used to satisfy additional thermal requirements associated with the industrial system. Topping cycle systems are most commonly implemented in power generation industries. For a bottoming cycle cogeneration system, the primary fuel is utilised in an industrial process

which produces thermal energy as a by-product at very high temperatures. This energy is normally considered to be waste energy and is recovered through the use of boilers or heat exchangers and transferred to a turbine generator in order to produce electrical power. Bottoming cycle systems are commonly implemented in industries with manufacturing processes that require heat at high temperatures in furnaces and kilns, and then reject heat at high temperatures as waste. This recovered waste heat is therefore utilised to produce additional electrical power [12].

An example of such a system is discussed in [11] whereby waste thermal energy is recovered from a sinter-cooling process and converted into electrical energy. The recovered waste energy is in the form of process off-gas which has a sufficient thermal energy potential to be used for power generation purposes. Cogeneration technologies can therefore be effectively implemented in the FeCr smelting industry as off gases extracted from the smelting processes are at an extremely high thermal energy level at temperatures of between 200 and 600 ^{o}C. This is sufficient thermal energy to be utilised to generate additional and useful electrical energy. Cogeneration processes however also generate thermal energy, usually at very low temperatures that are not suitable for re-use in the electrical generation process of the system. In essence this thermal energy is once again wasted.

The solution to this is the utilisation of low grade thermal energy for cooling and refrigeration purposes, as is discussed in [13] and [14]. Due to the broad evaporation range of ammonia-water absorption refrigeration systems, new cogeneration technologies with power generation and refrigeration capabilities have been developed. In these systems, the medium to high-grade extracted thermal energy from industrial processes is used to generate electrical energy utilising the Rankine Cycle, whereas the electrical energy generation by-product low-grade thermal energy is used for refrigeration and cooling processes, via the absorption refrigeration cycle [13].

The output of the power generation section of the cogeneration system is electrical energy and low temperature heat, or low-grade thermal energy. Recent studies have shown that by

using an ammonia-water or lithium bromide-water mixture working fluid and a gas heat exchanger, this low-grade thermal energy can be used for refrigeration purposes [13], [14]. This energy can therefore either be used to replace air-conditioning systems and provide comfort cooling to buildings, or it can be used for process refrigeration applications such as cold storage and the storage and preservation of food [13]. Industrial cooling applications can also utilise low-grade thermal energy to drive chillers which are capable of meeting facility and industrial cooling requirements. Such requirements include water and oil cooling processes [13], [14].

2.6 THE ORGANIC RANKINE CYCLE AND COGENERATION SYSTEM WORKING FLUID PROPERTIES

Power generation via cogeneration systems rely firmly on the Rankine Cycle. The Rankine Cycle is an idealised thermodynamic cycle of a working fluid that is used to predict the performance of the heat-to-electrical system in which the fluid is operating. The purpose of this section is to discuss the Organic Rankine Cycle (ORC), which is the Rankine Cycle of a specific organic fluid that is being used in a system. ORC systems utilise an organic fluid as the system working fluid as opposed to water and steam. Organic fluids allow for more efficient heat recovery and utilisation as opposed to water, although this is dependent on the capacity of the system in which the fluid operates. The system-related considerations that need to be made that affect the choice of working fluid utilised, organic or water, will also be discussed in this section.

In the case of this research, the ORC will be considered in conjunction with a heat recovery cogeneration system for electrical energy generation from recovered waste thermal energy. It is therefore important to understand what equipment is required for such a system and how the ORC can be analysed in order to recognise the thermal energy input and electrical energy output capacities of the system. The equipment that forms part of a heat recovery cogeneration system and on which the chosen working fluid ORC operates includes a heat exchanger or heat recovery vapour generator, a turbine expander for power generation, a condenser and a working fluid flow control and pressurising pump [14], [15], [16].

The working fluid undergoes phase, temperature, pressure and therefore energy changes throughout the power generation cycle, which are essential in the transfer of thermal energy to mechanical energy, and therefore electrical energy. These changes can be analysed using and are based firmly on the working fluid ORC. A representation of a power generation cycle and the comprising components are shown in Figure 2.1.

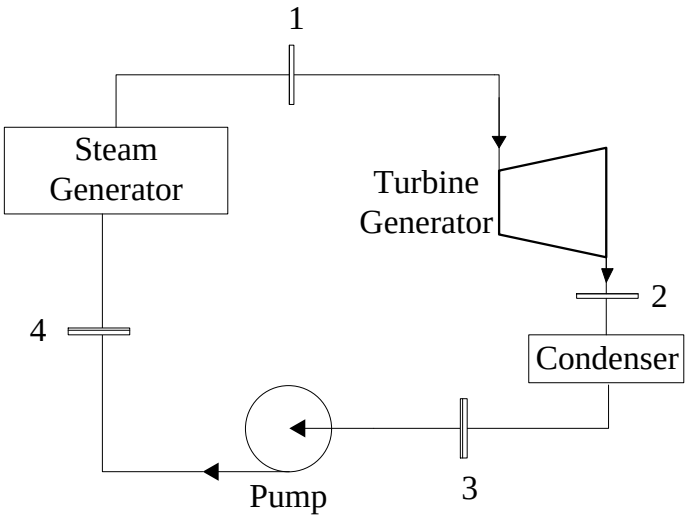

Figure 2.1: Power generation cycle

ORC cycles are analysed as 'Temperature vs. Entropy' (T-S) curves that show the phase and energy at which the working fluid exists at and in between each stage of the power generation cycle. A representation of such a curve is shown in Figure 2.2. Firstly, the heat exchanger transfers heat obtained via waste heat extraction and recovery to the working fluid. The incoming fluid is supplied with energy through this process which increases the temperature of the fluid until it becomes a saturated liquid. This saturated liquid is then evaporated to form a saturated vapour. The heat exchanger then further raises the temperature of the vapour to produce a superheated vapour. This corresponds to the working fluid change from 4 to 1 in Figure 2.2. The superheated vapour is the output of the heat exchanger and holds the thermal energy which will need to be converted into mechanical energy inside the turbine [14], [15], [16].

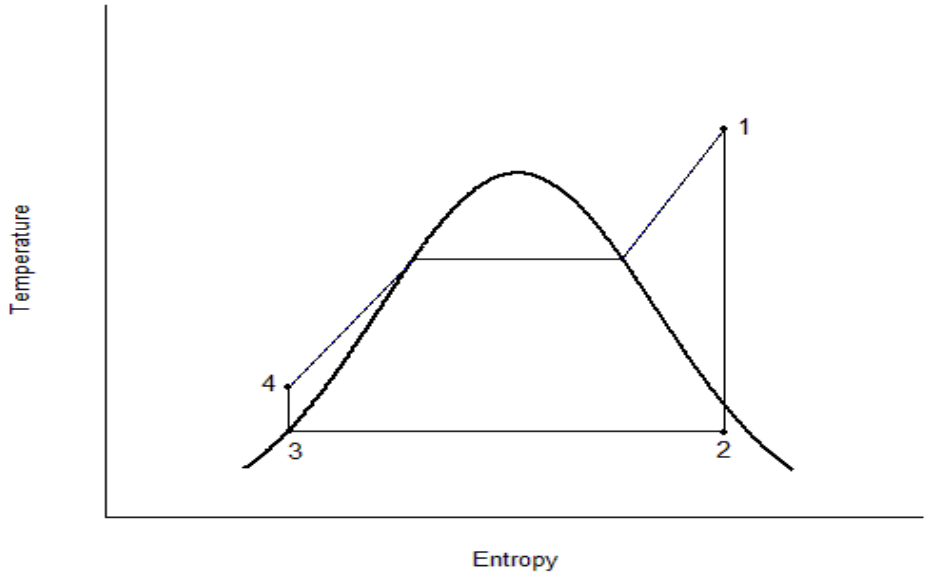

Figure 2.2: Power generation working fluid rankine cycle T-S curve

The superheated vapour is fed into the turbine where it is expanded over the turbine blades, thereby converting the working fluid thermal energy into mechanical energy. This mechanical energy is then transmitted to the turbine shaft in the form of a shaft rotational motion. This corresponds to the working fluid change from 1 to 2 in Figure 2.2. The turbine shaft drives an electrical generator which generates electrical power. As a result of the expansion of the superheated vapour inside the turbine and the conversion of most of the working fluid thermal energy into mechanical and electrical energy, the vapour exits the turbine at a pressure and temperature well below the entrance or throttle parameters. The power generation cycle re-uses the working fluid in a closed loop cycle, and therefore this exiting vapour must to be returned to the heat exchanger in the required pressurised and reduced-temperature state [14], [15], [16].

In order to return the turbine exiting vapour to the high pressure required by the heat exchanger to continue the cycle, the low pressure turbine exiting vapour is fed through a condenser and a flow control pressurising pump. The condenser reduces the temperature of the low pressure exiting vapour, converting the working fluid back to its starting form. This corresponds to the working fluid change from 2 to 3 in Figure 2.2. The condenser acts

as a reverse heat exchanger and utilises cooling water flowing inside copper tubes on which the low pressure exiting vapour either condenses or cools around depending on the category of fluid used, wet or dry. In both the heat exchanger and the condenser the fluids pass through with relatively low pressure drop and therefore it is common in ideal ORC evaluation to assume that heat exchangers and condenses operate on fluids of unchanging pressures.

The flow control pressurising pump is then used to pressurise and pump the working fluid back to its starting high pressure state as is required by the heat exchanger. This corresponds to the working fluid change from 3 to 4 in Figure 2.2. This pressurised and reduced temperature fluid is then fed back into the heat exchanger where the cycle begins once more [14], [15], [16].

The selection of a specific working fluid over another fluid, be it an organic fluid over water, or one category of organic fluid over another, is performed with the goal of developing the most efficient heat recovery process [15]. There are a variety of working fluids available, all suited to specific heat recovery processes and capacities, which is why the appropriate selection of a working fluid for a specific heat recovery process is extremely vital [17]. The performance of an ORC and the conjoining power generation cycle is determined very closely by the temperature and pressure ranges in which the fluid and the system as a whole operates [15]. With this in mind the two most important considerations when selecting a working fluid for a heat recovery system are total system heat recovery efficiency and working fluid thermal efficiency [17], [18], [19]. Ultimately, the aim of a heat recovery system, and more so the selection of an appropriate working fluid for the system, is to reduce both the power generation cycle and ORC inefficiencies and to increase the overall system energy conversion efficiencies [20].

There are four processes of the ORC that result in the ORC saturation vapour line curve shape. These processes occur as a result of the power generation cycle equipment and include [14]:

- The isentropic process that is the fluid pressurisation over the flow control pressurization pump,
- The heating process inside the heat exchanger where heat from a specific heat source is transferred to the working fluid,
- The fluid expansion process through the turbine in order to generate electrical energy which is ideally an isentropic process, and
- The condensation process of the working fluid whereby the turbine output fluid is cooled and returned back to the pump.

According to these four processes, ORC cycles are classified primarily according to the shape of the saturation vapour line of the 'Temperature vs. Entropy' (T-S) curve. The saturation vapour line for a working fluid can either be bell-shaped, categorised as "b-", or overhanging, categorised as "o-" [18]. The "b-" or "o-" saturation vapour line curve shape of a working fluid depends on the temperatures at which the ORC operates. It was found in [18] that ORC processes that operate at medium to high temperatures require an "o-" category working fluid.

In more detail, ORC working fluids can be classified into three main categories according to the slope of the T-S curve, either positive, infinite or negative. The three main categories are dry fluids with a positive slope, isentropic fluids with an infinite slope and wet fluids with a negative slope [16], [19]. The selection of the working fluid for a power generation and heat transfer process is essential and depends on factors such as thermodynamic performance, the elimination of the possibility of droplets forming on the turbine blades, a high vapour density, appropriate pressure and temperature operation ranges, a high stability and low boiling point temperature, low environmental impact, high availability and low cost [16], [18], [21]. In order to test the applicability of a chosen working fluid, system parameters such as the turbine inlet pressure and temperature, turbine fluid exit quality, condenser exit temperature, overall system irreversibility and system efficiency are considered [16].

Dry and isentropic working fluids are most appropriate for ORC and power generation systems due to the fact that these fluids are usually still in the superheated state after the isentropic expansion of the fluids through the turbine. This eliminates the risk of liquid droplets forming on the turbine blades which can be extremely damaging to the blades and the entire turbine. The disadvantage of using dry fluids however is that due to the superheated vapour turbine exit characteristic, the area of net work in the T-S curve for that fluid is reduced and the cooling process will require significantly more power to cool the superheated vapour, as opposed to wet fluids. In this light isentropic fluids are the most suitable, as the risk of droplet formation is eliminated, and the power required for the cooling process at the exit of the turbine is not as significant as for dry fluids. However, isentropic fluids do raise issues of concern such as cost, chemical stability and safety [16], [19]. Still, with these considerations in mind, isentropic working fluids are considered most appropriate for ORC and power generation cycles [16].

There are numerous working fluids to choose from, many of which are listed and discussed in [14], [15], [18], [20] and [21]. The most common fluids however include the refrigerant fluids R134a and R245fa, as well as n-pentane and silicone oil [21]. Currently, most power production systems are bottoming cycle systems utilising water and steam as the working fluid, although many have argued that the use of organic fluids will allow for much greater system efficiency. This however is not always the case and in fact depends on the temperature range and capacity at which the system operates [15], [18]. At low temperatures of about 100 ^{o}C, the advantages of utilising organic fluids over water as the working fluid are obvious. Organic fluids can have boiling point temperatures much lower than that of water and the volume ratio of the working fluid at the turbine inlet and outlet can be considerably smaller for organic fluids as opposed to water. This allows for simpler and cheaper turbines to be used for the same output power capacities [17], [18], [19]. At medium to high operation temperatures, 350 ^{o}C and higher, the advantages are not always as straight forward.

The significance of ORC working fluids is that the same equipment as conventional steam systems can be used, however the use of an organic working fluid allows for a reduced

boiling point and evaporating temperature and therefore a reduced amount of energy required to generate vapour in the heat exchanger or vapour generator. This is due to organic fluids having higher molecular masses and lower boiling points than water [20], [21]. Therefore some advantages of utilising organic working fluid systems over traditional steam-based systems include a significantly reduced boiler operating temperature and pressure, a reduced complexity and cost associated with the boiler equipment, and a decrease in the installation and system management costs due to the lower pressures that exist throughout the entire power generation cycle. The main advantage however is that low-grade heat can efficiently be utilised to generate additional useful power [14].

However, for systems that operate at higher temperatures, above 350 ^{o}C, the efficiency of power generation with an ORC begins to decrease and can become lower than that of a traditional steam cycle. A major drawback of organic fluid-based systems is in fact that the efficiency of power generation decreases as the plant size increases [14]. The efficiencies of power generation for bigger plant sizes are therefore often increased through the installation of additional power and heat generation systems, such as solar power systems and simple wood and coal burning systems. It is for this reason that ORC power generation systems are only applicable for the low to medium temperature range, between 80 and 350 ^{o}C. At temperatures beyond this, medium to high temperatures, traditional steam-based power generation systems are more effective and efficient. That is why power generation stations today are still primarily steam-based. As small-scale power generation picks up, so too will the utilisation of ORC power generation systems [14].

2.7 THE ORGANIC RANKINE CYCLE AND COGENERATION FOR THERMAL ENERGY RECOVERY AND UTILISATION

From the literature obtained regarding the capabilities of the ORC for heat recovery in a power generation system, it can be concluded that the ORC can be utilised in a bottoming cycle heat recovery cogeneration system. Such a system is well suited to the smelting industry as off gases from the smelting processes reach the current cooling stages at temperatures of between 200 and 400 ^{o}C. This low-medium grade waste thermal energy can be efficiently recovered and utilised by a power generation cycle with an organic fluid

as the working fluid, and the low temperature heat that is a by-product of the power generation process can be further utilised for refrigeration purposes [13], [16], [19].

In the smelting industry, a cogeneration system with the potential of recovering and utilising waste heat, will be coupled to the flue gas (off gas) extraction ducts. The thermal energy carried by the gases will therefore be transferred to the heat exchanger component of the cogeneration system, with the most likely case of thermal oil being used as the thermal energy transfer medium. The reason for this is that by using a thermal oil-based transfer medium fluid the risk of local overheating is significantly reduced, and the heat exchanger can be operated at atmospheric pressure [17]. This also reduces the load required by the pressurisation pump and therefore results in an increased overall system efficiency.

The implementation of such a system is extremely beneficial, but not only to the facility itself. It has been estimated in [20] that by 2030 the global energy consumption is likely to grow by 71%. Unfortunately, as energy consumption increases so too the generation of electrical energy is expected to increase in order to meet the new energy demand. By traditional electrical energy generation methods of burning coal in order to supply heat for the vaporisation of water, the energy generation-related carbon dioxide emissions are expected to rise in the same time by more than 40% [20]. In addition to this, the depletion of natural resources, and the increase in air and heat pollution and global warming due to the release of hot streams of system waste off gases, are all major global concerns [14], [20]. Therefore through the implementation of cogeneration systems that utilise this waste energy, three crucial benefits are achieved:

1. The power demand and generation burden can be eased as additional useful energy becomes available. The entire power generation system efficiency is also increased through this process and more electrical energy is produced from the same resources [14].
2. The amount of air and heat pollution is significantly reduced as waste thermal energy is almost completely utilised and the system-end by-product is thermal energy at very

low temperatures. The emission of harmful gases is also reduced as no additional fuel is required for the generation of more electrical energy [14].

3. ORC-based power generation and cogeneration systems can utilise and operate in conjunction with various types of low-grade thermal energy sources and topping cycle systems respectively, including solar, biomass and geothermal sources and systems. Furthermore, ORC systems can also operate in conjunction with traditional power generation plants with considerable ease and at low implementation costs [14], [18], [20].

Examples of current facilities and plants that are utilising ORC-based cogeneration system technologies are discussed in [18] and [21]. These include a 1 MW_{el} and a 0.2 MW_{el} power production capacity geothermal plant in Altheim, Austria and Neustadt-Glewe, Germany respectively. A 2 MW_{el} waste heat recovery cogeneration system at the CIMAR-ITALCEMENT GROUP in Morocco is one of the largest and leading ORC-based cogeneration system implementations that recovers and utilises waste thermal energy from an industrial process to generate additional useful electrical energy [22].

2.8 DISTRIBUTED GENERATION AND MULTI-CARRIER ENERGY SYSTEMS MODELLING

According to sections 2.1 to 2.7, a theoretical bottoming cycle waste heat recovery cogeneration system at a FeCr plant has the potential to generate additional useful electrical energy from extracted waste thermal energy. It is the objective of this research to dispatch the cogeneration generated power optimally between the furnace loads and the utility grid in order to obtain the maximum possible system associated energy savings. A system such as this is an example of a Distributed Generation (DG) energy system.

2.8.1 Energy Systems

The demand for energy is a continuously varying parameter in a technical and economic society. Energy systems can be defined as both technical and economic systems related to the supply of energy, as well as to the various and numerous society sub-systems that utilise energy every day in order to enhance the standard of living within the society [23].

The three main aspects of an energy system are electricity, heat and mobility [24]. Countries rely predominantly on the national electricity generation utility to meet electrical and heat demands, but frequently, there are significant interconnections between additional small-scale electrical and gas networks, and the main utility grid. These interconnections allow for the flow and trade of all country-wide generated energy. It is in this circumstance that the importance of mobility in an energy system is revealed.

The aim of energy systems and services is therefore to satisfy human needs and desires. However, the use of energy systems, and therefore energy itself, is in no way the termination of an energy system. Considerations concerning the energy-flow cycle, from primary energy sources to energy consumption and waste, need to be made. Energy systems have significant impacts on society, the economy and the environment, and therefore the modelling of these systems are imperative in order to monitor and control these impacts. An energy model is therefore aimed at assisting in decision making during the implementation and continuous utilisation of energy and energy systems, while ensuring the minimisation in the depletion of non-renewable primary energy resources, the minimisation of emissions of various energy system related pollutants, and the minimisation of the overall monetary and capital costs associated with energy systems [23].

2.8.2 Distributed Generation (DG)

Cogeneration, or Combined Heat and Power (CHP), is an effective method of utilising waste energy to meet additional energy demands, while obtaining additional technical and environmental benefits. Studies have shown that the implementation of cogeneration and trigeneration technologies in industries have led to the reduction in many industry related pollutants such as carbon dioxide and sulphur dioxide, as well as many sulphur and nitrogen oxides [25], [26], [27]. In conjunction with these environmental benefits, technical or efficiency-based benefits were also found to be considerable. Studies have shown that a conventional power generation unit is usually less than 60% efficient, whereas efficiencies of almost 90% can be obtained through the implementation of cogeneration and trigeneration technologies [28].

Cogeneration and trigeneration technologies fall under a broader energy generation system known as Distributed Generation (DG). DG is the application of small-scale and localised energy generation systems that are situated all around and throughout the main power supply utility grid. DG systems provide additional electrical power to customers in close proximity to the systems, and in doing so also provide support and assistance to the main supply utility grid. DG systems therefore offer additional and alternative sources of energy to industrial, commercial and residential customers. This has led to a substantial growth in interest in DG systems such as cogeneration [29]. DG systems are therefore not only capable of supplying additional energy to customers, but also increasing the reliability of on-site electrical and thermal supplies [30].

2.8.3 Distributed generation multi-carrier energy system considerations for modelling

Previously, the modelling of energy systems through the consideration of the conversion, transmission and distribution of energy, was accomplished by considering only one form of energy [31], [32]. With the increased implementation of DG, an increased coupling occurred between electricity generation, natural gas and district heating power systems. This coupling was found to be in the form of the interactions of these energy systems with each other through the transmission, distribution and conversion of energy between the respective energy systems [33].

The increased coupling of energy systems led to the necessity for modelling energy systems and energy flow through the consideration of multiple energy carriers and sources. These systems were referred to as Multi-Source Multi-Product (MSMP) systems, and were defined as systems with multiple energy inputs and multiple energy outputs. The modelling of MSMP systems was more significant as these systems resembled cogeneration and other DG systems substantially better than single-energy system models [31], [32]. An MSMP system energy flow model can therefore be implemented for systems that utilise waste energy to produce additional useful energy.

2.8.4 Energy hub concept

It is often beneficial, when modelling energy systems and energy flow, to utilise the concept of an energy hub. An energy hub is a single unit or interface that represents the inputs, outputs, conversion and transmission of energy throughout a single energy system. The single unit or interface therefore represents a single node of an entire energy network that describes the energy input-output model of the node, as well as all essential energy conversion and transmission features associated with the respective energy system. Energy hubs can therefore be interconnected to represent the exchange of energy between numerous energy systems, while a centralised energy hub supply is in place to represent the common utility grid supply that meets the demand of all connected energy hubs and systems [31], [32], [33].

2.8.5 The power flow and economic power dispatch (EPD) problem

The coupling of energy hubs or energy systems introduces a problem concerned with the optimal flow of power between systems, which results in the most advantageous economic and environmental outcomes associated with the systems. This is appropriately termed as an optimal power flow problem. Optimal power flow can be described as the determination of all power related operating conditions and constraints of an energy system that results in the 'best' operation of the system. This 'best' operation usually refers to the system operation that leads to the minimised system associated cost, impact on the environment and system failure rate [31], [34].

EPD relates to the optimal power flow problem, in that it is used to determine the optimal manner in which to share or dispatch available power between various loads, or loads between various generating units, in order to minimise the total system associated costs subject to various technological and physical constraints. EPD algorithms are usually in the form of half-hourly, hourly or daily power dispatch schedules that determine when and how much power is to be shared or distributed during the respective time intervals [26], [34], [35]. The increase in the use of DG systems has led to an increase in the requirement for EPD models to ensure the optimal flow of power within and between different energy

systems. An EPD algorithm is therefore essentially an optimisation model that solves and controls the optimal power flow problem of a single energy system or an interconnection of multiple energy carrier systems [36].

The specific DG system of importance in this research is a cogeneration or CHP system. The EPD model for this system can be termed as a Combined Heat and Power Economic Dispatch (CHPED) model. Conventional CHPED problems require models that represent the electrical-only, cogeneration (combined electrical and heat) and heat-only units of the cogeneration system. The objective of the CHPED model is to dispatch the generated heat and electricity between the loads while minimising the electrical and heat production costs [28].

2.8.6 EPD modelling and research applications

In order to establish and develop an EPD model, the multicarrier energy system under consideration needs to be re-established and considered as an interconnection of multiple energy hubs. This is the critical concept behind energy system modelling. The optimisation of the energy flow that forms the crux of the EPD model is separated into the optimisation of the energy flow between energy hubs, and the optimisation of energy flow within individual energy hubs. The difference that needs to be considered within these two sections is that within energy hubs, energy can be converted and changed into many different forms, whereas between energy hubs, energy can only be transmitted from one hub to another. Therefore, the two main energy-related quantities that are modelled are energy conversion and energy transmission [31].

The modelling of a multicarrier energy system can therefore be simplified into the following quantities [31], [33]:

- How much energy, from the different energy carriers, should the individual energy hubs consume?
- How and to what extent should the energy obtained from the various energy carriers be converted within individual energy hubs in order to meet the same energy hub load demand?

- How much energy should flow between the interconnected hubs and how should this energy flow be controlled?

The implementation of an EPD model, to determine the quantities specified above, requires assumptions and limitations in order to simplify the modelling process. These can be as follows [31], [32], [33], [36]:

- The overall multicarrier energy system is assumed to be in a steady state mode of operation, so that all transient responses associated with the system are ignored.
- The power or energy flow through converter devices are characterised by the quantity of power or energy and the converter efficiency only.
- Converters and transmission lines have efficiencies that are assumed to be constant.
- Losses within individual energy hubs only occur in the converter devices.
- Losses between energy hubs only occur due to transmission line losses.
- Unidirectional power or energy flow is assumed for all converter devices, from the input to the output of the energy hub.
- The cost of energy carriers is assumed to be polynomial functions of the associated energy or power.
- Throughout the multicarrier energy system, the cost associated with an energy carrier is assumed to be independent of the cost associated with a different energy carrier.

With these formulated assumptions in mind, various EPD models have been developed in [24], [26], [28], [31], [32], [33] and [36]. In [24], [31], [32], [33] and [36], simplified EPD models are developed for the optimal dispatch of electrical energy only, throughout an energy system. In essence, the models minimise the cost associated with the dispatch of power from an energy hub, while adhering to the load demand, power flow capacities, energy system power rating capacities, dispatch capacities and dispatch factors. In [33] and [36], the minimised cost is mathematically defined as a polynomial function of the dispatched power. Lastly, in [26] and [28], more complex stochastic models are presented that consider both the electrical and heat demands and requirements of CHP system.

In cogeneration or CHP industries, the generated thermal and electrical energy, as well as the industrial electrical and thermal demand, are all variables as determined by the industry specific operations and processes. Due to this variability, the energy processes are stochastic, and the modelling of these processes is achieved with stochastic models. All the EPD models presented in [24], [26], [28], [31], [32], [33] and [36] are stochastic based models.

From [28], [31], [32], [33] and [36], a power-only economic dispatch model for a single energy hub was obtained as is shown in equations (2.4) to (2.9):

$minmise$:

$$f(P_i) \tag{2.4}$$

$subject\ to$:

$$L_i - C_i P_i = 0 \quad (Load\ is\ always\ met), \tag{2.5}$$

$$P_{i,min} \leq P_i \leq P_{i,max} \quad (Energy\ hub\ and\ carrier\ input\ power\ range), \tag{2.6}$$

$$P_{ci,min} \leq NP_i \leq P_{ci,max} \quad (Converter\ input\ power\ range), and \tag{2.7}$$

$$0 \leq N \leq 1 \quad (Dispatch\ factor\ range). \tag{2.8}$$

where:

- P_i is the energy hub input and carrier i power,
- $f(P_i)$ is the cost function to be minimised, and is dependent on the i-th carrier input power P_i,
- L_i is the load associated with the energy hub input and carrier i,
- C_i is the converter efficiency associated with the energy hub input and carrier i, which couples the input power i to the dispatched power, sent to the coupled load,
- $P_{i,min}$ and $P_{i,max}$ are the input power minimum and maximum constraints associated with energy hub input and carrier i,
- $P_{ci,min}$ and $P_{ci,max}$ are the converter input power minimum and maximum constraints associated with energy hub input and carrier i, and
- N is a constant dispatch factor.

The cost function $f(P_i)$ can be expressed as a polynomial function of P_i:

$$f(P_i) = C_i = a_i + \begin{cases} \sum_{j=1}^{Q_i} b_{ij}(P_i + A_i)^j & if\ P_i \geq 0, \\ \sum_{k=1}^{R_i} c_{ik}|P_i + A_i|^k & if\ P_i < 0. \end{cases} \quad (2.9)$$

where:

- C_i is the total cost function related to the energy hub input and carrier i,
- A_i is the total network power losses for energy hub input and carrier i,
- a_i is a fixed energy cost related to energy hub input and carrier i,
- b_{ij} and c_{ik} are specific cost coefficients related to energy hub input and carrier i, and
- Q_i and R_i are the orders of the polynomial functions for energy hub input and carrier i.

A CHP economic dispatch model, considering both electrical and thermal energy was also obtained from [26] and [28], and is shown in equations (2.10) to (2.19):

$minmise$:

$$\sum_{i=1}^{N_p} C_i(P_{pi}) + \sum_{j=1}^{N_c} C_j(P_{cj}, H_{cj}) + \sum_{k=1}^{N_h} C_k(H_{hk}) \quad (2.10)$$

$subject\ to$:

$$\sum_{i=1}^{N_p} P_{pi} + \sum_{j=1}^{N_c} P_{cj} = P_d \quad (Power\ demand\ met) \quad (2.11)$$

$$\sum_{j=1}^{N_c} H_{cj} + \sum_{k=1}^{N_k} H_{hk} = H_d \quad (Heat\ demand\ met) \quad (2.12)$$

$$P_{pi,min} \leq P_{pi} \leq P_{pi,max} \quad for\ all\ i = 1\ to\ N_p \quad (Power - only\ capacity\ limits) \quad (2.13)$$

$$P_{cj,min} \leq P_{cj} \leq P_{cj,max} \quad for\ all\ j = 1\ to\ N_c \quad (Combined\ power\ capacity\ limits) \quad (2.14)$$

$$H_{cj,min} \leq H_{cj} \leq H_{cj,max} \quad for\ all\ j = 1\ to\ N_c \quad (Combined\ heat\ capacity\ limits) \quad (2.15)$$

$$H_{hk,min} \leq H_{hk} \leq H_{hk,max} \quad for\ all\ k = 1\ to\ N_h \quad (Heat - only\ capacity\ limits) \quad (2.16)$$

where:

- C_i, C_j and C_k are all cost functions associated with the power-only, combined heat and power, and heat-only units respectively,
- N_p, N_c and N_h are the number of power-only, combined heat and power, and heat-only units used respectively,
- i, j and k represent the i-th, j-th or k-th unit of the power-only, combined heat and power, and heat-only units used respectively,
- P_{pi} and H_{hk} represent the total power and heat generated respectively from the power-only and heat-only units,
- P_{cj} and H_{cj} represent the total power and heat generated respectively from the combined heat and power units,
- P_d is the overall power demand,
- H_d is the overall heat demand, and
- $P_{pi,max}$, $P_{pi,min}$, $P_{cj,max}$, $P_{cj,min}$, $H_{cj,max}$, $H_{cj,min}$, $H_{hk,max}$ and $H_{hk,min}$ represent the power and heat capacity limits for the power-only, combined heat and power, and heat-only units.

The cost functions were also assumed to be polynomial functions of the generated heat and/or power, and are presented below:

$$C_i(P_{pi}) = a_i(P_{pi})^2 + b_i P_{pi} + c_i \tag{2.17}$$

$$C_j(P_{cj}, H_{cj}) = a_j(P_{cj})^2 + b_j P_{cj} + c_j + d_j(H_{cj})^2 + e_j H_{cj} + f_j \tag{2.18}$$

$$C_k(H_{hk}) = a_k(H_{hk})^2 + b_k H_{hk} + c_k \tag{2.19}$$

where:

- a_i, b_i and c_i are the cost coefficients associated with the cost of power generation from the power-only units,
- a_j, b_j and c_j are the cost coefficients associated with the cost of power generation from the combined heat and power units,
- d_j, e_j and f_j are the cost coefficients associated with the cost of heat generation from the combined heat and power units, and

- a_k, b_k and c_k are the cost coefficients associated with the cost of heat generation from the heat-only units.

The models presented in [26], [28], [31], [32], [33] and [36] can be used to solve power-only economic dispatch problems for single energy systems, and CHP economic dispatch problems for combined electrical and thermal energy systems. In this research, an EPD model will be developed with the purpose of optimally dispatching cogeneration generated electrical energy between on-site loads and the utility grid. The on-site loads will also be supplied by the utility grid. The output or by-product of the proposed system will be low-grade heat which can also be used for refrigeration purposes. Therefore it is essential that all electrical and possibly refrigeration demands are met and that the model distributes the cogeneration generated electrical energy in an economically optimal manner between the on-site loads and the utility grid.

The development of the required EPD model will therefore require the concepts and models presented in [26], [28], [31], [32], [33] and [36]. However, the model in this research will consider specific utility contractual-based power, water and working fluid consumption and utilisation costs and incentives as the significant component of the model cost function. The cost of power generation will therefore not be modelled as a polynomial function of the generated power and in fact will be expressed as the actual power consumption tariff applied to the physical power required for the extraction of the waste heat and the operation of the bottoming cycle cogeneration system for power generation. This is made possible due to the real system operational data that will be used for the overall model development.

CHAPTER 3 RESEARCH METHODOLOGY

3.1 RESEARCH METHODOLOGY OVERVIEW

This research is divided into two main sub-sections as determined by the research questions posed in the Chapter 1. These two sub-sections deal with the methods, procedures, calculations and descriptions of how waste heat can be extracted from a FeCr plant (Glencore Ferrochrome in Rustenburg) and utilised for the generation of additional useful electricity, and how this additionally generated electrical energy should be optimally dispatched between the furnace loads and the utility grid resulting in the maximum possible system associated energy and cost savings. In each of these two sub-sections, the methods that are used as well as all process related calculations and system optimisation algorithms will be extensively discussed. The explanations will follow the flow of the optimisation algorithm from raw data input to final EPD, and will include discussions of code and algorithms that are used throughout the optimisation model.

3.2 WASTE HEAT EXTRACTION, RECOVERY AND UTILISATION FOR ELECTRICAL ENERGY GENERATION

3.2.1 EPD model raw data input and working array formation

The EPD model requires the FeCr plant operating conditions and capacities in order to calculate exactly how much electrical energy can be obtained from the heat recovery bottoming cycle cogeneration system coupled to the plant furnace heat extraction ducts for thermal energy recovery. The operating conditions and capacities are in the form of raw process-related data obtained from the plant control and monitoring system that displays and stores current and historical data. The model that will be developed in this research will be built and tested utilising historical data, however the purpose of the model will be real-time operation and power dispatch and will therefore operate utilising current data. This however does not affect the model development, only the considerations that are made if the model is physically implemented into the entire system.

The plant operation raw data is stored in a spread sheet with the following column headings: Date and Time, F1 MVA, F1 MW, F1 Stack Temp 1, F1 Stack Temp 2, F1 Stack Temp 3, Bagplant 1 Inlet Temp, F2 MVA, F2 MW, F2 Stack Temp 1, F2 Stack Temp 2, F2 Stack Temp 3, Bagplant 2 Inlet Temp, F3 MVA, F3 MW, F3 Stack Temp 1, F3 Stack Temp 2, F3 Stack Temp 3, Bagplant 3 Inlet Temp, F4 MVA, F4 MW, F4 Stack Temp 1, F4 Stack Temp 2, F4 Stack Temp 3 and Bagplant 4 Inlet Temp.

It is essential for the Date and Time data to be formatted as a general numerical value rather than as date and time, as these values can only be imported into the chosen modelling program in a numerical format. For example, the date-time stamp of 2014/08/01 01:00:00 AM, will need to be formatted to the general numerical form of 41852.04167, before it can be imported into the chosen modelling program. This is done by simply formatting the Date and Time cells to General. An additional change to the Date also has to be performed in the modelling program in the form of a reference date adjustment. This is due to a difference that exists between the reference dates of the spread sheet and the modelling program. This adjustment is shown in the EPD model algorithm in Addendum A.

The MVA and MW raw data values are the real and apparent furnace operating power values that will be considered as the plant real and apparent load respectively within the system-established boundary of the furnaces and bagplants only. Each furnace has three stacks that are coupled to a single extraction duct per furnace. Currently these ducts carry hot extracted material to the trombone coolers before the material reaches the bagplants for treatment. Since the proposed cogeneration heat recovery system will be considered as a replacement for the current cooling components, the trombone coolers, the material temperatures before and after the coolers will be used as the material temperatures expected to exist before and after the proposed cogeneration system for each furnace. Therefore each furnace 1 to 4 stack temperature (Stack Temp 1 to 3) and each bagplant inlet temperature (Bagplant 1 to 4 Inlet Temp) is required and will be stored in the raw data spread sheet.

The chosen time interval for the raw data storage and utilisation is half-hourly (every 30 minutes). Therefore the load and temperature information that is required and stored is done so every 30 minutes. The system operates as a back-filling system, meaning every 30 minutes the data is averaged for that past half hour and the average value taken to represent that past 30 minute time interval. The EPD model depends on an overall system energy cost function that requires an entire month's data. Therefore the raw data for an entire month is imported with a unique date-time stamp for each input time interval within the month, and is essential for the effective operation of the optimisation model. This stamp is obtained from the Date and Time stored in conjunction with the operation and capacity data. It is important to note from this that all raw data exist and are used by the EPD model in 30 minute time intervals for an entire month. For a 31 day month such as December, this results in 1488 data points for each raw data column or field.

The mathematical modelling and technical computing language MATLAB will be used for the data handling and optimisation model development. Before optimisation can be performed, it is essential to read all required data into useful program information arrays and to develop a model working array. All temperature and power information and raw data is therefore imported from the raw data spread sheet into appropriate information arrays. For the EPD model developed in this research, an information array is generated for each raw data field of the raw data spread sheet. These information arrays, as they are used by the model, are F1MVA, F1MW, F1S1T, F1S2T, F1S3T, B1T, F2MVA, F2MW, F2S1T, F2S2T, F2S3T, B2T, F3MVA, F3MW, F3S1T, F3S2T, F3S3T, B3T, F4MVA, F4MW, F4S1T, F4S2T, F4S3T and B4T. It is required to have a single cogeneration system input temperature, or single furnace outlet temperature, that exists in the single extraction duct per furnace. Therefore the stack temperatures for each furnace are used to calculate an overall per furnace outlet temperature according to equation (3.1). The result from equation (3.1) is an outlet temperature information array for each furnace, F1T, F2T, F3T and F4T.

$$F_xT = \frac{1}{3} \times (F_xS1T + F_xS2T + F_xS3T) \tag{3.1}$$

where:

- F_xT is the extracted material temperature at the input of the heat recovery cogeneration system for furnace x, where x = 1 to 4, and
- F_xS1T, F_xS2T and F_xS3T are the extracted material temperatures at each furnace x stack 1 to 3 respectively, where x = 1 to 4.

Equation (3.1) is obtained through the conservation of heat and arithmetic mean of the heat transfer equation when gas flow from multiple ducts merging into a single duct is considered. This is illustrated in Figure 3.1 and equations (3.2) to (3.8).

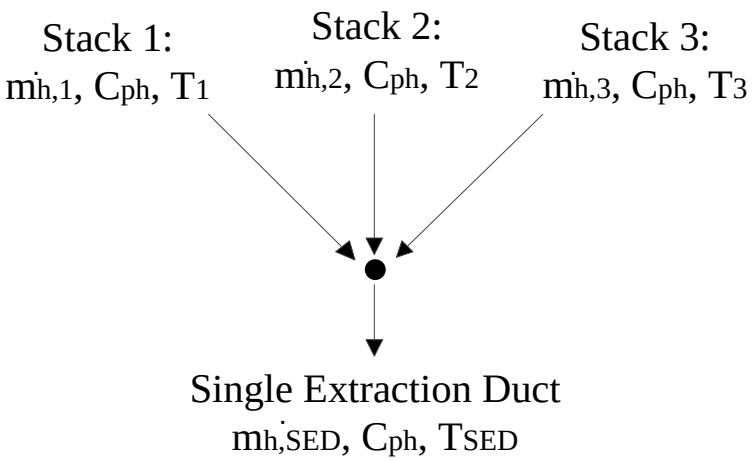

Figure 3.1: Multiple stack to single duct off gas flow

General heat transfer equation:

$$\dot{Q}_h = \dot{m}_h \times C_{ph} \times \Delta T \tag{3.2}$$

where:

- $\dot{Q}_h$ is the heat transfer in kW,
- $\dot{m}_h$ is the mass flow rate of the extracted hot material in kg/s,
- C_{ph} is the specific heat of the extracted hot material in kJ/kg.K, and
- ΔT is the temperature difference in K.

For each stack, equation (3.2) can be used as follows:

$$Stack\ 1\ heat = \dot{Q}_{h,1} = \dot{m}_{h,1} \times C_{ph} \times T_1 \quad (3.3)$$

$$Stack\ 2\ heat = \dot{Q}_{h,2} = \dot{m}_{h,2} \times C_{ph} \times T_2 \quad (3.4)$$

$$Stack\ 3\ heat = \dot{Q}_{h,3} = \dot{m}_{h,3} \times C_{ph} \times T_3 \quad (3.5)$$

For the single extraction duct (SED) into which the three stacks merge, equation (3.2) to (3.5) can be combined to form:

$$\dot{Q}_{h,SED} = \dot{m}_{h,SED} \times C_{ph} \times T_{SED} = \dot{Q}_{h,1} + \dot{Q}_{h,2} + \dot{Q}_{h,3} \quad (3.6)$$

But, $\dot{m}_{h,1} = \dot{m}_{h,2} = \dot{m}_{h,3} = \frac{1}{3} \times \dot{m}_{h,SED}$ (3.7)

$$\therefore \dot{m}_{h,SED} \times T_{SED} = \frac{1}{3} \times \dot{m}_{h,SED} \times T_1 + \frac{1}{3} \times \dot{m}_{h,SED} \times T_2 + \frac{1}{3} \times \dot{m}_{h,SED} \times T_3 \quad (3.8)$$

Eliminating $\dot{m}_{h,SED}$ from equation (3.8) yields the form of equation (3.1).

The EPD model requires a program working array. This working array is dependent on the date-time stamp of each time interval data point imported into the various information arrays and is essential in assisting the model with linking all the calculations and procedures to be performed at each date-time stamp and time interval, to each corresponding data point. In addition to this, the working array is also vital in determining the specific T.O.U period for each data point. This is an essential component of the model cost function. The program working array is comprised of single columned arrays for each data point, arranged as follows:

FWorkArray = [i, j, Y, M, d, h, m, DayNumber, Day],

where:

- FWorkArray is the program working array,

- i = 1 to n, holds the i-th day of the given month where n is the maximum number of days in that given month,
- j = 1 to 48, holds the j-th 30 minute time interval of the day,
- Y holds the year,
- M = 1 to 12, holds the month in the year Y,
- d = 1 to n, holds the day in the month and year, M and Y respectively, and is used in the generation of the i data array,
- h = 0 to 23, holds the hour of the day d,
- m = 0 or 30, holds the minute of the hour h, and only consists of 0 and 30 as the time interval characteristic of the model was chosen as half hourly,
- DayNumber = 1 to 7, holds the day number of the week where 1 is equivalent to Sunday, and
- Day = 1 to 3, holds the day type of the day d, Weekdays, Saturdays and Sundays respectively.

The i and j columns of the working array are the most important columns of the array as it is the values of i and j that ensure the linking of all the calculations and procedures to be performed at each data point time interval, to each corresponding data point. The final requirements of the raw data import and working array development is the setting of the high demand season flag, as well as the generation of the Peak, Standard and Off-Peak flag arrays. The high demand season flag, SHigh, is set to 1 when the current month of the data is a high demand season month. High demand season months are June, July and August, while the remaining months are all low demand season months [37].

The Peak, Standard and Off-Peak flag arrays are arrays consisting of peak, standard and off-peak T.O.U flag values respectively, for each data point. The purpose of these arrays is to indicate when a specific data point time value falls in a peak, standard or off-peak T.O.U period, which is essential for applying the T.O.U consumption and generation energy tariff structures. The Peak, Standard and Off-Peak flag array values are set to 1 when that T.O.U period is to be considered. The consideration of the three T.O.U periods is dependent on

the time of day as well as the type of day, Weekdays, Saturdays or Sundays, and is in accordance with the tariff structure on which the facility is billed [37]. Therefore the working array elements j and Day are used for the generation of these flag arrays.

3.2.2 Process chemical calculations and determination of available heat

In order to obtain the system electrical energy value out from a system thermal energy value in, it is important to consider the chemistry that occurs inside the furnaces, resulting in the production of the off gases that are recovered. The chemistry involves the furnace internal process chemical reactions that generate off gases, the individual constituent gases of the generated off gas and the mass flow rate, temperature and enthalpy values of these off gas constituents. Therefore, to understand what gases are coming out of the furnaces, it is essential to know what raw materials are going in to the smelting process as well as the rate at which these materials are fed. At Glencore Ferrochrome in Rustenburg, a specific recipe of raw materials is fed into the furnaces in batches, at a specific number of batches per day per furnace. Table 3.1 shows the facility raw materials that are fed in to the furnaces and the important constituent percentages of these materials. Table 3.2 shows the specific furnace feed batch recipe. Only the ores and reductants are considered as the fluxes play no part in the chemical reactions resulting in the production of FeCr.

Table 3.1: Furnace feed raw materials

Ores	Feed Type and Bin	% Moisture	% FeO	% Cr_2O_3
ORE CR PEL OUT ME	TSWELOPELE Bin 7	4.6	25.8	40.6
ORE CR PEL OUT ME	TSWELOPELE Bin 10	4.6	25.8	40.6
ORE CR PEL OUT ME	TSWELOPELE Bin 12	4.6	25.8	40.6
ORE CR LUMPY UG	KD LUMPY Bin 1	0.4	23.6	40.3
Reductants	Feed Type and Bin	% Moisture	% FC	
RED COAL PEAS LP	EXXARO Bin 8	3.6	61.1	
RED COKE COBS LP	UKRAINE COKE Bin 2	2.1	85.2	
RED COKE NUT HP	MET COKE Bin 5	10.3	86	
RED CHAR NUT LP	ACM CHAR Bin 4	4.7	73.4	

Table 3.2: Furnace feed batch recipe

Ores	Feed Type and Bin	% Required	Mass Required (kg)
ORE CR PEL OUT ME	TSWELOPELE Bin 7	30	1200
ORE CR PEL OUT ME	TSWELOPELE Bin 10	30	1200
ORE CR PEL OUT ME	TSWELOPELE Bin 12	20	800
ORE CR LUMPY UG	KD LUMPY Bin 1	20	800
	Total Ore Feed Batch size (kg)		4000
Reductants	Feed Type and Bin	% Required	Mass Required (kg)
RED COAL PEAS LP	EXXARO Bin 8	36	501
RED COKE COBS LP	UKRAINE COKE Bin 2	18	177
RED COKE NUT HP	MET COKE Bin 5	10	106
RED CHAR NUT LP	ACM CHAR Bin 4	36	422
	Total Reductant Feed Batch Size (kg)		1205

When it comes to the chemical calculations, only the ore materials are important, as excess carbon is always a large constituent of the process waste slag. Therefore the reduction processes only use as much carbon as is required for complete metal reduction, the value of which is not of importance in the furnace chemical process calculations. The metal ores also constitute some other compounds such as CaO, Al_2O_3 and MgO, however only FeO, Cr_2O_3 and moisture are of concern.

The furnace raw material feed rates are expressed in terms of batches per day. As can be seen in Table B.4 they are:

- Furnace 1: 110 batches per day,
- Furnace 2: 110 batches per day,
- Furnace 3: 110 batches per day, and
- Furnace 4: 160 batches per day.

The raw material make-up, batch recipe and batch feed rate are used in conjunction with the furnace internal process chemical reactions to calculate the amount of available heat that is extracted and recovered from each furnace by the potential cogeneration system.

This is shown in equations (3.9) to (3.40). The calculations are performed for each furnace separately and for each 30 minute time interval in the given month. The calculation temperatures that are required are taken as the furnace outlet and bagplant inlet temperatures that are obtained from the raw data spread sheet, and which are imported into MATLAB as discussed in section 3.2.1. Tables of results for the time independent calculations performed for each furnace are shown in Addendum B. Addendum B also shows the additional time-independent constants that are required for the overall chemical reaction and heat calculations.

The off gas constituent and heat calculations begin with the calculation of the actual percentage FeO and Cr_2O_3 in the different raw material feed ores. This is done due to the fact that the current constituent percentages are obtained on a dry sample of ore, whereas a sample with the specified moisture content is what is actually fed into the furnaces. The actual percentages of FeO and Cr_2O_3 per ore sample per feed bin are obtained via equations (3.9) to (3.13), which apply to the various ore types. The results of these equations are shown in Table B.1.

$$TM_s = \frac{\%TM_s}{100} \times m_s \tag{3.9}$$

$$AMFeO_s = \frac{\%FeO_s}{100} \times (m_s - TM_s) \tag{3.10}$$

$$\%AFeO_s = \frac{AMFeO_s}{m_s} \times 100 \tag{3.11}$$

$$AMCr_2O_{3_s} = \frac{\%Cr_2O_{3_s}}{100} \times (m_s - TM_s) \tag{3.12}$$

$$\%ACr_2O_{3_s} = \frac{AMCr_2O_{3_s}}{m_s} \times 100 \tag{3.13}$$

where:

- TM_s is the total moisture in the ore sample in kg,
- $\%TM_s$ is the percentage total moisture in the ore sample,
- m_s is the ore sample mass required in the feed, in kg,

- $AMFeO_s$ and $AMCr_2O_{3_s}$ are the actual mass of FeO and Cr_2O_3 in kg, in the ore sample required mass, and
- $\%AFeO_s$ and $\%ACr_2O_{3_s}$ are the actual %FeO and $\%Cr_2O_3$ in the ore sample required mass.

Using the actual percentages of FeO and Cr_2O_3, the total percentage of FeO and Cr_2O_3 can be obtained for an entire batch by utilising the batch recipe ore sample constituents. This is shown in equations (3.14) and (3.15). Results of these equations are shown in Table B.1.

$$\%TFeO = \frac{\left(\frac{\%AFeO_{Bin7}}{100}\times m_{Bin\ 7}+\frac{\%AFeO_{Bin10}}{100}\times m_{Bin\ 10}+\frac{\%AFeO_{Bin12}}{100}\times m_{Bin\ 12}+\frac{\%AFeO_{Bin1}}{100}\times m_{Bin\ 1}\right)}{BS}\times 100 \quad (3.14)$$

$$\%TCr_2O_3 = \frac{\left(\frac{\%ACr_2O_{3\,Bin7}}{100}\times m_{Bin\ 7}+\frac{\%ACr_2O_{3\,Bin10}}{100}\times m_{Bin\ 10}+\frac{\%ACr_2O_{3\,Bin12}}{100}\times m_{Bin\ 12}+\frac{\%ACr_2O_{3\,Bin1}}{100}\times m_{Bin\ 1}\right)}{BS}\times 100 \quad (3.15)$$

where:

- $\%TFeO$ and $\%TCr_2O_3$ are the total %FeO and $\%Cr_2O_3$ in the feed batch,
- $\%AFeO_{Bin7}$, $\%AFeO_{Bin10}$, $\%AFeO_{Bin12}$ and $\%AFeO_{Bin1}$ are the actual %FeO in the ore sample required mass from Bin 7, Bin 10, Bin 12 and Bin 1 respectively,
- $\%ACr_2O_{3_{Bin7}}$, $\%ACr_2O_{3_{Bin10}}$, $\%ACr_2O_{3_{Bin12}}$ and $\%ACr_2O_{3_{Bin1}}$ are the actual $\%Cr_2O_3$ in the ore sample required mass from Bin 7, Bin 10, Bin 12 and Bin 1 respectively,
- $m_{Bin\ 7}$, $m_{Bin\ 10}$, $m_{Bin\ 12}$ and $m_{Bin\ 1}$ are the ore sample masses required in the feed, in kg, from Bin 7, Bin 10, Bin 12 and Bin 1 respectively, and
- BS is the overall feed batch size in kg.

The furnace internal chemical reaction equations are then used to calculate how much CO gas is produced from the smelting process. This is done by considering the $\%TFeO$ and $\%TCr_2O_3$ in a single feed batch, the molecular weight of the compounds as well as a constant mass ratio of the compounds in the two chemical equations and the conservation

of mass that applies to the chemical reaction processes. As shown in Table B.1, the actual mass of FeO and Cr_2O_3 per single batch feed is calculated as 975.67 kg and 1 560.55 kg respectively. Equations (3.16) and (3.17) show the forms of the mass ratios for both reactions which remain constant for all the compounds in that reaction, and how these mass ratios are used to calculate the mass of another compound in the chemical equation, for example CO gas. Equations (3.18) and (3.19) show the overall reduction chemical reactions with the actual compound masses and molecular weights, the most important of which is the overall mass of produced CO gas from the two reduction chemical reactions that occur in the furnaces during the smelting processes. The results of these equations are shown in Table B.2.

$$MR_{Fe\ reaction} = \frac{AM\,(FeO)}{MW(FeO)} = \frac{AM\,(C)}{MW(C)} = \frac{AM\,(Fe)}{MW(Fe)} = \frac{AM\,(CO)}{MW\,(CO)} \tag{3.16}$$

$$MR_{Cr\ reaction} = \frac{AM(Cr_2O_3)}{MW(Cr_2O_3)} = \frac{AM(3C)}{MW(3C)} = \frac{AM\,(2Cr)}{MW(2Cr)} = \frac{AM\,(3CO)}{MW\,(3CO)} \tag{3.17}$$

where:

- $MR_{Fe\ reaction}$ and $MR_{Cr\ reaction}$ are the mass ratios for the FeO and Cr_2O_3 reduction reaction respectively,
- AM is the actual mass of the bracketed compound in kg, and
- MW is the molecular weight of the bracketed compound.

$$\begin{array}{lccccccc} Actual\ Mass\,(kg) & & 975.67 & & 162.61 & & 758.85 & 379.43 \\ Reduction\ Reaction & : & FeO & + & C & = & Fe & + & 3CO \\ Molecular\ Weight & & 72 & & 12 & & 56 & & 28 \end{array} \tag{3.18}$$

$$\begin{array}{lccccccc} Actual\ Mass\,(kg) & & 1560.55 & & 369.60 & & 1067.74 & 862.41 \\ Reduction\ Reaction & : & Cr_2O_3 & + & 3C & = & 2Cr & + & 3CO \\ Molecular\ Weight & & 152 & & 36 & & 104 & & 84 \end{array} \tag{3.19}$$

Due to the Glencore Ferrochrome furnaces in Rustenburg being open furnaces and the fact that these furnaces operate at temperatures well above the autoignition temperature of CO gas, CO gas will react with the oxygen in the surrounding air to produce carbon dioxide

gas (CO_2). The same mass ratio and chemical reaction calculation forms as above can be used to calculate the combined overall amount of CO_2 gas that is produced from the two reduction chemical reactions. Equation (3.20) shows the combined produced CO gas whereas the mass ratio and chemical reactions that occur in order to produce CO_2 gas are shown in equations (3.21) and (3.22). The results of these equations are shown in Table B.2.

$$AM(CO) = AM(CO)_{Fe\,reaction} + AM(CO)_{Cr\,reaction}$$
$$= 379.43 + 862.41 = 1241.83\ kg \tag{3.20}$$

$$MR_{CO\,reaction} = \frac{AM(CO)}{MW(CO)} = \frac{AM(O_2)}{MW(O_2)} = \frac{AM(2CO_2)}{MW(2CO_2)} \tag{3.21}$$

where:

- $MR_{CO\ reaction}$ is the mass ratio for CO reaction.

$$\begin{array}{lccccc} Actual\ Mass\ (kg) & & 1241.83 & & 709.62 & 1951.45 \\ Reduction\ Reaction & : & 2CO & + & O_2 & = & 2CO_2 \\ Molecular\ Weight & & 56 & & 32 & & 88 \end{array} \tag{3.22}$$

The next step for calculating the overall available heat for each furnace is to calculate the off gas constituent masses for a single batch reaction. For an open furnace, the CO gas from the two metal reduction reactions autoignites with surrounding air to produce CO_2 gas. The open furnace characteristic therefore allows for air to be in the furnaces. The main constituents of the overall extracted off gas are therefore CO_2 gas and air. A certain amount of air is required to produce CO_2 gas from CO gas, as oxygen is needed in the CO – CO_2 reaction. The extraction of air however, is controlled via large induced draft (ID) extraction fans for each furnace that extract a fixed volume of off gas no matter how much CO_2 gas is produced. Therefore excess air will also be present in the extracted off gas. The three constituents of the off gas which will therefore be considered are CO_2 gas, air that holds the required oxygen for the CO – CO_2 reaction, and excess extracted air.

The excess air depends firmly on the air extraction capabilities of the ID extraction fans. For now though, the amount of air that is required for the CO – CO_2 reaction per batch can be calculated. Assuming an air composition of 77% N_2 (nitrogen) and 23% O_2 (oxygen), the amount of air, nitrogen and oxygen that is required is calculated via equations (3.23) and (3.24). From equation (3.22), an amount of 709.62 kg of O_2 is required to combust the total CO (2CO) to total CO_2 ($2CO_2$). Therefore:

$$\frac{23\%}{100} \times TM_{air} = TM_{O_2} = 709.62\ kg, \quad \therefore\ TM_{air} = \frac{709.58}{0.23} = 3085.30\ kg\ air \tag{3.23}$$

$$\therefore \frac{77\%}{100} \times TM_{air} = TM_{N_2} = 2375.68\ kg\ N_2 \tag{3.24}$$

where:

- TM_{air}, TM_{O_2} and TM_{N_2} are the total mass of air, oxygen and nitrogen respectively per batch reaction.

The results of these equations are shown in Table B.3.

Next, a volumetric and mass flow rate per off gas constituent can be calculated. This is done according to the following gas law assumption, the constants of which are obtained from Table B.4:

$$1\ mol\ of\ gas\ occupies\ 22.414\ l = 22.414\ m^3\ @\ STP,$$
$$where\ STP = 1\ atm\ and\ 273.15\ K$$

The remainder of the calculations that are to be performed are time dependant calculations that require the results from the time independent calculations, additional time independent constants as shown in Table B.4, as well as the time dependant furnace and bagplant operating temperatures. Equations (3.25) to (3.27) utilise the gas law assumption in order to calculate the volumetric gas flow rate of each off gas constituent per furnace. The flow rates require a raw material feed rate, which in this case is the batches fed per day.

$$\dot{V_{CO_2}} = \frac{TM_{CO_2}}{MW(CO_2)} \times \frac{F_{BR}}{24} \times 22.414\ m^3 \times \frac{T+237.15\ K}{273.15\ K} \quad (3.25)$$

$$\dot{V_{O_2}} = \frac{TM_{O_2}}{MW(O_2)} \times \frac{F_{BR}}{24} \times 22.414\ m^3 \times \frac{T+237.15\ K}{273.15\ K} \quad (3.26)$$

$$\dot{V_{N_2}} = \frac{TM_{N_2}}{MW(N_2)} \times \frac{F_{BR}}{24} \times 22.414\ m^3 \times \frac{T+237.15\ K}{273.15\ K} \quad (3.27)$$

where:

- $\dot{V_{CO_2}}$, $\dot{V_{O_2}}$ and $\dot{V_{N_2}}$ are the volumetric flow rates in m^3/h of CO_2, O_2 and N_2 respectively,
- MW is the molecular weight of the bracketed compound,
- F_{BR} is the furnace batch feed rate in batches per day, and
- T is the temperature the off gas is extracted at, in ^oC.

The off gas temperature T is taken as the furnace combined stack outlet, and therefore furnace outlet temperature in ^oC, just before the proposed heat recovery cogeneration system, as is calculated via equation (3.1). The next step is to determine how much excess air is extracted with the currently considered off gases. As previously mentioned the excess air depends on the volumetric air extraction capabilities of the ID fans. They are:

- Furnace 1 ID fan: 106 900.8 m^3/h,
- Furnace 2 ID fan: 106 900.8 m^3/h,
- Furnace 3 ID fan: 106 900.8 m^3/h, and
- Furnace 4 ID fan: 155 492 m^3/h.

The batch feed rate and ID fan volumetric air extraction capabilities are directly proportional to each other, and remain in a constant ratio for all four furnaces. Due to a higher batch feed rate and a larger furnace ID extraction fan for furnace 4, the volumetric air extraction capability of furnace 4 will also be higher. Equation (3.28) shows this proportionality.

$$\frac{F_{1-3,BR}}{F_{4,BR}} = \frac{\dot{V_{1-3,off\ gas}}}{\dot{V_{4,off\ gas}}} \quad (3.28)$$

where:

- $F_{1\text{-}3,BR}$ and $F_{4,BR}$ are the furnace raw material batch feed rates in batches per day for furnace 1-3 and furnace 4 respectively, and
- $\dot{V}_{1-3,off\ gas}$ and $\dot{V}_{4,off\ gas}$ are the off gas volumetric flow rates in m^3/h for furnace 1-3 and furnace 4 respectively.

The excess amounts of air can therefore be calculated by subtracting the sum of the furnace extracted constituents already considered from the overall total ID fan extraction volumetric flow per furnace. Utilising the 77% N_2 (nitrogen) and 23% O_2 (oxygen) air composition, the excess N_2 and O_2 can also be calculated. Finally, adding the excess N_2 and O_2 to the off gas N_2 and O_2 already considered for the CO – CO_2 reaction, a final amount of N_2 and O_2 per furnace can be obtained. The excess air plays no additional role to the amount of CO_2 already considered and therefore this CO_2 is also the overall amount of extracted CO_2 per furnace. Equations (3.29) to (3.34) show how the excess and total amounts of all off gas constituents per batch reaction are calculated.

$$\dot{Exc}_{air} = \dot{V}_{off\ gas} - \dot{V}_{CO_2} - \dot{V}_{O_2} - \dot{V}_{N_2} \tag{3.29}$$

$$\dot{Exc}_{O_2} = \frac{23\%}{100} \times \dot{Exc}_{air} \tag{3.30}$$

$$\dot{Exc}_{N_2} = \frac{77\%}{100} \times \dot{Exc}_{air} \tag{3.31}$$

$$\dot{TV}_{CO_2} = \dot{V}_{CO_2} \tag{3.32}$$

$$\dot{TV}_{O_2} = \dot{Exc}_{O_2} + \dot{V}_{O_2} \tag{3.33}$$

$$\dot{TV}_{N_2} = \dot{Exc}_{N_2} + \dot{V}_{N_2} \tag{3.34}$$

where:

- $\dot{Exc}_{air}$, $\dot{Exc}_{O_2}$ and $\dot{Exc}_{N_2}$ are the volumetric excess amounts of extracted air, O_2 and N_2 in m^3/h respectively, and
- $\dot{TV}_{CO_2}$, $\dot{TV}_{O_2}$ and $\dot{TV}_{N_2}$ are the total volumetric amounts of extracted off gas constituents CO_2, O_2 and N_2 in m^3/h respectively.

In order to apply the heat equation as in equation (3.2) an off gas material mass flow rate is required, in kg/s. The total volumetric amount of each extracted off gas constituent is therefore used next to calculate the mass flow rate of these constituents per single batch and process reaction, per furnace. This is shown in equations (3.35) to (3.37).

$$\dot{m_{CO_2}} = \frac{\dot{TV_{CO_2}} \times MW(CO_2) \times \frac{273.15\ K}{T+273.15\ K}}{22.414\ m^3} \times \frac{1\ h}{3600\ s} \quad (3.35)$$

$$\dot{m_{O_2}} = \frac{\dot{TV_{O_2}} \times MW(O_2) \times \frac{273.15\ K}{T+273.15\ K}}{22.414\ m^3} \times \frac{1\ h}{3600\ s} \quad (3.36)$$

$$\dot{m_{N_2}} = \frac{\dot{TV_{N_2}} \times MW(N_2) \times \frac{273.15\ K}{T+273.15\ K}}{22.414\ m^3} \times \frac{1\ h}{3600\ s} \quad (3.37)$$

where:

- $\dot{m_{CO_2}}$, $\dot{m_{O_2}}$ and $\dot{m_{N_2}}$ are the off gas constituent mass flow rates in kg/s of CO_2, O_2 and N_2 respectively.

The final step in calculating the overall available heat is the utilisation of the heat equation. Equation (3.2) is used to calculate the available heat in kW by using the specific heat of the gas multiplied by the mass flow rate multiplied by the change in temperature. For simplicity purposes, the specific heat multiplied by the change in temperature can be expressed as a difference in enthalpy at the considered temperatures. This is shown in equation (3.38).

$$\dot{Q_h} = \dot{m_h} \times C_{ph} \times \Delta T = \dot{m_h} \times C_{ph} \times (T_{hot} - T_{cold}) = \dot{m_h} \times \left(H_{T_{hot}} - H_{T_{cold}}\right) \quad (3.38)$$

where:

- $\dot{Q_h}$ is the heat transfer in kW for a considered off gas constituent,
- $\dot{m_h}$ is the mass flow rate of the considered extracted hot off gas constituent in kg/s,
- T_{hot} and T_{cold} are the temperatures of the extracted off gas constituent before and after the heat recovery component of the proposed cogeneration system respectively, in ^{o} C or K, and

- $H_{T_{hot}}$ and $H_{T_{cold}}$ are the enthalpy values of the off gas constituent in kJ/K or kJ/^{o}C, at T_{hot} and T_{cold} respectively.

Equation (3.38) and the mass flow rates of $\dot{m_{CO_2}}$, $\dot{m_{O_2}}$ and $\dot{m_{N_2}}$ are therefore used for the available heat calculations. The enthalpy values are obtained from the off gas constituent thermodynamic and enthalpy tables, the three of which are shown in Table 3.3.

Table 3.3: Thermodynamic enthalpy table for off gas constituents

CO2		N2		O2	
T (° C)	H @ T (kJ/mol)	T (° C)	H @ T (kJ/mol)	T (° C)	H @ T (kJ/mol)
25	0	25	0	25	0
100	2.963	100	2.197	100	2.239
200	7.276	200	5.164	200	5.317
300	11.848	300	8.174	300	8.47
400	16.604	400	11.227	400	11.683
500	21.508	500	14.322	500	14.949
600	26.539	600	17.46	600	18.264
700	31.687	700	20.64	700	21.627
800	36.944	800	23.863	800	25.034
900	42.305	900	27.129	900	28.487
1000	47.768	1000	30.438	1000	31.983

In order for the EPD model to determine the overall available heat, an interpolation function is required with the purpose of utilising the enthalpy tables shown in Table 3.3. The interpolation function has the enthalpy tables in Table 3.3 loaded as lookup tables, and upon receiving a certain off gas constituent furnace outlet or bagplant inlet temperature, the function looks in the appropriate constituent table and performs a linear interpolation within the table temperature range that holds the received temperature. The interpolation function, Find_Enthalpy, is therefore used to determine the enthalpy value for every single model data point off gas constituent at every single constituent furnace outlet temperature and bagplant inlet temperature, for all four furnaces, and to generate enthalpy information arrays for all off gas constituents at all required temperatures. The Find_Enthalpy function is shown in Addendum A.

The generated enthalpy value information arrays are ECF1, ENF1, EOF1, ECB1, ENB1, EOB1, ECF2, ENF2, EOF2, ECB2, ENB2, EOB2, ECF3, ENF3, EOF3, ECB3, ENB3, EOB3, ECF4, ENF4, EOF4, ECB4, ENB4 and EOB4. ECF, ENF and EOF information arrays hold the enthalpy values of the off gas constituents CO_2, N_2 and O_2 respectively, at the considered furnace outlet temperatures, just before the heat recovery component of the cogeneration system. ECB, ENB and EOB information arrays hold the enthalpy values of the off gas constituents CO_2, N_2 and O_2 respectively, at the considered bagplant inlet temperatures, just after the heat recovery component of the cogeneration system.

All chemical calculations and calculated variables such as the mass flow rates of the off gas constituents for each furnace, are also stored in appropriate information arrays. The i and j columns of the model working array are used to ensure that all calculations and calculated variables are performed and stored in information arrays at the appropriate specific time interval or data point. With the off gas constituent mass flow rate and enthalpy value information arrays generated for all furnaces at all time instances within the given month, an available heat at each time instance can be calculated using equation (3.38), and an available heat information array for each furnace can be generated.

The overall system available heat in MW can then be calculated. However, due to certain facility and power generation system operational aspects, two vital assumptions or limitations have to be made before an overall available heat value can be calculated. These aspects include the furnaces being off at certain time intervals for maintenance, a minimum temperature of operation that will allow for the recovery of heat via the ORC cogeneration system, and the potential for faults in the temperature sensors at the outlet of the furnaces and inlet of the bagplants. Therefore the assumptions or limitations which apply to each furnace individually are:

- If the combined single duct hot extracted material temperature is below 200 ^{o}C, the actual furnace itself, i.e. the furnace electrodes and the smelting processes that occur inside the furnace, is assumed to be off, and it is highly likely that there will be insufficient thermal energy from the furnace extracted off gas to be recovered and

utilised by the heat recovery cogeneration system. Therefore the overall heat recovery cogeneration system will not consider this specific furnace during this time interval.

- If the measured bagplant inlet temperature is higher than the measured furnace outlet temperature, the heat recovery process cannot occur, and the overall heat recovery cogeneration system will once again not consider this specific furnace during this time interval.

The furnace output temperature minimum of 200 ^{o}C is a limitation that exists due to the actual power generation cycle and components. The furnace output temperature limitation determines when useable furnace process off gas temperatures are produced, and therefore only during these time intervals will heat recovery and power generation be able to take place. This limitation will be further discussed in Section 3.2.3. Other instances were noticed from the raw data where the measured bagplant inlet temperature was found to be greater than the measured furnace outlet temperature for certain time intervals. During all of these intervals, cogeneration will not take place for that specific furnace, and the overall available heat will only account for extracted off gases from the other furnaces with sufficient process off gas temperatures.

The control of when individual furnace off gases will be used or considered for the overall cogeneration process and when they won't is achieved through the variable control of the ID extraction fans. If any of the aforementioned limitations occur, the ID fan for the specific limited furnace will be turned off during the limitation time interval, and off gas extraction will not occur for that furnace. This is appropriate as the limited furnace smelting processes and loads are not operational during these time intervals and therefore off gas extraction is not required. Another advantage of this is that cold extracted off gases, almost entirely normal air if the furnaces are off, will not be allowed to come into contact with and cool hot extracted off gases from other furnaces that are operational during that specific limitation time interval.

With the aforementioned considerations in mind, the overall furnace load contribution of the ID fans and the overall extracted and recovered heat available for cogeneration for each time interval can be calculated using equations (3.39) and (3.40) respectively.

$$FL_{ID\ fans} = F1L_{ID\ fan} + F2L_{ID\ fan} + F3L_{ID\ fan} + F4L_{ID\ fan} \quad (3.39)$$

$$\dot{Q_{h,total}} = \dot{Q_{h,F1}} + \dot{Q_{h,F2}} + \dot{Q_{h,F3}} + \dot{Q_{h,F4}} \quad (3.40)$$

where:

- $FL_{ID\ fans}$ is the furnace load contribution due to the operation of each furnace ID fan in MW,
- $F1L_{ID\ fan}$, $F2L_{ID\ fan}$, $F3L_{ID\ fan}$ and $F4L_{ID\ fan}$ are the furnace load contributions for furnace 1 to 4 as a result of the operation of ID fans 1 to 4 in MW respectively,
- $\dot{Q_{h,total}}$ is the overall system extracted and recovered heat in MW that is available to the cogeneration system for electrical energy generation, and
- $\dot{Q_{h,F1}}$, $\dot{Q_{h,F2}}$, $\dot{Q_{h,F3}}$ and $\dot{Q_{h,F4}}$ are the extracted and recovered heats in MW from furnace 1 to 4 respectively, with the furnace operation limitations as discussed above taken into consideration.

It is important to note that all the calculations performed are done so at every single time interval or data point in the given month. Therefore each 30 minute time interval will require all calculations and the determination of a system overall available heat in MW that will be used by the cogeneration system for electrical energy generation. In order for all the calculations to be performed, time-independent information and constants are loaded into the EPD model in a time-independent information function, Time_Indep_Info. This can be seen in Addendum A.

3.2.3 Potential electrical and cooling energy cogeneration output from extracted and recovered thermal energy

In order to obtain an electrical energy output from the calculated recovered and available thermal energy input, technical information and an understanding of a potential heat

recovery and power generation system that could be implemented at the chosen facility, Glencore Ferrochrome in Rustenburg, needs to be obtained. Upon contact and consultation, this information was acquired from Turboden s.r.l

Turboden s.r.l, based in Italy, is a leading company in the production and development of ORC heat recovery and turbo generator solutions, with approximately 289 plants in 32 countries around the world, generating a staggering 397.32 MW of additional electrical power from numerous industrial waste energy sources [38]. Turboden s.r.l also specialises in the utilisation of thermal oil as a heat transfer medium which is essential in the intermediate extraction and transfer of heat from various heat sources such as industrial process off gases, when a direct exchange of heat is not possible. The company designs and builds ORC heat recovery and power generation units suited to various applications depending on the waste energy source. These applications include biomass cogeneration, waste heat recovery, geothermal cogeneration and solar thermodynamic applications [22], [38]. In the case of this research, a waste heat recovery application will be used.

Therefore, an evaluation of the recovery of heat from FeCr smelting furnaces, more specifically the four furnaces at Glencore Ferrochrome in Rustenburg, to generate additional electrical power, was required. This evaluation was performed by Turboden s.r.l utilising site specific and customer defined data and descriptions pertaining to the available energy source. The data and descriptions were obtained directly from the facility, as used for the research-resulting EPD model, and are shown in Table 3.4. A few assumptions also had to be made by the evaluation team at Turboden s.r.l, the results of which are also shown in Table 3.4.

Table 3.4: Customer supplied and assumed system data descriptions

Data Description	Source	Data Value	Unit
Thermal energy source	Customer	Smelting furnace off gases	-
Number of furnaces	Customer	4	-
Total exhaust gas flow rate	Customer	73.5	kg/s
Average exhaust gas temperature	Customer	413	°C
Minimum exhaust gas temperature	Customer	200	°C
Average air temperature (dry bulb)	Assumed	23	°C
Average cooling water temperature (tower water)	Assumed	30	°C
Grid voltage connection for unit	Assumed	Medium voltage	-

The system evaluation utilising the data and descriptions as in Table 3.4 resulted in two potential solutions, i.e. a direct exchange and an indirect exchange solution. The direct exchange solution allows for the direct exchange of heat between the furnace fumes or waste heat and the ORC working fluid by means of a dedicated heat exchanger component. The indirect exchange solution performs an indirect heat exchange between the furnace fumes or waste heat and the ORC working fluid through the utilisation of an intermediate heat exchanger system. The heat from the primary heat source is transferred to a thermal oil via the intermediate heat exchanger system and this heat is transferred to the ORC working fluid via the main power generation heat exchanger component. The working fluid that was selected by Turboden s.r.l that would be the most appropriate for this application was Hexamethyldisiloxane.

The direct exchange solution allows for a higher system thermodynamic efficiency as well as a reduced investment and implementation cost due to fewer required system components (there is no intermediate heat exchanger system). However, the direct exchange solution can only be used for fumes that do not possess erosion capabilities, i.e. non-dusty fumes. In the case of this research, the off gases extracted from the furnaces possess an ash content of approximately 4.32 g/m^3, as dust particles thrown up from the feed of raw materials are also extracted with the process off gases. Even though the dust volume and mass is

negligible in relation to the overall extracted off gas volume and mass, the existence of dust particles does bring about erosion problems. Therefore for the purpose of this research, an indirect heat exchange solution will be most appropriate. The indirect exchange ORC heat recovery cogeneration system diagram is shown in Figure 3.2.

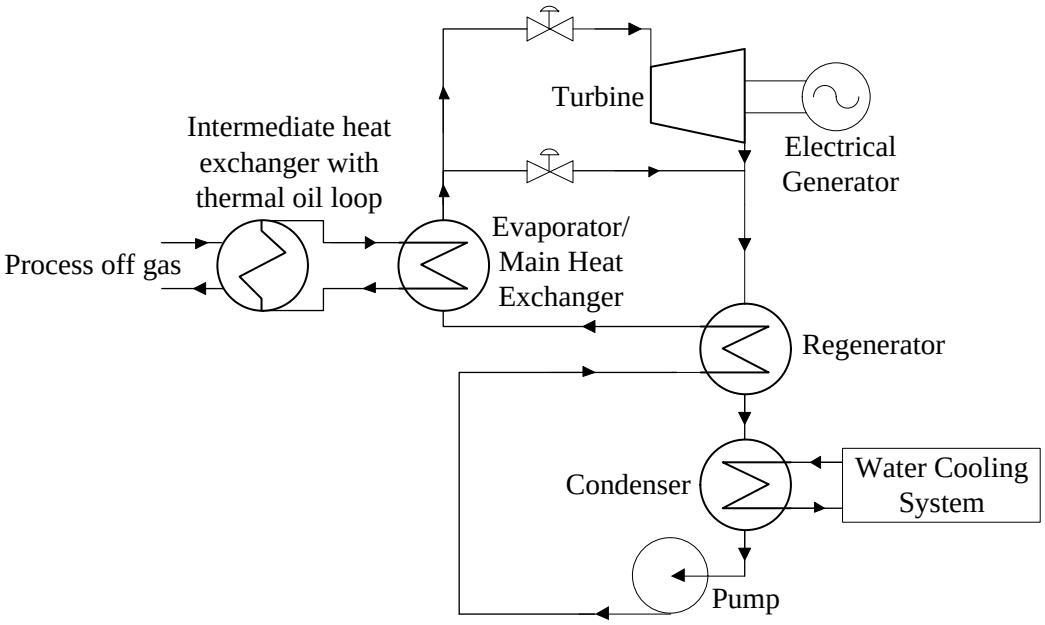

Figure 3.2: Turboden s.r.l indirect exchange ORC heat recovery cogeneration system

In Figure 3.2, the thermal energy is transferred from the furnace off gases to the power generation ORC working fluid via the intermediate heat exchanger system which utilises thermal oil as the heat transfer medium. In transferring this heat to the ORC working fluid in the main heat exchanger or evaporator, the working fluid is vaporised and the fluid vapour expanded through the turbine which drives an electric generator. The ORC working fluid then leaves the turbine, still in the vaporous phase, and passes through the regenerator component. Then, the working fluid is condensed utilising the condenser and water cooling sub-systems. Finally, the working fluid is brought back to the required pressure by means of the flow control pressurising pump, pre-heated by means of an internal heat exchanger bringing heat from the regenerator, and passed back to the main heat exchanger or evaporator where the cycle begins once more.

Therefore, the power generation cycle in Figure 3.2 produces electricity and low temperature heat through the closed thermodynamic cycle that enforces the working fluid changes as defined by the working fluid's characteristic ORC. Traditionally, the low temperature heat is dissipated into the atmosphere via the cooling sub-systems, however the utilisation of the absorption refrigeration cycle allows for the use of this low grade heat for numerous cooling and refrigeration applications, thereby further improving the overall system efficiency.

From the evaluation performed by Turboden s.r.l utilising the data and descriptions as shown in Table 3.4, a resulting proposed system was obtained. The system characteristics and performance calculations as determined by Turboden s.r.l are shown in Table 3.5.

Table 3.5: Turboden s.r.l system characteristics and performance calculations

Data Description	Source	Data Value	Unit
Heat source calculations			
Output temperature from exchanger	Turboden	200	°C
Exhaust gas average specific heat capacity	Turboden	1.1	kJ/kg.K
Heat losses from heat exchanger	Turboden	2	%
Net available thermal power	Calculated	17060	kW
ORC power generation unit			
ORC unit type	Turboden	TD40	-
Heat exchange configuration	Turboden	Indirect exchange	-
ORC gross power output at generator terminals	Calculated	4130	kW
ORC captive power consumption	Calculated	195	kW
ORC net output power	Calculated	3935	kW
Thermal power to cooling source	Calculated	12700	kW
Electrical generator			
Generator type	Turboden	Asynchronous	-
Generator frequency	Turboden	50	Hz
Generator voltage	Turboden	Medium voltage	-
Cooling sub-system (if required)			
Cooling type (ORC condenser)	Turboden	Dry WCC	-
Cooling system internal consumption	Calculated	180	kW

From Table 3.5, the Turboden TD40 ORC unit provides a gross and net electrical efficiency as calculated using equations (3.41) and (3.42) respectively.

$$Gross\ electrical\ efficiency\ (\%) =$$

$$\eta_{ge} = \frac{Gross\ electrical\ output\ power\ (MW)}{Net\ available\ thermal\ power\ (MW)} \times 100 = \frac{4130}{17060} \times 100 = 24.21\% \quad (3.41)$$

$$Net\ electrical\ efficiency\ (\%) =$$

$$\eta_{ne} = \frac{Net\ electrical\ output\ power\ (MW)}{Net\ available\ thermal\ power\ (MW)} \times 100 = \frac{4130-195}{17060} \times 100 = \frac{3935}{17060} \times 100 = 23.07\% \quad (3.42)$$

Therefore, approximately 23% of the thermal power available at each data point will be converted into and utilised as the amount of cogeneration generated electrical power $\dot{W}_{t,j}^{T}$ at that data point. In addition to this, the remaining low temperature thermal power, which would traditionally be sent to the cooling sub-system, is available for utilisation by the facility for cooling and refrigeration purposes, the capacity of which is determined by the absorption refrigeration cycle. The amount of low temperature thermal power available at each data point, 12.7 MW in the system design case shown in Table 3.5, can be calculated using equation (3.43).

$$Net\ available\ low\ temperature\ thermal\ power\ (MW) =$$

$$\dot{QMW}_{low} = \frac{100\% - \eta_{ne} - 2\%}{100\%} \times Net\ available\ thermal\ power\ (MW) \quad (3.43)$$

The low temperature thermal power as calculated in equation (3.43) is in the form of hot water. This is because it is the water in the cooling sub-system that picks up this low grade heat from the power generation cycle circuit via the condenser component. For the suitable operation of an absorption refrigeration cycle, the cooling system fuel or supply heat must be in the form of hot water at temperatures around 92 ^{o}C, steam at pressures of approximately 1 bar, or exhaust flue gases at temperatures above 300 ^{o}C. Since the low grade heat is transmitted to water via the condenser unit, the most appropriate fuel for the purpose of this research will be hot water.

Although the proposed power generation system usually operates with condenser design inlet and outlet cooling water temperatures of 23 ^{o}C and 30 ^{o}C respectively, these design values can be altered with a relatively small reduction in the power generation cycle net electrical efficiency, about a 2% reduction in order to obtain a condenser cooling water outlet of approximately 90 ^{o}C. Therefore, for the purpose of this research, it will be assumed that the cooling water exiting the condenser component of the power generation system will be an acceptable fuel source as required by the absorption refrigeration system, hot water at approximately 92 ^{o}C, and a resulting net electrical efficiency decrease of 2% will be obtained.

The two most common absorption refrigeration cycles are ammonia-water solution and lithium bromide-water solution based cycles. Ammonia is an extremely toxic substance and systems incorporating this compound are required to be designed with significantly increased safety measures and precautions as opposed to lithium bromide based absorption refrigeration systems. Therefore, upon further consultation with Voltas Technologies, a leading engineering firm in the supply and development of mostly cooling based sustainable energy solutions, a lithium bromide-water solution absorption refrigeration cycle was chosen for theoretical system incorporation. The proposed system is shown in Figure 3.3.

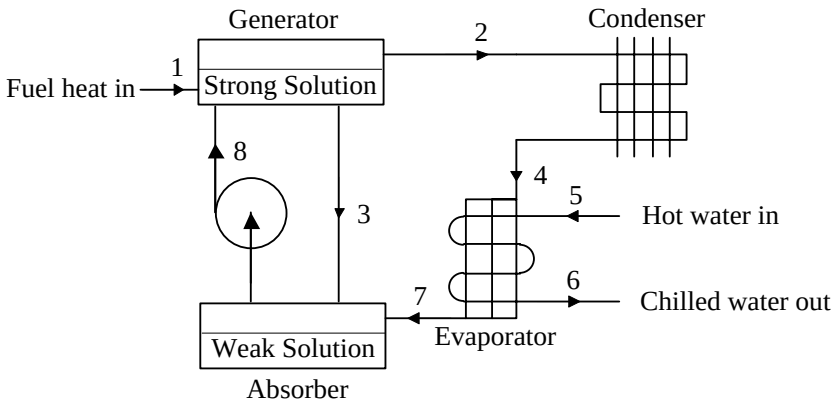

Figure 3.3: System incorporated lithium bromide-water solution absorption refrigeration cycle

The system operation begins with the heat input to the absorption refrigeration cycle at 1. The heat is obtained from the system supplied fuel which is hot water from the power

generation condenser component. The heat is supplied to the generator component of the cycle, which holds a pressurised strong lithium bromide-water solution. The heat supplied to the generator raises the temperature of the solution to a point where the water in the strong solution is vaporised and exits the generator at 2. The heating of the solution causes the lithium bromide in the solution to percolate out of the generator at 3, and drip into the absorber at a reduced pressure where it will once again absorb the water at a later stage in the cycle. Therefore the absorber holds a weak lithium bromide-water solution.

The vaporised water enters the condenser component of the cycle, from 2, and heat is extracted from the vapour by means of cooling fins or cooling water. The vapour therefore condenses to form liquid water, which then progresses to the evaporator via 4. Lithium bromide has a high affinity to water vapour and therefore absorbs water strongly in the vaporous state. This quality forces a vigorous evaporation of the liquid water in the evaporator and the vapour exits the evaporator at 7 and is absorbed by the weak lithium bromide-water solution in the absorber. The vigorous evaporation of water brings about an extreme cooling effect as heat is strongly absorbed from hot water entering the evaporator at 5, thereby producing chilled water, at about 5 ^{o}C, which exits the evaporator at 6, and can be used for numerous cooling requirements. The now strong lithium bromide-water solution is then pumped back to the generator via 8, where the cycle begins once more.

The performance of any cooling system is evaluated in terms of a coefficient of performance (COP), which can be described as the ratio of the output cooling power, chilled water at 5 ^{o}C, to the supplied input thermal power, hot water at 92 ^{o}C. The COP of a single-effect chiller, the representation of which is shown in Figure 3.3, as obtained from Voltas Technologies, is 0.7. Therefore equation (3.44) is used to calculate what theoretical cooling power can be obtained via a lithium bromide-water solution absorption refrigeration system that utilises the net available low temperature power as calculated in equation (3.43).

$$Available\ cooling\ power\ (MW) =$$

$$\dot{QMW}_{cold} = COP \times \dot{QMW}_{low} = 0.7 \times \dot{QMW}_{low} \quad (3.44)$$

3.3 EPD MODEL FOR COGENERATION OUTPUT POWER OPTIMAL DISPATCH SCHEDULE DEVELOPMENT

3.3.1 Facility input requirements

The effective operation of the EPD model developed in this research requires specific user or facility inputs. These inputs are required for the consumption and generation tariff structures applicable to the facility and include the consumption and generation transmission zone, the consumption and generation transmission voltage level, a consumption customer category and a generation maximum export capacity. The consumption and generation transmission zones are determined by the distance of the facility from Johannesburg, South Africa [37]. It is expected for a combined consumer and generator facility that the consumption and generation transmission zones are the same, and therefore only a single input is required for both. The four transmission zones are [37], [39]:

- ≤ 300 km,
- > 300 km and ≤ 600 km,
- > 600 km and ≤ 900 km, and
- > 900 km.

The consumption and generation transmission voltage level is the voltage level at which the facility receives and produces electricity from and to the utility grid respectively. Although it is highly likely that the transmission voltage level for consumption and generation will be the same for a facility that is a combined electrical consumer and generator, this might not always be the case. Therefore a separate input is required for the consumption and the generation transmission voltage level. The four transmission voltage levels are [37], [39]:

- < 500 V,
- ≥ 500 V and < 66 kV,
- ≥ 66 kV and ≤ 132 kV, and
- > 132 kV (only applicable for consumption).

The consumption customer category is dependent on the facility's agreement with the utility and can either be [37]:

- > 1 MVA or
- Key Customer.

Key customers often have additional agreements with the utility that applies to periods of extremely high overall nationwide electrical energy consumption and demand. During these time periods the utility can ask its key customers to reduce its load in order to alleviate grid pressures and assist with meeting the nationwide electrical demand without having to shed power from commercial and residential areas.

Lastly, the generation maximum export capacity is a maximum supply value that is safely the maximum possible real power that the facility can generate and feed back to the utility grid. The generation maximum export capacity is divided into five main categories which are [39]:

- ≤ 100 kW,
- > 100 kW and ≤ 500 kW,
- > 500 kW and ≤ 1 MW,
- > 1 MW and
- Transmission Connected.

The user or facility input requirements are important in determining all active energy consumption and generation related charges as well as service and administration charges for the utility grid connection accommodating both electrical consumption and generation. The EPD model requests these inputs before the dispatch schedule can be generated, using these inputs to determine which energy consumption and generation charges as well as service and administration charges need to be utilised in the overall model cost function.

3.3.2 Utility defined facility consumption and generation tariff structure and cost function development

From Figure 1.1 the EPD model is implemented at the output of the cogeneration system. The purpose of the model is to determine the optimal manner in which to dispatch the cogeneration generated power between the furnace loads and the utility grid, for each time interval under consideration, so that the maximum possible overall energy and cost savings are obtained. The objective function for this research will therefore be the overall energy cost (costs - incentives) associated with the operation of the furnace loads and the generation of additional useful energy via the cogeneration system. The development of the overall system energy cost function is essential in acquiring energy and cost saving results from the EPD model.

As previously stated, the overall system energy cost can only be calculated on a monthly basis as is depicted by the energy consumption and generation tariff structures formulated by the country's electrical utility, Eskom [37], [39]. The monthly cost function requires system operational information or data for each time interval under consideration, for an entire month, in order to determine the real-time optimal manner in which to dispatch the cogeneration generated power at each time interval within the month. From this the overall monthly energy cost and savings can be determined. However, this poses a problem in the form of a time interval incompatibility.

The purpose of the optimisation model is to determine the real-time optimal power dispatch schedule for any given time interval in a month, yet the cost function requires system operational data for the entire month. The solution to this problem is the implementation of a prediction or forecasting model to determine all system operational data points beyond the current time interval of consideration. This allows for the determination of the real-time optimal power dispatch schedule, using the monthly based cost function, at any specific time interval within the given month. The prediction model will be further discussed in section 3.3.3.

The system overall objective/cost function can be defined as the sum of the overall system related energy cost (costs - incentives), all Use-of-System (U.o.S) charges and costs, and all costs associated with the generation of energy via the cogeneration system. The overall energy cost accounts for all costs associated with the consumption of energy from the utility grid supply less the financial incentives obtained through the sell-back of cogeneration generated power to the utility grid or a third party customer. The U.o.S charges and costs account for all costs associated with the supply of the utility grid connection, including administration and network reliability costs. Lastly, the power generation costs include all costs that are incurred through the process of generating additional useful electricity via the cogeneration system. Figure 3.4 shows a summary of these costs for a combined consumption and generation facility and is essential in the development of the final optimisation model objective function as obtained from [39].

The cost of power generation via the theoretical cogeneration system has been simplified as the sum of all individual costs for power that is required in order to generate additional useful energy via the cogeneration system. Captive power consumption is the internal power consumed by the cogeneration system, consisting of heat recovery and power generation. This power is essentially the power consumed by all the power generation system components, for example the flow control pressurising pump, the condenser cooling water flow control pump and all the auxiliary loads required for the operation of the cogeneration components. The captive power value is already accounted for by the net electrical efficiency calculation as shown in equation (3.42), and therefore does not need to be considered as an additional power consumption and therefore additional energy cost associated with the generation of additional electrical energy via the proposed cogeneration system. Therefore the only additional cost incurred through the generation of additional energy is the cost associated with the operation of the ID extraction fans for the extraction of the furnace off gases from the furnaces to the proposed cogeneration unit.

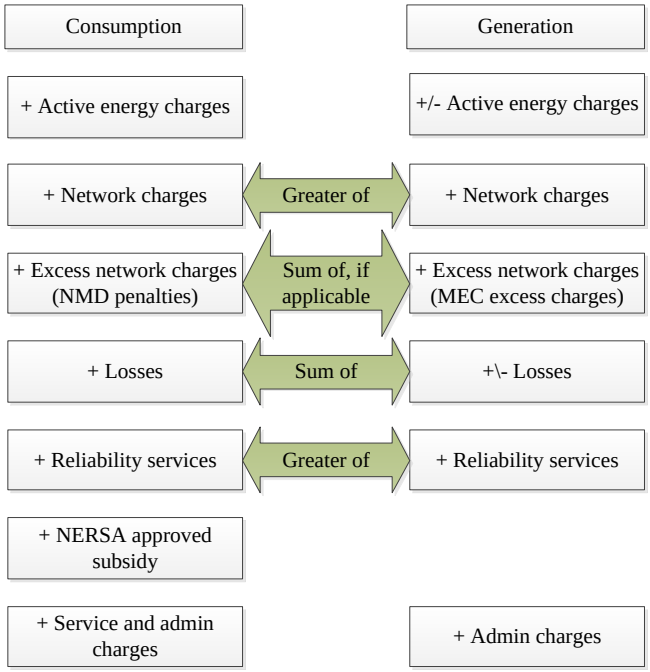

Figure 3.4: Summary of charges and incentives applicable to combined consumption/generation systems

The model objective/cost function for the EPD model developed in this research is therefore summarised as in equation (3.45).

$$\begin{aligned} &Overall\ Cost = Cost\ of\ all\ furnace\ energy\ consumption\ (from\ Eskom) \\ &- Total\ Insentive\ from\ sold\ generated\ energy\ (to\ Eskom) \\ &+ All\ U.o.S\ Charges \\ &+ ID\ fan\ heat\ extraction\ system\ charges \\ &+ Working\ fluid\ consumption\ charges \end{aligned} \tag{3.45}$$

The tariff structure that will be considered for this research and the EPD model is the MEGAFLEX local authority rates and tariff structure [37]. The cost function in equation (3.45) is a monthly based cost function that is used to determine the cogeneration power dispatch schedule for each half-hour time interval in the given month. According to the consumption and generation tariff structures in [37] and [39], overall energy consumption and generation costs require energy calculations for peak, standard and off-peak operating

time intervals. Therefore the cost function must account for these energy consumption T.O.U periods. In order to account for the energy consumption T.O.U period variations for different days of the week, flag variables for each of these periods must be implemented. The T.O.U period flag variables can only have values of 1 or 0, and are set to 1 only when that desired energy consumption T.O.U period (peak, standard or off-peak) is being considered. It is these flag variables that are stored in the Peak, Standard and Off-Peak flag arrays discussed in section 3.2.1. The energy consumption T.O.U period flag variables are defined in equations (3.46) to (3.49).

$$P_{i,j}(Peak) = 1$$
$$for\ Day(i) = 1,\ \ j = 15\ to\ 20\ and\ j = 37\ to\ 40 \tag{3.46}$$

$$S_{i,j}(Standard) = 1$$
$$for\ Day(i) = 1,\ \ j = 13\ to\ 14,\ j = 21\ to\ 36\ and\ j = 41\ to\ 44,\ \ and$$
$$for\ Day(i) = 2,\ \ j = 15\ to\ 24\ and\ j = 37\ to\ 40 \tag{3.47}$$

$$O_{i,j}(Off\ Peak) = 1$$
$$for\ Day(i) = 1,\ \ j = 1\ to\ 12\ and\ j = 45\ to\ 48,$$
$$for\ Day(i) = 2,\ \ j = 1\ to\ 14, j = 25\ to\ 36\ and\ j = 41\ to\ 48,\ \ and$$
$$for\ Day(i) = 3,\ \ j = 1\ to\ 48 \tag{3.48}$$

$$where\ Day(i) = \begin{matrix} 1 \\ 2 \\ 3 \end{matrix} \quad \begin{matrix} for\ day\ i\ being\ a\ Weekday\ (Monday\ to\ Friday) \\ for\ day\ i\ being\ a\ Saturday \\ for\ day\ i\ being\ a\ Sunday \end{matrix} \tag{3.49}$$

Using half-hour (30 minute) time intervals, the total number of daily time intervals that must be considered is 48 (24 h/day x 2 intervals/h). The EPD model determines the optimal amount of cogeneration generated power in MW that is dispatched back to the furnace loads, denoted as C_i in Figure 1.1, for each 30 minute time interval in the given month that will result in the maximum possible system related energy and cost savings. The optimisation variables for the power dispatch optimisation problem, for a given month of n days, are therefore formulated as is shown in equation (3.50).

$C_{i,j}\ (MW)$ (3.50)

where

- $1 \leq i \leq n$ denotes the i-th day in a given month,
- n denotes the total number of days in the given month, and
- $1 \leq j \leq 48$ denotes the j-th 30 minute time interval of the given day.

With the optimisation variables and energy consumption T.O.U periods defined, an overall system cost function can be developed. A consumption and generation combination energy network under the MEGAFLEX tariff structure will consist of the following network and energy consumption and generation costs, charges or financial incentives [37], [39]:

- A consumption Network Demand Charge (NDC) for the cogeneration system maximum consumption demand, shown in equations (3.51) to (3.56),
- A consumption Network Access Charge (NAC) based on the voltage of the utility grid supply to the system and the annual energy system utilised capacity, shown in equations (3.57) and (3.58),
- A Peak, Standard and Off-Peak Active Energy Consumption Charge (PEC, SEC and OEC respectively) for the total amount of energy consumed for each T.O.U period, shown in equations (3.59) to (3.64),
- An Electrification and Rural Subsidy Charge (ERC) applied to the total amount of active energy consumed, shown in equations (3.65) and (3.66),
- A Reactive Energy Charge (REC) based on the total amount of excess reactive energy required by the energy system, shown in equations (3.67) to (3.69),
- A Consumption Administration Charge (CAC) and Consumption Service Charge (CSC) for the utilisation of the utility grid supply for consumption, shown in equations (3.70) and (3.71),
- A Transmission Network Charge (TNC) for the transmission of the supply from the primary generation zone, shown in equation (3.72),

- An Urban Low Voltage Subsidy Charge (ULVSC) based on the voltage of the utility grid supply to the system and the annual energy system utilised capacity, shown in equation (3.73),
- A generation Network Access Charge (gNAC) based on the voltage of the utility grid supply the system feeds to and the annual energy system generated capacity, shown in equations (3.74) and (3.75),
- A Peak, Standard and Off-Peak Active Energy Generation Incentive (PEI, SEI and OEI respectively) for the total amount of active energy sold to or wheeled through the utility grid for third party customers, and a Total Rebate to be subtracted from the generation Network Access Charge, for each T.O.U period, shown in equations (3.76) to (3.82),
- A Generation Administration Charge (GAC) and Generation Service Charge (GSC) for the utilisation of the utility grid supply for generation, shown in equations (3.83) and (3.84),
- A combined Reliability Service Charge (RSC) based on the utility grid supply voltage for all energy consumption and generation T.O.U periods, shown in equations (3.85) to (3.88).

The cost functions for each individual charge or cost as introduced above are formulated in equations (3.51) to (3.88).

3.3.2.1 Network Demand Charge

$$Max\ Demand\ (kVA) = max\big(Peak\ Max\ Demand\ (MVA), Standard\ Max\ Demand\ (MVA)\big) \times 1000 \quad (3.51)$$

$$Peak\ Max\ Demand\ (MVA) = \max\left[\left(\left|\boldsymbol{S}_{i,j}^{load} - \boldsymbol{C}_{i,j}\right|\right) \times P_{i,j}\right] \quad for\ all\ i\ and\ j \quad (3.52)$$

$$Standard\ Max\ Demand\ (MVA) = \max\left[\left(\left|\boldsymbol{S}_{i,j}^{load} - \boldsymbol{C}_{i,j}\right|\right) \times S_{i,j}\right] \quad for\ all\ i\ and\ j \quad (3.53)$$

The power that is generated via the cogeneration system can either be dispatched to the furnace loads or fed back to the utility grid. This cogeneration output power is a real value (MW). The power that is fed back to the furnace load has to match the load itself in terms of power factor as the power factor is determined by the load. Therefore, whatever real power value is dispatched to the furnace loads as determined by the EPD model, will be dispatched at the same power factor as the current furnace load power factor. Therefore, the apparent power consumed from the utility grid supply once cogeneration power is dispatched to the furnace loads and used to substitute some of the utility grid supply, as shown in equations (3.52) and (3.53), can be calculated using equation (3.54).

$$\left|\boldsymbol{S}_{i,j}^{load} - \boldsymbol{C}_{i,j}\right| = \left|\boldsymbol{S}_{i,j}^{load}\right| \times \left(1 - \frac{C_{i,j}}{P_{i,j}^{load}}\right) \quad for\ all\ i\ and\ j \tag{3.54}$$

$$\therefore Max\ Demand\ (kVA) =$$

$$\max\left[\left|\boldsymbol{S}_{i,j}^{load}\right| \times \left(1 - \frac{C_{i,j}}{P_{i,j}^{load}}\right) \times (P_{i,j} + S_{i,j})\right] \times 1000 \quad for\ all\ i\ and\ j \tag{3.55}$$

$$\therefore NDC = Max\ Demand\ (kVA) \times NDC_r\ (R/kVA) \tag{3.56}$$

where:

- $\left|\boldsymbol{S}_{i,j}^{load}\right|$ is the magnitude of the furnace consumed apparent power in MVA during the i,j time interval,
- $P_{i,j}^{load}$ is the furnace load in MW consumed during the i,j time interval,
- NDC_r is the Network Demand Charge rate in R/kVA.

3.3.2.2 Consumption Network Access Charge

$$Maximum\ Installed\ Access\ Demand\ for\ Consumption(AD)(kVA) =$$

$$AD\ (MVA) \times 1000 \tag{3.57}$$

$$\therefore NAC = AD\ (kVA) \times NAC_r\ (R/kVA) \tag{3.58}$$

where NAC_r is the consumption Network Access Charge rate in R/kVA.

3.3.2.3 Active Energy Consumption Charges

$$Total\ Utility\ Consumed\ Peak\ Energy\ (kWh) = 0.25\ h \times \sum_{i=1}^{n} \sum_{j=1}^{48} \left[\left(P_{i,j}^{load} - C_{i,j} \right) \times 1000 \times P_{i,j} \right] \quad (3.59)$$

$$\therefore PEC = Total\ Utility\ Consumed\ Peak\ Energy\ (kWh) \times P_r\ (c/kWh) \times \frac{1}{100} \quad (3.60)$$

$$Total\ Utility\ Consumed\ Standard\ Energy\ (kWh) = 0.25\ h \times \sum_{i=1}^{n} \sum_{j=1}^{48} \left[\left(P_{i,j}^{load} - C_{i,j} \right) \times 1000 \times S_{i,j} \right] \quad (3.61)$$

$$\therefore SEC = Total\ Utility\ Consumed\ Standard\ Energy\ (kWh) \times S_r\ (c/kWh) \times \frac{1}{100} \quad (3.62)$$

$$Total\ Utility\ Consumed\ Off\ Peak\ Energy\ (kWh) = 0.25\ h \times \sum_{i=1}^{n} \sum_{j=1}^{48} \left[\left(P_{i,j}^{load} - C_{i,j} \right) \times 1000 \times O_{i,j} \right] \quad (3.63)$$

$$\therefore OEC = Total\ Utility\ Consumed\ Off\ Peak\ Energy\ (kWh) \times O_r\ (c/kWh) \times \frac{1}{100} \quad (3.64)$$

where P_r, S_r and O_r are the Peak, Standard and Off-Peak Active Energy Consumption Charge rates in c/kWh respectively.

3.3.2.4 Electrification and Rural Subsidy Charge

$$\begin{aligned} Total\ Utility\ Consumed\ Energy\ (kWh) &= Total\ Utility\ Consumed\ Peak\ Energy\ (kWh) \\ &+ Total\ Utility\ Consumed\ Standard\ Energy\ (kWh) \\ &+ Total\ Utility\ Consumed\ Off\ Peak\ Energy\ (kWh) \end{aligned}$$

$$= 0.25\ h \times \sum_{i=1}^{n} \sum_{j=1}^{48} \left[\left(P_{i,j}^{load} - C_{i,j} \right) \times 1000 \times \left(P_{i,j} + S_{i,j} + O_{i,j} \right) \right] \quad (3.65)$$

$$\therefore ERC = Total\ Utility\ Consumed\ Energy\ (kWh) \times ERC_r\ (c/kWh) \times \frac{1}{100} \quad (3.66)$$

where ERC_r is the Electricity and Rural Subsidy Charge rate in c/kWh.

3.3.2.5 Reactive Energy Charge

A reactive energy charge is only applied if the reactive energy required from the utility grid exceeds 30% of the real energy required from the grid. If the 30% condition is applicable, equation (3.67) is used to calculate the total excess reactive energy in kVArh.

$$Q_{i,j}^{exc} = \left(\left(P_{i,j}^{load} - C_{i,j}\right) \times 1000 \times \sqrt{\left(\frac{\left|S_{i,j}^{load}\right|}{P_{i,j}^{load}}\right)^2 - 1} \right) - 0.3 \times \left(P_{i,j}^{load} - C_{i,j}\right) \times 1000$$

$$= \left(P_{i,j}^{load} - C_{i,j}\right) \times \left(\sqrt{\left(\frac{\left|S_{i,j}^{load}\right|}{P_{i,j}^{load}}\right)^2 - 1} - 0.3 \right) \times 1000 \quad for\ all\ i\ and\ j \tag{3.67}$$

$$Total\ Excess\ Reactive\ Energy\ (kVArh) =$$

$$0.25\ h \times \sum_{i=1}^{n} \sum_{j=1}^{48} \left[Q_{i,j}^{exc} \times (P_{i,j} + S_{i,j}) \times REC_{i,j}^{test} \right] \tag{3.68}$$

$$\therefore REC = Total\ Excess\ Reactive\ Energy\ (kVArh) \times REC_r\ (c/kVarh) \times \frac{1}{100} \tag{3.69}$$

where:

- $Q_{i,j}^{exc}$ is the excess reactive energy in kVAr during the i,j time interval,
- $REC_{i,j}^{test}$ is a reactive energy charge test flag for each i,j time interval that is set to 1 if the 30% reactive energy condition occurs during that i,j time interval, and
- REC_r is the Reactive Energy Charge rate in c/kVarh.

The $REC_{i,j}^{test}$ flag is set utilising the REC_Test_Condition function of the EPD model which can be seen in Addendum A. The REC_Test_Condition function calculates the reactive load data array utilising the MVA and MW load arrays for each time interval and then compares all the reactive load array elements in MVAr to the corresponding time interval real load array elements in MW, applying the 30% test condition. If the reactive load exceeds 30% of the real load, the $REC_{i,j}^{test}$ flag for that specific time interval is set to 1.

3.3.2.6 Consumption Service and Administration Charges

$$CAC = n\ (days) \times CAC_r(R/day) \tag{3.70}$$

$$CSC = n\ (days) \times CSC_r(R/day) \tag{3.71}$$

where:

- CAC_r is the Consumption Administration Charge rate in R/day, and
- CSC_r is the Consumption Service Charge rate in R/day.

3.3.2.7 Consumption Transmission Network Charge

$$TNC = AD\ (kVA) \times TNC_r\ (R/kVA) \tag{3.72}$$

where TNC_r is the Transmission Network Charge rate in R/kVA.

3.3.2.8 Urban Low Voltage Subsidy Charge

$$\therefore ULVSC = AD\ (kVA) \times ULVSC_r\ (R/kVA) \tag{3.73}$$

where $ULVSC_r$ is the urban low voltage subsidy charge rate in R/kVA.

3.3.2.9 Generation Network Access Charge

$$Maximum\ Installed\ Access\ Demand for\ Generation(gAD)(kVA) = gAD\ (MVA) \times 1000 \tag{3.74}$$

$$\therefore gNAC = gAD\ (kVA) \times gNAC_r\ (R/kVA) \tag{3.75}$$

where $gNAC_r$ is the generation Network Access Charge rate in R/kVA.

3.3.2.10 Active Energy Generation Incentives and Total Rebate

$$Total\ Peak\ Sold\ Generated\ Energy\ (kWh) = 0.25\ h \times \sum_{i=1}^{n} \sum_{j=1}^{48} \left[\left(\dot{W}_{i,J}^{T} - C_{i,j}\right) \times 1000 \times P_{i,j}\right] \tag{3.76}$$

$$\therefore PEI = Total\ Peak\ Sold\ Generated\ Energy\ (kWh) \times WP_r\ (c/kWh) \times \frac{1}{100} \tag{3.77}$$

$$Total\ Standard\ \ Sold\ Generated\ Energy\ (kWh) =$$

$$0.25\ h \times \sum_{i=1}^{n} \sum_{j=1}^{48} \left[\left(\dot{W}_{i,j}^{T} - \ C_{i,j} \right) \times 1000 \times S_{i,j} \right] \quad (3.78)$$

$$\therefore SEI = Total\ Standard\ \ Sold\ Generated\ Energy\ (kWh) \times WS_r\ (c/kWh) \times \frac{1}{100} \quad (3.79)$$

$$Total\ Off\ Peak\ Sold\ Generated\ Energy\ (kWh) =$$

$$0.25\ h \times \sum_{i=1}^{n} \sum_{j=1}^{48} \left[\left(\dot{W}_{i,j}^{T} - \ C_{i,j} \right) \times 1000 \times O_{i,j} \right] \quad (3.80)$$

$$\therefore OEI = Total\ Off\ Peak\ Sold\ Generated\ Energy\ (kWh) \times WO_r\ (c/kWh) \times \frac{1}{100} \quad (3.81)$$

$$Total\ Rebate = (PEI + SEI + OEI) \times (DLF \times TLF - 1) \quad (3.82)$$

where:

- $\dot{W}_{i,j}^{T}$ is the total cogeneration generated power in MW during the i,j time interval,
- WP_r, WS_r and WO_r are the base WEPS (Wholesale Electricity Pricing System) energy rates in c/kWh,
- DLF is the Distribution Loss Factor, as shown in Table 3.6,
- TLF is the Transmission Loss Factor, as shown in Table 3.7, and
- Total Rebate is the rebate to be subtracted from the generation Network Access Charge only if this charge is applicable. If the generation Network Access Charge is not applicable, the Total Rebate will be 0.

Table 3.6: Distribution Loss Factors

Distribution Loss Factor		
Voltage	Urban Loss Factor	Rural Loss Factor
< 500 V	1.1111	1.1527
≥ 500 V and < 66 kV	1.0957	1.1412
≥ 66 kV and ≤ 132 kV	1.0611	
> 132 kV	1	

Table 3.7: Transmission Loss Factors

Transmission Loss Factor		
Transmission Zone Distances	Zone	Loss Factor
≤ 300 km	0	1.0107
> 300 km and ≤ 600 km	1	1.0208
> 600 km and ≤ 900 km	2	1.031
> 900 km	3	1.0413

3.3.2.11 Generation Service and Administration Charges

$$GAC = n\ (days) \times GAC_r(R/day) \tag{3.83}$$

$$GSC = n\ (days) \times GSC_r(R/day) \tag{3.84}$$

where:

- GAC_r is the Generation Administration Charge rate in R/day, and
- GSC_r is the Generation Service Charge rate in R/day.

3.3.2.12 System Network Reliability Service Charge

$$Consumption\ Reliability\ Service\ Charge\ (CRC) = Total\ Utility\ Consumed\ Energy\ (kWh) \times CRC_r\ (c/kWh) \times \frac{1}{100} \tag{3.85}$$

$$\begin{aligned} Total\ Sold\ Generated\ Energy\ (kWh) &= Total\ Peak\ Sold\ Generated\ Energy\ (kWh) \\ &+ Total\ Standard\ Sold\ Generated\ Energy\ (kWh) \\ &+ Total\ Off\ Peak\ Sold\ Generated\ Energy\ (kWh) \end{aligned}$$

$$= 0.25\ h \times \sum_{i=1}^{n} \sum_{j=1}^{48} \left[\left(\dot{W}_{i,j}^{T} - C_{i,j} \right) \times \left(P_{i,j} + S_{i,j} + O_{i,j} \right) \times 1000 \right] \tag{3.86}$$

$$\therefore Generation\ Reliability\ Service\ Charge\ (GRC) = Total\ Sold\ Generated\ Energy\ (kWh) \times GRC_r\ (c/kWh) \times \frac{1}{100} \tag{3.87}$$

$$\therefore RSC = \max(CRC : GRC) \tag{3.88}$$

where:

- CRC_r is the Consumption Network Reliability Service Charge rate in c/kWh, and
- GRC_r is the Generation Network Reliability Service Charge rate in c/kWh.

The charges and incentives in equations (3.51) to (3.88) are the active energy consumption charges, the energy generation incentives and all U.o.S charges relating to the complete installed cogeneration (consumption and generation) system. As previously suggested, the power generation costs must account for the cost associated with the extraction of the hot material from the furnaces. These costs are essentially the costs associated with the operation of the ID extraction fans, the combined load of which can simply be added to the furnace load as is shown in equation (3.89).

$$P_{i,j}^{load} + P_{i,j}^{ID} \tag{3.89}$$

where $P_{i,j}^{ID}$ is the total combined power rating of the hot material ID extraction fans in MW during the i,j time interval.

Due to the cyclic operation of the proposed cogeneration system, it will be assumed that the working fluid is continuously recycled and reused, and only replaced during specific maintenance time intervals which are not of concern in this research. Therefore a working fluid utilisation cost will not be considered. The final optimal power dispatch cost function is therefore shown in equation (3.90).

$$Cost\ (R) = NDC + (PEC + SEC + OEC) + ERC + REC + CAC + CSC + TNC + ULVSC + \max[NAC{:}\, gNAC - Total\ Rebate] - (PEI + SEI + OEI) + GAC + GSC + RSC \tag{3.90}$$

Given equations (3.46) to (3.50) and substituting equations (3.51) to (3.89) into equation (3.90), the detailed mathematical system objective function is expanded and simplified into the cost function shown in equation (3.91). It is important to note that all power-

related data is obtained as MW and MVA, but all power tariffs give a cost value per kW, kVA or kWh. Therefore an appropriate conversion from the mega-range to the kilo-range (x 1000) is required. This too is shown in equation (3.91).

$$
\begin{aligned}
&Cost\,(R) = \\
&\max\left[\left|\boldsymbol{S}_{i,j}^{load}\right| \times \left(1 - \frac{C_{i,j}}{P_{i,j}^{load} + P_{i,j}^{ID}}\right) \times (P_{i,j} + S_{i,j})\right] \times 1000 \times NDC_r \\
&+ 0.25 \times \sum_{i=1}^{n} \sum_{j=1}^{48} \left(\left(\left(P_{i,j}^{load} + P_{i,j}^{ID}\right) - C_{i,j}\right) \times 1000 \times \left(\frac{P_{i,j} \times (P_r + ERC_r)}{100} + \frac{S_{i,j} \times (S_r + ERC_r)}{100} + \right.\right. \\
&\left.\left.\frac{O_{i,j} \times (O_r + ERC_r)}{100}\right)\right) \\
&- 0.25 \times \sum_{i=1}^{n} \sum_{j=1}^{48} \left(\left(\dot{W}_{i,j}^{T} - C_{i,j}\right) \times 1000 \times \left(\frac{P_{i,j} \times WP_r}{100} + \frac{S_{i,j} \times WS_r}{100} + \frac{O_{i,j} \times WO_r}{100}\right)\right) \\
&+ \left[0.25 \times \sum_{i=1}^{n} \sum_{j=1}^{48} \left[\left(\left(P_{i,j}^{load} + P_{i,j}^{ID}\right) - C_{i,j}\right) \times \left(\sqrt{\left(\frac{\left|\boldsymbol{S}_{i,j}^{load}\right|}{P_{i,j}^{load} + P_{i,j}^{ID}}\right)^2} - 1 - 0.3\right) \times 1000 \times \right.\right. \\
&\left.\left.(P_{i,j} + S_{i,j}) \times REC_{i,j}^{test}\right] \times \left(\frac{REC_r}{100}\right)\right] \\
&+ \left[n \times (CAC_r + CSC_r + GAC_r + GSC_r)\right] \\
&+ \left[\max\left[(AD(MVA) \times 1000 \times NAC_r) : \left((gAD(MVA) \times 1000 \times gNAC_r) - \right.\right.\right. \\
&\left.\left.\left.Total\ Rebate\right)\right]\right] \\
&+ \left(AD(MVA) \times 1000 \times (TNC_r + ULVSC_r)\right) \\
&+ \left[\max\left[\begin{array}{l}\left(\frac{0.25 \times CRC_r}{100} \times \sum_{i=1}^{n} \sum_{j=1}^{48} \left(\left(P_{i,j}^{load} + P_{i,j}^{ID}\right) - C_{i,j}\right) \times 1000 \times \left(P_{i,j} + S_{i,j} + O_{i,j}\right)\right) \\ : \left(\frac{0.25 \times GRC_r}{100} \times \sum_{i=1}^{n} \sum_{j=1}^{48} \left(\dot{W}_{i,j}^{T} - C_{i,j}\right) \times 1000 \times \left(P_{i,j} + S_{i,j} + O_{i,j}\right)\right)\end{array}\right]\right]
\end{aligned}
\tag{3.91}
$$

3.3.3 EPD model development

3.3.3.1 Model and raw data prediction and forecasting

An important aspect of the optimisation model developed in this research is that the model cost function is a monthly-based cost function, requiring a month's data, and yet the model is a real-time operational model that is expected to generate a real-time EPD schedule. As mentioned in Section 3.3.2 the solution is a prediction or forecasting model. The prediction

model is a section of the EPD model that predicts what the future furnace operation data is in order to apply the monthly cost function at any time interval in the given month. A linear prediction can be used whereby all data after the current time interval of consideration is assumed to be a specific reasonable constant value, but the most accurate overall EPD model will be achieved through the utilisation of a historical data-based prediction model.

The historical data-based prediction model utilises data from months that have already occurred, often months that are similar to the current month of consideration in terms of days in the month, the season, months with similar furnace breakdown or maintenance schedules, etc. Once sufficient historical data for each month is obtained, a general raw data prediction array can be generated for each month or month type. The EPD model therefore executes the optimisation and cost function model procedures by utilising the raw data prediction array for all data points beyond the current time interval of consideration in conjunction with actual acquired data for the current month up until the current time interval.

However, for this research, due to a lack of historical data available at Glencore Ferrochrome in Rustenburg, the raw data prediction array could only be generated utilising historical data obtained for the time period range 2014/08/01 00:00 to 2014/11/12 12:30. All historical raw data obtained from Glencore Ferrochrome in Rustenburg was stored, filtered and grouped in a prediction data spread sheet, PredData, and used to generate a forecast or prediction model data array. It was noticed that the furnace operation varied slightly during summer and winter months with the overall load approximately 15% less in winter. Although this variation is not insignificant, due the limited historical data obtained, only a single prediction data array was developed, for all months.

Historical data filtering is the process whereby "off" furnace condition data points are filtered out and replaced with a general average of each specific raw data field or type, furnace load power, furnace stack temperatures and bagplant inlet temperatures for each furnace. This is because furnace trips or faults at individual and unique data point time

intervals which resulted in the furnaces being non-operational for short and unscheduled periods of time are not data points and time instances that are of concern, and therefore should not affect the general furnace operational data condition averages and corresponding predicted data points.

Furnace "off" or non-operational conditions were decided upon based on the bagplant inlet temperatures for each furnace. It was assumed that a bagplant inlet temperature of less than or equal to 80 ^{o}C meant that the corresponding furnace was in the "off" or non-operational condition, as a bagplant inlet temperature at this low temperature level could only be reached if furnace smelting processes were not being performed at that specific time interval. The specific historical raw data type averages were obtained by neglecting all established "off" or non-operational condition data points for each data field, and averaging the remaining operational condition data points. The resulting filtered raw data therefore consisted of only operational condition data points by replacing all non-operational condition data points with the calculated specific data field averages.

The final model prediction data array was generated using a pivot table applied to the filtered historical raw data. A pivot table was used to group all the filtered raw data according to the hour and minute of each data point. Therefore the final predication data array was generated as an average daily data array with an overall average of each raw data field for each grouped half our time interval range in a day, 00:30 to 24:00 (00:00). The prediction data array therefore consisted of a single day's half-hourly data, a total of 48 predicted data point time intervals, and represented an average overall furnace operation condition, and therefore average specific data field values, for a single day. The prediction data array generated in this research is further discussed in Chapter 4.

Therefore, the data array utilised at the beginning of the EPD model is a combination of all acquired operation data points and conditions up until a current time interval in the month of operation, and predicted raw data for all time intervals beyond the current. Therefore all raw data field values for each half hour time interval beyond the current were set to the corresponding half hour time interval prediction data point from the prediction data array.

This ensures a level of accuracy in the past-to-present power dispatch schedule as the operational data points beyond the current are represented by average accepted system operation conditions based firmly on historical data. The data handling required in order to develop the final raw data array to be used by the EPD model can be seen at the beginning of the EPD optimisation algorithm in Addendum A.

3.3.3.2 EPD optimisation modelling

The optimisation model is highly dependent on the model cost function, which is shown in equation (3.91). The cost function however requires the consumption and generation tariff structure costs, charges and incentives. All applicable tariffs are acquired utilising a Determine_Cons_Charges and Determine_Gen_Charges function as is shown in Addendum A. Both of these functions take the user or facility input requirements (transmission zone, voltage level and maximum import or export capacity) as well as the high demand season flag, and utilise the information to generate a CTariff and GTariff array which hold the actual MEGAFLEX consumption and generation tariff structures, i.e. costs, charges and incentives, respectively, that are applicable for all the current input information. Within these two functions, the MEGAFLEX charges and incentives as shown in [37] and [39] are loaded into lookup tables and the appropriate tariffs obtained utilising the function inputs. The CTariff and GTariff arrays are arranged as follows:

CTariff = [HDP_r, HDS_r, HDO_r, LDP_r, LDS_r, LDO_r, TNC_r, NAC_r, NDC_r, ULVSC, CRC_r, CSC_r, CAC_r, ERC_r, REC_r], and
GTariff = [TLF, $gNAC_r$, DLF, GRC_r, WPr, WSr, WOr, GSC_r, GAC_r],

where:

- HD and LD are high demand and low demand tariff charges, and
- All other variables are as they are used in Section 3.3.2.

The cost function in equation (3.91) is utilised in MATLAB by generating cost function constant arrays and variables. These constants are calculated at each time interval and data point and stored in arrays for utilisation by the Cost_Function function within the EPD

model, as can be seen in Addendum A. The constant arrays and variables are simplified and calculated using equations (3.92) to (3.106).

$$A_{i,j} = \left|\boldsymbol{S}_{i,j}^{load}\right| \times (P_{i,j} + S_{i,j}) \times 1000 \times NDC_r \quad (3.92)$$

$$B_{i,j} = \left|\boldsymbol{S}_{i,j}^{load}\right| \times \left(\frac{1}{P_{i,j}^{load} + P_{i,j}^{ID}}\right) \times (P_{i,j} + S_{i,j}) \times 1000 \times NDC_r \quad (3.93)$$

$$D_{i,j} = P_{i,j}^{load} + P_{i,j}^{ID} \quad (3.94)$$

$$E_{i,j} = 1000 \times \left(\frac{P_{i,j} \times (P_r + ERC_r)}{100} + \frac{S_{i,j} \times (S_r + ERC_r)}{100} + \frac{O_{i,j} \times (O_r + ERC_r)}{100}\right) \quad (3.95)$$

$$F_{i,j} = \dot{W}_{i,J}^{T} \quad (3.96)$$

$$G_{i,j} = 1000 \times \left(\frac{P_{i,j} \times WP_r}{100} + \frac{S_{i,j} \times WS_r}{100} + \frac{O_{i,j} \times WO_r}{100}\right) \quad (3.97)$$

$$H_{i,j} = 1000 \times \left(\sqrt{\left(\frac{\left|\boldsymbol{S}_{i,j}^{load}\right|}{P_{i,j}^{load} + P_{i,j}^{ID}}\right)^2 - 1} - 0.3\right) \times (P_{i,j} + S_{i,j}) \times REC_{i,j}^{test} \times \left(\frac{REC_r}{100}\right) \quad (3.98)$$

$$K = n \times (CAC_r + CSC_r + GAC_r + GSC_r) \quad (3.99)$$

$$L = AD(MVA) \times 1000 \times NAC_r \quad (3.100)$$

$$M = gAD(MVA) \times 1000 \times gNAC_r \quad (3.101)$$

$$N = (DLF \times TLF - 1) \quad (3.102)$$

$$Q = AD(MVA) \times 1000 \times (TNC_r + ULVSC_r) \quad (3.103)$$

$$R = \frac{0.25 \times CRC_r}{100} \quad (3.104)$$

$$T = 1000 \times (P_{i,j} + S_{i,j} + O_{i,j}) \quad (3.105)$$

$$U = \frac{0.25 \times GRC_r}{100} \quad (3.106)$$

The model cost function, as it is simplified and implemented in MATLAB, is shown in equations (3.107) to (3.110).

$$Cost\,(R) = \lambda_1 + 0.25 \times \left(\sum_{i=1}^{n}\sum_{j=1}^{48}\left[\left(E_{i,j} + H_{i,j}\right) \times \left(D_{i,j} - C_{i,j}\right)\right] - \sum_{i=1}^{n}\sum_{j=1}^{48}\left[G_{i,j} \times \left(F_{i,j} - C_{i,j}\right)\right]\right) + \lambda_2 + \lambda_3 + K + Q \quad (3.107)$$

where:

$$\lambda_1 = \max\left[A_{i,j} - \left(B_{i,j} \times C_{i,j}\right)\right] \quad (3.108)$$

$$\lambda_2 = \max\left[L{:}\left(M - \left(N \times 0.25 \times \sum_{i=1}^{n}\sum_{j=1}^{48}\left[G_{i,j} \times \left(F_{i,j} - C_{i,j}\right)\right]\right)\right)\right] \quad (3.109)$$

$$\lambda_3 = \max\left[\left(R \times \sum_{i=1}^{n}\sum_{j=1}^{48} T \times \left(D_{i,j} - C_{i,j}\right)\right), \left(U \times \sum_{i=1}^{n}\sum_{j=1}^{48} T \times \left(F_{i,j} - C_{i,j}\right)\right)\right] \quad (3.110)$$

It has been stated that the correspondence of the specific i, j time interval data to calculations, procedures and optimisation steps to be performed using that specific data point, is controlled via the model working array. This is because the working array holds the values of i and j in the first two columns of the array. Therefore the time interval i and j values can be obtained utilising the model working array as is shown in the generic data correspondence equation (3.111).

$$x(i,j) = x\left(FWorkArray(dp,1), FWorkArray(dp,2)\right) = y(dp,1) \quad (3.111)$$

where:

- x(i,j) is a [n x 48] array that holds information array data specific to the i,j time interval of the month,
- i = FWorkArray(dp,1),
- j = FWorkArray(dp,2),
- dp is the data point from, 1 to (48n), that corresponds to the specific i,j time interval, and
- y(dp,1) is a [(48n) x 1] information array that is originally imported from the raw data spread sheet.

The purpose of the EPD model is to calculate the model optimisation variable $C_{i,j}$ for all i, j data points, which is the amount of cogeneration generated power that is dispatched to the furnace loads for each data point that results in the minimum possible overall cost (R). The optimisation is performed utilising the built-in 'sqp' MATLAB optimisation algorithm as is shown in Addendum A. The optimisation process utilises the cost function to solve an optimisation variable array x which represents the model optimisation variable $C_{i,j}$. The solved x array that is the result of the optimisation process is the model optimisation

variable array $C_{i,j}$ for all the i,j data points that is used to calculate the overall system obtained energy cost and savings.

This research deals with the consideration of a heat recovery cogeneration system that replaces the current furnace off gas cooling system. Therefore, for a system implementation energy saving figure to be calculated, an initial system and final system energy cost is required. The optimisation model process as discussed above is used to calculate the energy cost after the energy saving measure is put in place. In order to calculate the energy cost prior to the implementation of the energy saving measure, the heat recovery cogeneration system is neglected. Therefore the cogeneration output power $\dot{W}_{i,j}^{T}$ and the x array are both assumed as and set to zero before Cost_Function is recalled.

In this case the cost function simply calculates the overall system energy cost with the cogeneration system output neglected, meaning that the only energy costs are the costs associated with the consumption of energy directly from the utility grid. The total energy system implementation savings are finally calculated as is shown in equation (3.112).

$$TotalSavings\ (R) = ICost - FCost \tag{3.112}$$

where:

- ICost is the initial system calculated energy cost in R, and
- FCost is the system final calculated energy cost in R, after the heat recovery cogeneration system implementation.

The EPD model then completes its operation by exporting the generated EPD schedule, the available cooling power and the monthly savings to a CogenOutput spread sheet for analysis. The generated schedule is for the entire month of consideration. Segments of example EPD schedules for the chosen months of analysis are shown in Addendum C.

CHAPTER 4 RESULTS

4.1 OVERVIEW OF RESULTS

The main objective of the EPD model is to provide the facility or user with a developed real-time optimal power dispatch schedule for the cogeneration generated additional power between the furnace loads and the utility grid, so as to achieve the maximum possible system and facility associated energy and cost savings. Therefore, the primary and most important research associated result is the overall system associated energy and cost savings that can be obtained through the consideration of a theoretical heat recovery cogeneration system and an associated EPD model that develops the optimal power dispatch schedule. There are however additional system and model associated results that need to be realised before simply considering and accepting the overall cost savings figure. These results include:

- The overall capacity of previously wasted thermal energy that can be recovered and the overall capacity of additional electrical energy that can be generated via the proposed cogeneration system,
- The overall cooling power capacity that can be additionally catered for as a result of the utilisation of the cogeneration system by-product of low grade thermal energy,
- The system prediction data array that is essential in the operation of a real-time optimal power dispatch system, and
- The final past-to-present optimal power dispatch schedule that determines the quantity of additionally generated power that is dispatched to the furnace loads or back to the utility grid, ensuring the primary result, energy and cost savings, are obtained.

The results will be presented and discussed for a single winter and a single summer month in order to provide just a perspective of the overall potential of energy and cost savings that can be obtained via the proposed cogeneration system and associated EPD model. This is due to the limited raw data that could be obtained from Glencore Ferrochrome in Rustenburg. The two months that were chosen for the purpose of results were August 2014 (winter) and October 2014 (summer). In terms of the user or facility specified inputs, for Glencore Ferrochrome in Rustenburg, these inputs are as follows:

- Consumption and Generation Transmission Zone = Zone 1, ≤ 300 km,
- Consumption and Generation Supply Voltage Level = Level 2, ≥ 500 V & < 66 kV,
- Consumption Customer Category = Category 1, Key Customer, and
- Maximum Generation Export Capacity = Category 4, > 1 MVA/MW.

4.1.1 Total system heat recovery and additional power generation capacities

An average combined furnace 1 to 4, daily, real load profile for the chosen winter and summer month is shown in Figure 4.1 and 4.2 respectively. The corresponding daily average combined extracted thermal power and average combined generated electrical power profiles, as a result of the proposed cogeneration system, for the chosen winter and summer month, are shown in Figure 4.3 and 4.4 respectively. The generated electrical power profile is well below the recovered heat profile, as a 21% efficiency of electrical power generation from recovered heat was obtained from the proposed power generation unit.

The averages were obtained in a similar fashion to the prediction data array, through the process of grouping and averaging the chosen data type for each half hour time interval range 00:30 to 24:00 (00:00) throughout the given months.

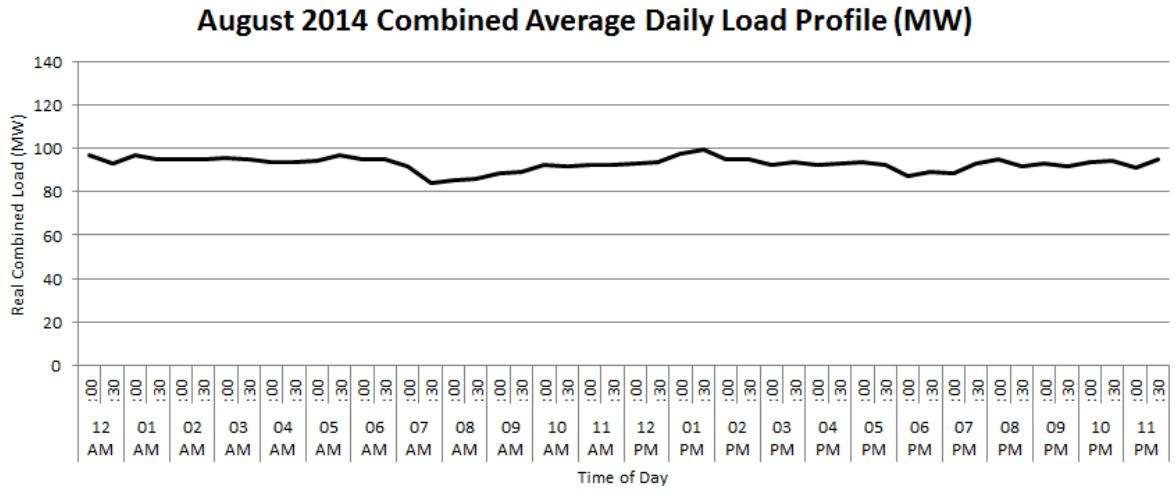

Figure 4.1: Combined average daily real load profile in MW for August 2014

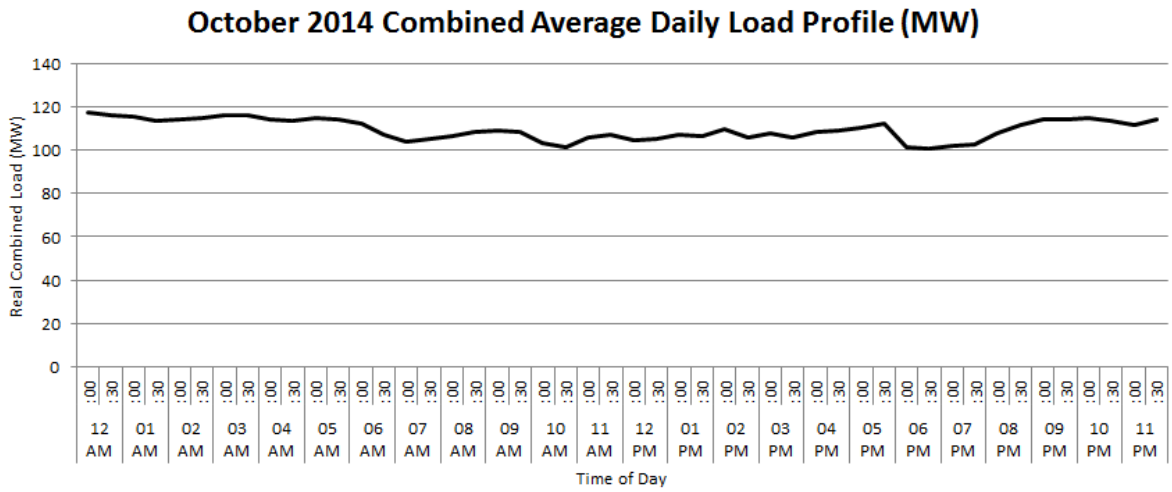

Figure 4.2: Combined average daily real load profile in MW for October 2014

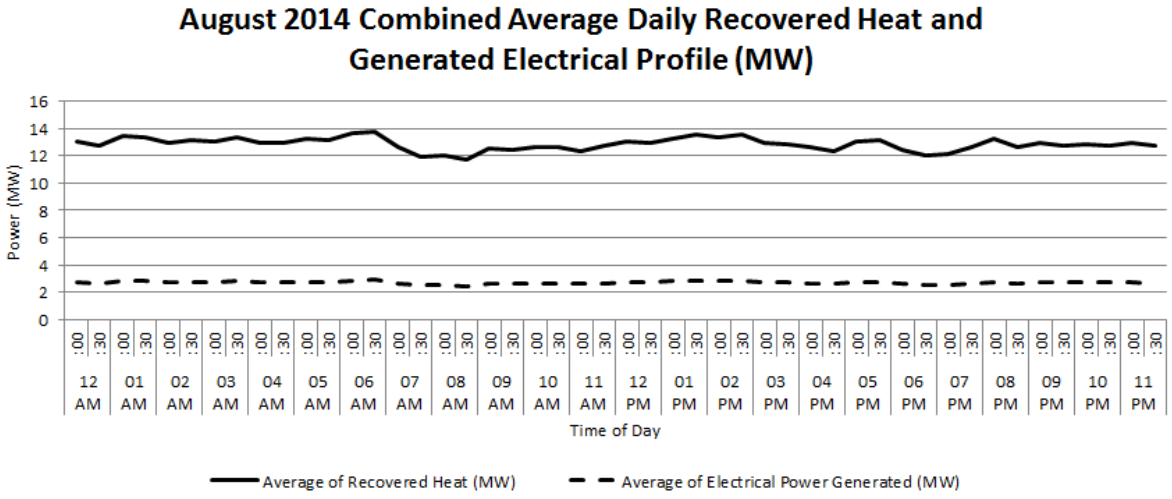

Figure 4.3: Combined average daily recovered heat and generated electricity profiles in MW, for August 2014

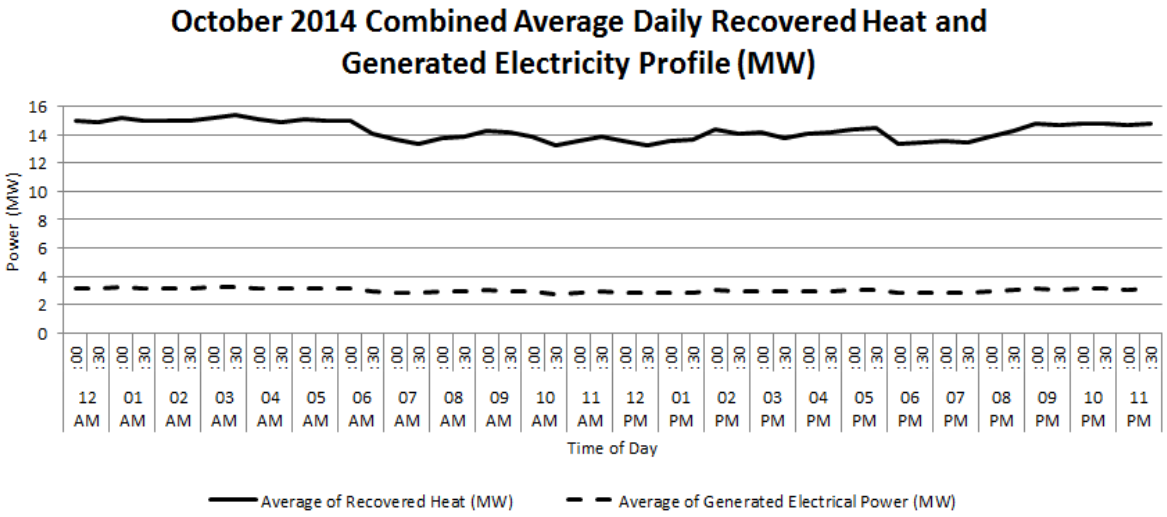

Figure 4.4: Combined average daily recovered heat and generated electricity profiles in MW, for October 2014

From Figure 4.1 it can be seen that in a winter season the furnace real load exists within the range of 84 to 100 MW with an average load of 92.81 MW. Figure 4.3 shows the total combined recovered thermal power of between 11 and 14 MW with an average of 12.85 MW of recovered thermal power. Lastly, Figure 4.3 also shows the total combined generated electrical power of between 2.4 and 2.9 MW with an average generated electrical power of 2.71 MW.

From Figure 4.2 it can be seen that in a summer season the furnace real load exists within the range of 100 to 118 MW with an average load of 109.5 MW. Figure 4.4 shows the total combined recovered thermal power of between 13 and 16 MW with an average of 14.26 MW of recovered thermal power. Lastly, it also shows the total combined generated electrical power of between 2.7 and 3.3 MW with an average generated electrical power of 3 MW.

A table of these results is shown in Table 4.1.

4.1.2 Total system resulting cooling power capacity

Average combined daily available cooling power profiles for the chosen winter and summer month are shown in Figure 4.5 and 4.6 respectively. The averages were once again obtained through the process of grouping and averaging the cooling power for each half hour time interval range 00:30 to 24:00 (00:00) throughout the given months. From Figure 4.5 it can be seen that an average available cooling power of 6.92 MW was obtained for the chosen winter month, with a range of between 6.2 and 7.4 MW of available cooling power. From Figure 4.6 it can be seen that an average available cooling power of 7.68 MW was obtained for the chosen summer month, with a range of between 7.1 and 8.3 MW of available cooling power. These results are also summarised in Table 4.1.

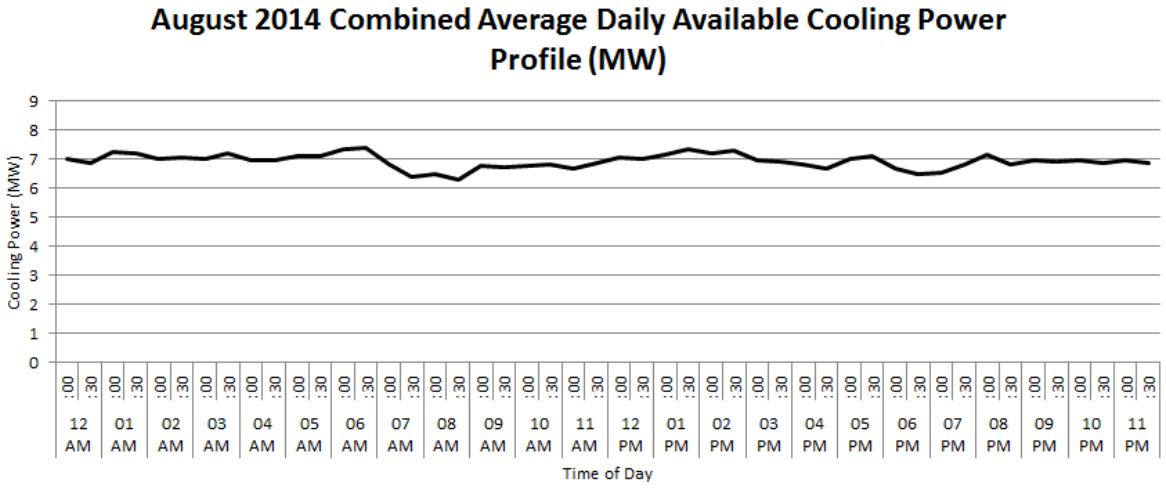

Figure 4.5: Combined average daily available cooling power profile in MW for August 2014

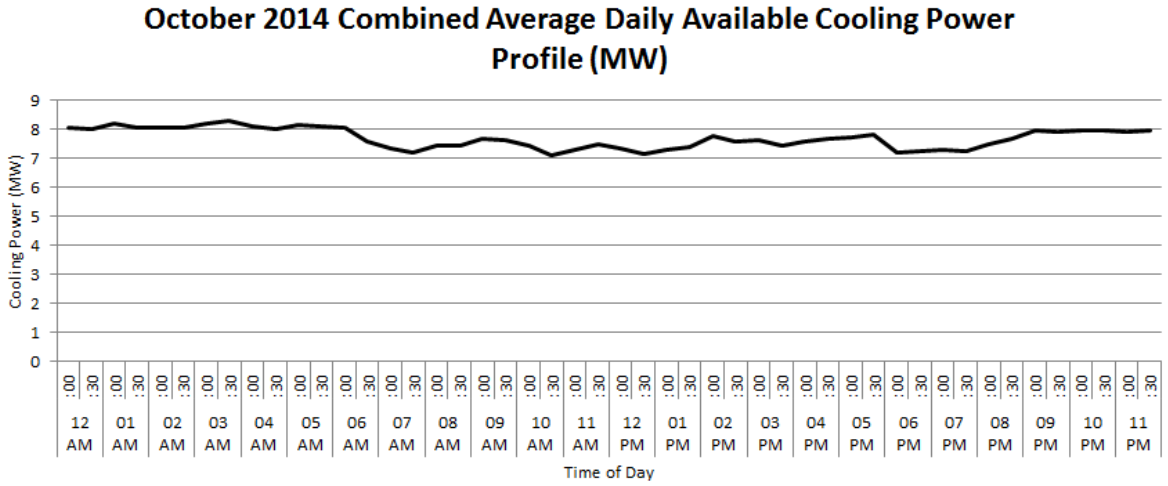

Figure 4.6: Combined average daily available cooling power profile in MW for October 2014

Table 4.1: Table of results from combined averaged daily profiles

Result	Aug-14			Oct-14		
	Min	Average	Max	Min	Average	Max
Combined average daily load: P_{load} (MW)	84	92.81	100	100	109.5	118
Combined average daily recovered heat: $\dot{Q}_{h,total}$ (MW)	11	12.85	14	13	14.26	16
Combined average daily generated electricity: $\dot{W}_T$ (MW)	2.4	2.71	2.9	2.7	3	3.3
Combined average daily available cooling power: $QM\dot{W}_{cold}$ (MW)	6.2	6.92	7.4	7.1	7.68	8.3
Average thermal energy recovery efficiency (%)	13.85			13.02		
Average combined load-to-generated electricity efficiency (%)	2.92			2.74		
Total average combined utilised waste energy (cooling + electrical) efficiency (%)	74.94			74.89		

4.1.3 Prediction data array

The prediction data array was generated utilising the historical raw data obtained from Glencore Ferrochrome in Rustenburg. This historical raw data can always be expanded as time progresses and more historical data is obtained, and therefore the prediction data array is subject to change and an improvement in accuracy. From the limited historical data that

was obtained from Glencore Ferrochrome for the purpose of this research, the prediction data array was developed in the form of a [48 x 24] array with an average combined daily profile of each furnace operation data field according to the historical raw data of each data field.

4.1.4 Optimal power dispatch schedule

The optimal power dispatch schedule is generated at each half hour time interval in the given month. At each time interval this schedule consists of the following:

- The i and j data stamp values,
- The T.O.U period,
- The apparent and real furnace load power values in MVA and MW respectively,
- The amount of thermal power that is extracted from the process off gas in MW,
- The amount of additional electrical power generated via the cogeneration system in MW,
- The amount of this electrical power that is dispatched to the furnace loads in MW,
- The remaining electrical power that is dispatched back onto the utility grid in MW, and
- The available cooling power in MW.

The model operates in real-time and the schedule is updated constantly every 30 minutes. The past-to-present schedule is the EPD model-generated schedule from the start of the month up until the current time interval. Examples of EPD model-generated schedule segments for specific chosen time ranges in the winter and summer months, 2014/08/18 10:00 to 2014/08/19 00:00 (winter month) and 2014/10/10 17:00 to 2014/10/11 07:00 (summer month), as they were written to the CogenOutput result spread sheet, are shown in Table C.1 and C.2 respectively. Figures 4.7 and 4.8 show a graphical representation of these EPD schedule segments. As time goes on and the following time interval is reached, a new optimal power dispatch schedule is calculated for this time interval and the overall past-to-present schedule updated with this latest schedule result. This process continues until the end of the given month and starts again at the beginning of the following month.

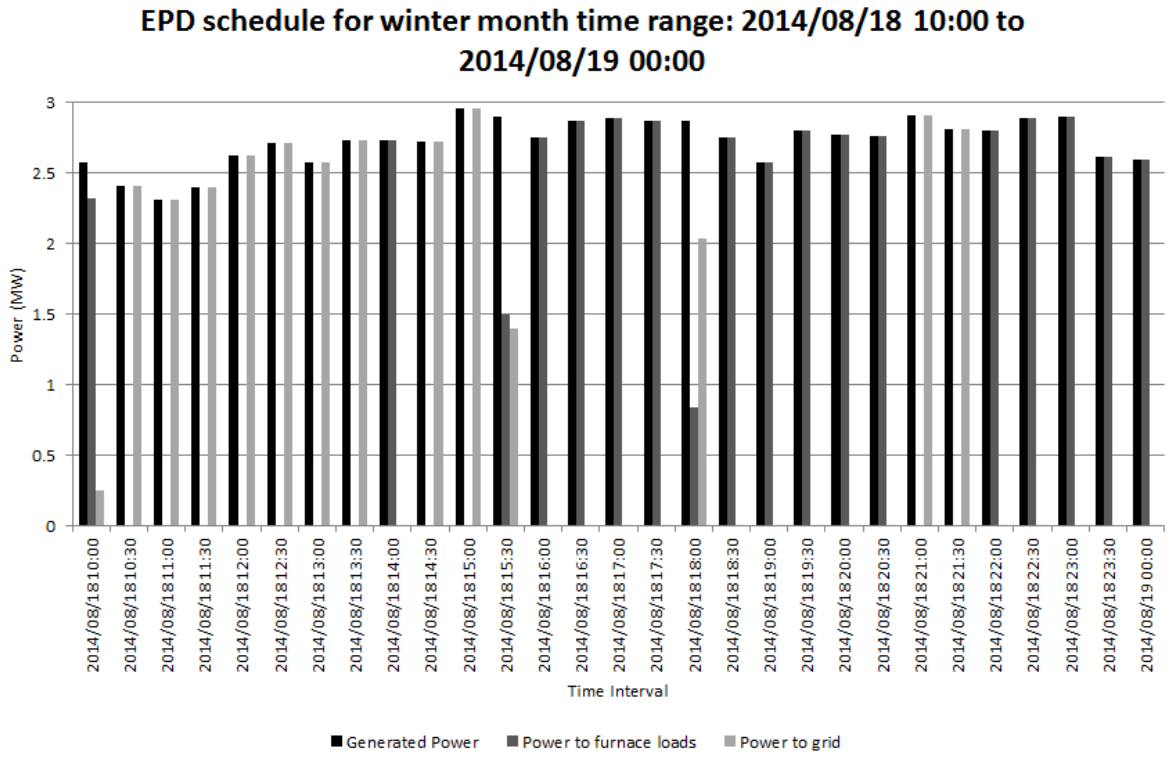

Figure 4.7: Graphical representation of EPD schedule for chosen winter month time range

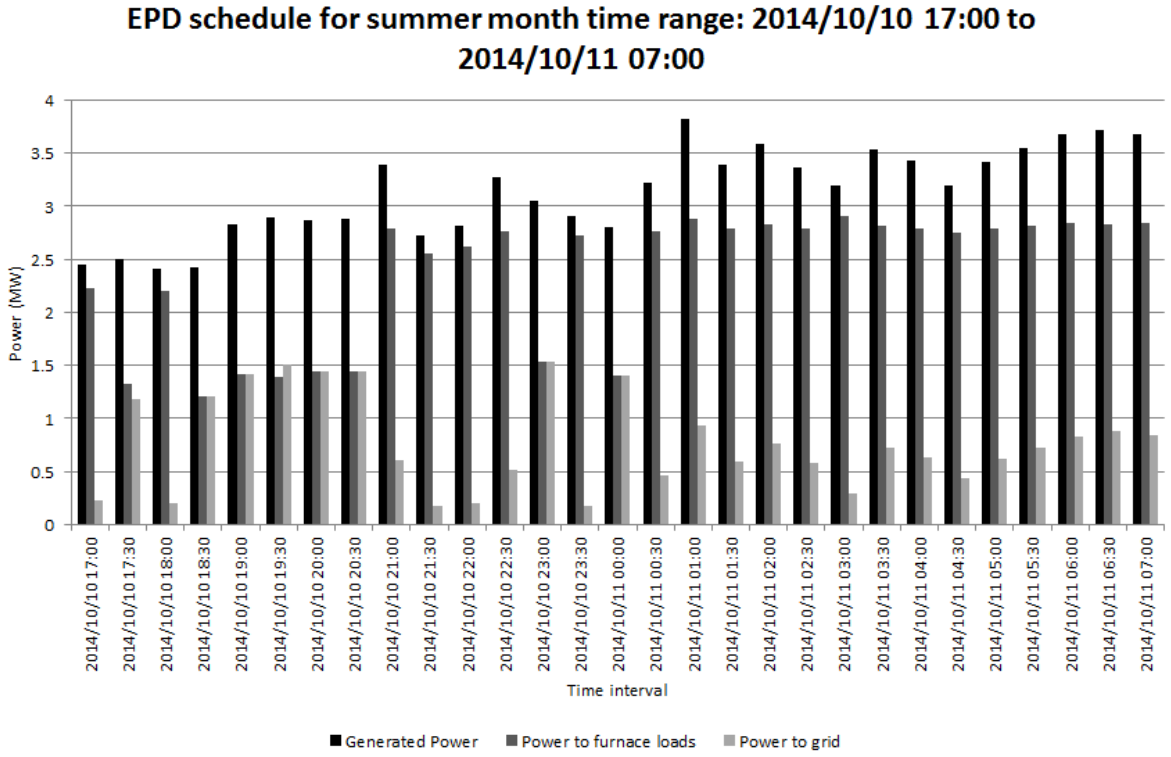

Figure 4.8: Graphical representation of EPD schedule for chosen summer month time range

4.1.5 Final system and facility associated energy savings

The final system associated cost savings are calculated as per equations (3.112). It is often more useful however to refer to energy and cost savings as a percentage of the original energy cost. Therefore a percentage cost savings is also calculated by taking the percentage of the total system associated cost savings divided by the total initial energy cost. Although the model optimisation operates on the basis of minimising the overall cost of energy at each time interval, using all acquired system operation data up until the current time interval and predicted data for time intervals beyond the current, the overall energy and cost savings figure that is of the most importance is the cost savings calculated at the end of the month. This is because at the end of the month only real system operation data has been utilised.

For the chosen winter and summer month the final calculated cost savings were obtained as shown in Table 4.2.

Table 4.2: Table of total energy cost and savings for chosen winter and summer month

August 2014 Cost and Savings		October 2014 Cost and Savings	
Total Initial Cost	R 58 100 771.05	Total Initial Cost	R 45 664 431.30
Total Final Cost	R 56 571 653.57	Total Final Cost	R 44 545 569.01
Total Savings	R 1 529 117.48	Total Savings	R 1 118 862.29
% Savings	2.63%	% Savings	2.45%

Therefore, assuming the costs and savings as obtained in Table 4.2 are similarly achieved for each summer and winter month in the given year, 2014, an approximate annual energy savings figure of R 14 657 113.05 could potentially be obtained for Glencore Ferrochrome in Rustenburg.

CHAPTER 5 DISCUSSION OF RESULTS

5.1.1 Potential for additional savings from available cooling power

There are many requirements for cooling throughout the plant at Glencore Ferrochrome in Rustenburg, the most prominent being the cooling plant of the facility that provides cooling water for the furnace shells. Additional cooling requirements include cooling fans throughout the plant in numerous plant rooms such as the transformer rooms or the hydraulic rooms, cooling fans for the cooling of transformer and hydraulic oil, and office building, control room and MCC room comfort cooling provided by specialised industrial air conditioners. From this it can be concluded that the majority of all cooling requirements are fulfilled through the utilisation of electric motors for fans and air conditioning units.

It was therefore assumed that the cooling power could be determined by considering the size of the electric motors that operate the numerous fans throughout the facility that are responsible for meeting the cooling requirements. In the case of air conditioners, the cooling power could also be determined by considering the electrical load size of the various air conditioning units. With these considerations in mind and through consultation with the facility concerning the aforementioned cooling equipment sizes and quantities, an estimated cooling capacity requirement in kW was obtained. This is shown in Table 5.1.

Table 5.1: Glencore Ferrochrome sectional cooling capacity requirements

Section Requiring Cooling	Calculated Cooling Capacity (kW)
Cooling Plant	576.82
Furnaces 1 to 4	876.52
Block Plant	47
Dispatch	200

In addition to the facility sections covered in Table 5.1, all cooling requirements, comfort cooling and air conditioners, within the section of workshops and offices also need to be accounted for. A combined sectional load of 355 kW was obtained for workshops and offices at the facility. According to [40], 40% of the energy consumption in commercial

buildings can be attributed to air conditioners. However, since workshops are composed of some non-commercial equipment such as heavy machinery, this percentage is slightly higher for the workshops and offices section. Therefore it was assumed that 30% of the energy consumed in the workshops and offices was due to air conditioning and comfort cooling systems. Utilising this assumption in conjunction with the information in Table 5.1, the overall facility estimated cooling capacity requirement in MW was calculated as is shown in equation (5.1) and (5.2).

$$Cooling\ Capacity\ (kW) = 576.82 + 876.52 + 47 + 200 + 30\% \times (355) = 1806.84 \quad (5.1)$$

$$Cooling\ Capacity\ (MW) = \frac{Cooling\ Capacity\ (kW)}{1000} = 1.81\ MW \quad (5.2)$$

Therefore a total facility-wide cooling capacity of 1.81 MW is required. From Chapter 4, a total combined average available cooling power, obtained via the utilisation of the cogeneration system by-product of low grade heat for cooling purposes, of 6.92 and 7.68 MW, for the chosen winter and summer month respectively, was found. This is significantly more than the facility required cooling capacity of 1.81 MW. Therefore it can be assumed that the cooling power obtained via the proposed absorption refrigeration system that utilises the cogeneration system wasted low grade thermal energy is more than sufficient to meet all facility cooling demands.

Although the sections of the facility that require cooling, except for the furnaces, do not fall within the established model boundary, additional savings can be calculated simply by applying the MEGAFLEX active energy charges to the now substituted cooling power capacity of the facility. In addition to this the furnace load can be reduced to account for the cooling power capacity required by the furnaces, which fall within the established model boundary. Utilising the chosen winter and summer months to calculate additional savings outside the model boundary and by decreasing the combined furnace load by 876.52 kW, as shown in Table 5.1, at an assumed power factor equal to the current combined furnace load power factor, the overall energy savings were obtained as:

- Combined additional furnace savings for August 2014: R 507 005.82
- Combined additional furnace savings for October 2014: R 325 489.04
- Additional facility savings from substituted cooling power for August 2014: R 473 558.28
- Additional facility savings from substituted cooling power for October 2014: R 493 562.02

On top of the savings incurred as a result of the implementation of the proposed heat recovery cogeneration system, and again assuming these savings are similarly achieved for each summer and winter month in the given year, 2014, an approximate annual cost savings figure of R 24 970 264.89 could potentially be obtained for Glencore Ferrochrome in Rustenburg, an increase in R 10 313 151.84 annually due to the utilisation of the available cooling power from the proposed power generation system.

5.1.2 Potential project payback period

It is clear from Chapter 4 that significant energy savings can be achieved through the utilisation of a heat recovery cogeneration system and associated EPD model for the optimal power dispatch schedule development. However, cogeneration and power generation technologies are still relatively expensive and the success of such a proposed system or project is often determined by the payback period of the project. The payback period is the time it takes for the project savings to equal the cost of implementation and installation of the entire system, basically for the savings to pay back the capital or system start-up costs. Therefore before a conclusion can be made on the success of the system proposed in this research, a payback period needs to be established. A summary of the potential costs required for the implementation of the proposed cogeneration and cooling systems is shown in Table 5.2.

The costs in Table 5.2 were converted from € to R utilising the current exchange rate: € 1 = R 13.71. Taking into account additional costs for installation and labour (works costs), the payback period for the proposed entire system was found to be approximately 4 to 5 years.

Table 5.2: Capital costs associated with the ORC cogeneration and absorption refrigeration systems

System Component	Cost	Currency
Turboden TD40 ORC Unit	3 905 000.00	€
	53 537 550.00	R
Intermediate Gas/Oil Thermal Exchanger	2 600 000.00	€
	35 646 000.00	R
2 MW single stage hot water chiller	3 000 000.00	R
Total cost in R:	92 183 550.00	R

5.1.3 Direct CO gas combustion and closed furnaces

The furnaces at Glencore Ferrochrome in Rustenburg are open furnaces. This means that the CO gas that is produced, as a result of the furnace internal chemical reactions, exits the top of the furnace material, comes into contact with surrounding air and autoignites to form CO_2, which is not flammable in its current state. Closed furnaces allow for CO gas exiting the top of the furnace to remain in the current state as free air does not exist and autoignition does not occur. CO gas is highly flammable and possesses a heat of combustion of 10.1 MJ/kg CO gas.

Assuming the furnaces at Glencore Ferrochrome in Rustenburg operated in the exact same manner, but were closed furnaces, if the produced CO gas was ignited, a potential combined available heat, as is calculated via equation (5.3) and (5.4), can be determined. According to Table B.2, the amount of CO gas produced per batch feed is 1 241.83 kg/batch. With the furnace batch feed rates as specified in Table B.4, the total combined mass flow rate of CO gas is calculated as shown in equation (5.3). Multiplying this mass flow rate with the heat of combustion of CO gas, an overall available heat can be calculated as is shown in equation (5.4).

$$\dot{m_{CO\ gas}} = \frac{1241.83\ kg}{batch} \times \left(3 \times \left(\frac{110\ batches}{day}\right) + \left(\frac{160\ batches}{day}\right)\right) \times \frac{1\ day}{86400\ s} = 7.04\ kg/s \quad (5.3)$$

$$\dot{Q_{CO\ gas}} = \frac{10.1\ MJ}{kg\ CO\ gas} \times \dot{m_{CO\ gas}} = 71.10\ MW \quad (5.4)$$

The direct burning of CO gas can be utilised in a gas turbine to generate electrical energy. Gas turbines are capable of operating at efficiencies of greater than 80% [41]. The gas turbine potential electrical power output from the heat of combustion calculated in equation (5.4) is calculated via equation (5.5).

$$\dot{W_{T,gas}} = 80\% \times \dot{Q_{CO\,gas}} = 56.88\ MW \tag{5.5}$$

This electrical power output from the same amount of CO produced from the current furnace operations, is significantly higher than the electrical power obtained through the methods followed in this research. The reason for this is that heat exchangers are considerably less efficient than the direct burning of fuel. This shows that the utilisation of closed furnaces as opposed to open furnaces, offers a much greater potential for heat recovery and the generation of additional useful electrical energy.

5.1.4 WEPS energy rates

The WEPS are the base energy rates that Eskom utilises outside of already established energy pricing tariff structures. Due to the relatively recent nature of the feed of electrical power back to the utility grid, no specific generation and feed-in energy tariff structure has yet been implemented. As was used in this research, in the development of the EPD model objective and cost function, a facility feeding electrical power back onto the grid obtains a financial incentive from a third-party customer, or Eskom itself, who buys this electrical power. The rates that are implemented for this transaction are the base or WEPS energy rates.

It was noticed however that the WEPS energy rates had a significant impact on the EPD model schedule and the overall system associated savings. The WEPS energy rates as they are established in Eskom's Tariffs and Charges Booklet for 2013-2014 [37] were found to be too low to allow for or encourage the feed of electrical power back onto the utility grid, as the EPD schedule developed dispatched all additionally generated electrical energy to the furnace loads instead. Essentially the financial incentive offered for the feed of electrical power back onto the utility grid to be used by third party customers, or Eskom

itself, was too low. Therefore, for the purpose of this research, the WEPS energy rates were adjusted in order to test the dispatch of additionally generated electrical energy, not only to the furnaces, but back onto the grid as well. All results and savings as they appear in Chapter 4 are based on the adjusted WEPS energy rates. Table 5.3 shows the initial and adjusted WEPS energy rates.

Table 5.3: Initial and adjusted WEPS energy rates

	Local Authority WEPS Energy Rates					
	High demand season			Low demand season		
	Peak	Standard	Off Peak	Peak	Standard	Off Peak
Initial WEPS rates [37]	186.14	56.39	30.62	60.72	41.79	26.52
Adjusted WEPS rates	211.06	68.01	39.21	72.56	51.58	34.66
% Increase	13.39%	20.61%	28.05%	19.50%	23.43%	30.69%

Therefore for the successful implementation of a system that will potentially feed electrical energy back onto the utility grid, incentive energy rates, currently the WEPS energy rates, will need to be established that will encourage the feed of electricity back onto the utility grid. In addition to this, the proposed rate can be flexible. During times of severely high nationwide electricity demand and strain the utility could introduce much higher incentive energy rates that will encourage the facility to dispatch most, if not all, of its additionally generated power back to the grid, which will assist and support the grid considerably with the meeting of this increased demand.

Glencore Ferrochrome in Rustenburg is situated very close to rural township and housing communities. These townships often have very limited access to electricity. If an average household maximum demand of 2 kW was assumed, the amount of additionally generated electrical power has the potential to feed more than 1000 households. Therefore, Eskom could also offer the facility increased energy incentives for the feed of additionally generated electrical energy back onto the utility grid, to assist with the supply of a stable electrical connection for these communities.

5.1.5 Seasonal system variations

It is important to note the differences in the system and model outputs and results that occur as a result of the change in season, winter months versus summer months. Although the results do not differ significantly between the seasons, the comfort cooling required throughout the facility is considerably less in winter. In fact, during winter months, heating is required rather than cooling. An improvement in the system could also be made to provide the facility with comfort heating in addition to comfort cooling, when it is preferred during winter months.

It was noticed that slightly more cost savings were obtained for winter months as opposed to summer months, about 0.18%. This can be attributed to a decrease in the ambient temperature, but more significantly to the high active energy consumption rates, especially during peak and standard T.O.U energy consumption periods. Being able to significantly reduce the amount of active energy consumed from the utility grid through the substitution of this energy via the cogeneration system, during these T.O.U periods with very high active energy consumption rates in comparison to summer months, allowed for the slight increase in the overall system associated energy and cost savings during winter months.

5.1.6 Improvements

There were a number of improvements that were identified with regards to this research. The most significant improvements identified are:

- The thermal energy recovery efficiency can be improved by allowing for a lower bagplant inlet temperature, thereby improving the cogeneration system heat exchanger efficiency.
- The excess cooling power, more than 5 MW of cooling power, can be sold and dispatched to outlying or adjacent facilities to meet additional cooling requirements and to allow for additional financial incentives.
- The EPD model generated schedule and savings can be further improved by improving the accuracy of the generated prediction or forecast data array. Significantly more and up-to-date historical data is required for this improvement.

CHAPTER 6 CONCLUSION

The proposed overall system, consisting of the heat recovery cogeneration system for electrical energy generation, the EPD model for the development of the optimal power dispatch schedule, and the absorption refrigeration system for cooling power generation, has the potential to produce significant energy and associated cost savings for Glencore Ferrochrome in Rustenburg, while supporting the facility, the utility grid and the surrounding community with a stable supply of electrical power of between 2 and 3 MW. An annual system associated energy savings for the facility of approximately R 24 970 264.89, with a project payback period of between 4 and 5 years, was found. For the mining and smelting industry, this is an acceptable project payback period.

Even with the savings calculated as above and the acceptance of the project payback period, there are a few improvements that can be made to the project that will allow for even more energy and associated cost savings. One such improvement that has not previously been mentioned is the complete revamp of the furnaces to convert them to closed furnaces. Although this will introduce significantly higher energy savings due to the improved heat extraction and power generation efficiencies, the cost associated with the facility revamp is also expected to be extremely high. However, this is a unique and separate project that can be considered at a later stage in the facility's development.

In conclusion, with a continuous rise in the demand for energy, and more so electricity, and the rapid rate in which natural resources are depleted, the field of renewable energy sources and waste energy recovery and utilisation has never been more important. The system proposed in this research, the first of its kind not only in the country, but the whole of Africa as well, is a small but vital stepping stone in managing our current energy crisis.

REFERENCES

[1] R. T. Jones, "Electric Smelting in Southern Africa," 2013, http://www.mintek.co.za/Pyromet/, Directory: 2013, File: Presentation: Electric Smelting in Southern Africa (Plenary address at EMC 2013).pdf. Last accessed 31 October 2014.

[2] P. Niemelä & M. Kauppi, "Production, Characteristics and Use of Ferrochromium Slags," in *11th Int. Ferro Alloys Congress (INFACON XI), 18-21 February, 2007, New Delhi, India:* International Committee on Ferro Alloys, 2007, pp. 171-179.

[3] X. Pan, "Effect of South Africa Chrome Ores on Ferrochrome Production," in *Int. Conf. on Mining, Mineral Processing and Metallurgical Eng. (ICMMME'2013), 15-16 April, 2013, Johannesburg, South Africa*, 2013, pp. 106-110.

[4] P. C. Hayes, "Aspects of SAF Smelting of Ferrochrome," in *10th Int. Ferro Alloys Congress (INFACON X), 1-4 February, 2004, Cape Town, South Africa:* Transformation through Technology, 2004.

[5] E. N. Cameron, "Chromite in the central sector of the Eastern Bushveld Complex, South Africa," *American Mineralogist*, vol. 62, no. 1977, pp. 1082-1096, 1977.

[6] R. G. Cawthorn, "The Platinum Group Element Deposits of the Bushveld Complex in South Africa," *Platinum Metals Rev.*, vol. 54, no. 4, pp. 205-215, 2010.

[7] J. G. Roos & A. M. Hearn, "Optimising the Effective Use of Energy in the Ferroalloy Industry through Innovative Technology," in *10th Int. Ferro Alloys Congress (INFACON X), 1-4 February, 2004, Cape Town, South Africa*, 2004.

[8] H. Takahashi, K. Ichihara & T. Homma, "Operational Improvement of a Submerged Arc Furnace in Kashima Works (KF-1)," in *13th Int. Ferro Alloys Congress (INFACON XIII), 9-13 June, 2013, Almaty, Kazakhstan*, 2013.

[9] J. Daavittila, M. Honkaniemi & P. Jokinen, "The transformation of ferrochromium smelting technologies during the last decades," in *10th Int. Ferro Alloys Congress (INFACON X), 1-4 February, 2004, Cape Town, South Africa*, 2004.

[10] *Standard Handbook for Electrical Engineers.* 16th ed., The McGraw-Hill Companies, pp. 5.111–5.115, 2013.

[11] D. Hui, L. Jie, L. Zhi-ming, Z. Yong & C. Jiu-ju, "Cogeneration system utilising waste heat from sinter-cooling process," in *2010 2nd Int. Symp. on Power Electron. for Distributed Generation Syst. (PEDG)*, 2010, pp. 674-677.

[12] S. Bhawan & R.K. Puram, "Cogeneration," in *Energy Efficiency in Thermal Utilities*, 3rd ed., New Delhi, India: Bureau of Energy Efficiency, 2010, ch. 7, pp. 115–167.

[13] L. Sun, W. Han, W. Jing, D. Zheng & H. Jin, "A power and cooling cogeneration system using mid/low-temperature heat source," *Applied Energy*, vol. 112, no. 2013, pp. 886-897, May 2013.

[14] D. Wei, X. Lu, Z. Lu & J. Gu, "Performance analysis and optimisation of organic Rankine cycle (ORC) for waste heat recovery," *Energy Conversion and Management*, vol. 48, no. 2007, pp. 1113-1119, Dec. 2006.

[15] R. Chacartegui, D. Sánchez, J. M. Muñoz & T. Sánchez, "Alternative ORC bottoming cycles FOR combined cycle power plants," *Applied Energy*, vol. 86, no. 2009, pp. 2162-2170, Mar. 2009.

[16] T. C. Hung, S. K. Wang, C. H. Kuo, B. S. Pei & K. F. Tsai, "A study of organic working fluids on system efficiency of an ORC using low-grade energy sources," *Energy*, vol. 35, no. 2010, pp. 1403-1411, Dec. 2009.

[17] U. Drescher & D. Brüggemann, "Fluid selection for Organic Rankine Cycle (ORC) in biomass power and heat plants," *Applied Thermal Eng.*, vol. 27, no. 2007, pp. 223-228, July 2006.

[18] B. Saleh, G. Koglbauer, M. Wendland & J. Fischer, "Working fluids for low-temperature organic Rankine cycles," *Energy*, vol. 32, no. 2007, pp. 1210-1221, 2006.

[19] B. T. Liu, K. H. Chien & C. C. Wang, "Effect of working fluids on organic Rankine cycle for waste heat recovery," *Energy*, vol. 29, no. 2004, pp. 1207-1217, 2004.

[20] V. Minea, "Power generation with ORC machines using low-grade waste heat or renewable energy," *Applied Thermal Eng.*, vol. 69, no. 2014, pp. 143-154, Apr. 2014.

[21] S. Quoilin & V. Lemort, "Technological and Economical Survey of Organic Rankine Cycle Systems," in *5th European Conf., 14-17 April, 2009, Algarve, Portugal*, 2009.

[22] Turboden, "Turboden ORC plants for Industrial Heat Recovery," 2014, http://www.turboden.eu/en/downloads/downloads.php/, Directory: Presentations, File: Presentation: Heat Recovery Presentation - 2014.pdf. Last accessed 31 October 2014.

[23] H.M. Groscurth, T. Bruckner & R.Kummel, "Modelling of energy-services supply systems," *Energy*, vol. 20, no. 9, pp. 941–958, Sept. 1995.

[24] T. Krause, L. Yang & G. Andersson, "Modelling interconnected national energy systems using an energy hub approach," in *2011 IEEE Trondheim Power Tech*, Trondheim, June 19-23. 2011.

[25] M. Liu, Y. Shi & F. Fang, "Optimal power flow and PGU capacity of CCHP systems using a matrix modelling approach," *Applied Energy*, vol. 102, pp. 794–802, Feb. 2013.

[26] L. Wang & C. Singh, "Stochastic combined heat and power dispatch based on multi-objective particle swarm optimisation," *Int. J. Elect. Power Energy Syst.*, vol. 30, no. 3, pp. 226–234, Mar. 2008.

[27] J.H. Talaq, F. El-Hawary & M.E. El-Hawary, "A summary of environmental/economic dispatch algorithms," *IEEE Trans. Power Syst.*, vol. 9, no. 3, pp. 1508–1516, Aug. 1994.

[28] B. Mohammadi-Ivatloo, M. Moradi-Dalvand & A. Rabiee, "Combined heat and power economic dispatch problem solution using particle swarm optimisation with time varying acceleration coefficients," *Electric Power Syst. Research*, vol. 95, pp. 9–18, Feb. 2013.

[29] G. Carpinelli, G. Celli, A. Russo & F. Pilo, "Distributed generation siting and sizing under uncertainty," in *2001 IEEE Porto Power Tech Proc.*, vol. 4, 2001.

[30] M. Pipattanasomporn, M. Willingham & S. Raham, "Implications of on-site distributed generation for commercial/industrial facilities," *IEEE Trans. Power Syst.*, vol. 20, no. 1, pp. 206–212, Feb. 2005.

[31] M. Geidl & G. Andersson, "Optimal Power Flow of Multiple Energy Carriers," *IEEE Trans. Power Syst.*, vol. 22, no. 1, pp. 145–155, Feb. 2007.

[32] K. Hemmes, J.L. Zachariah-Wolf, M. Geidl & G. Andersson, "Towards multi-source multi-product energy systems," *Int. J. Hydrogen Energy*, vol. 32, no. 10-11, pp. 1332–1338, July-Aug. 2007.

[33] M. Geidl & G. Andersson, "A modelling and optimisation approach for multiple energy carrier power flow," in *2005 IEEE Russia Power Tech*, pp. 1–7, St. Petersburg, June 27-30. 2005.

[34] J. Carpentier, "Optimal power flows," *Int. J. Elect. Power Energy Syst.*, vol. 1, no. 1, pp. 3–15, Apr. 1979.

[35] L.D. Coelho & V.C. Mariani, "An improved harmony search algorithm for power economic load dispatch," *Energy Conversion and Management*, vol. 50, no. 10, pp. 2522–2526, Oct. 2009.

[36] M. Geidl & G. Andersson, "Optimal power dispatch and conversion in systems with multiple energy carriers," in *2005 Power Syst. Computation Conf. (PSCC)*, Zurich, 2005.

[37] Eskom, "Tariff & Charges Booklet 2013/14," April 2013, http://www.eskom.co.za/CustomerCare/TariffsAndCharges/Pages/, Directory: Tariffs and Charges, Tariff history, File: 2013/14.pdf. Last accessed 31 October 2014.

[38] Turboden, 2014, http://www.turboden.eu/en/home.index.php. Last accessed 31 October 2014.10.31

[39] Eskom, "Generator tariff charges 2013/14," http://www.eskom.co.za/CustomerCare/TariffsAndCharges/Pages/, Directory: Tariffs and Charges, Pricing Related Information for Generators. Last accessed 31 October 2014.

[40] W. Cass, J. Zhang & X. Xia, "Energy management of commercial buildings – A case study from a POET perspective of energy efficiency," *J. Energy South Africa*, vol. 23, no. 1, pp. 23–31, Feb. 2012.

[41] *Standard Handbook for Electrical Engineers.* 16th ed., The McGraw-Hill Companies, pp. 6.25, 2013.

ADDENDUM A MATLAB PROGRAMMING CODE

A.1 MAIN EPD MODEL FILE

```
%%  Author: Michael Chennells
%%  Naming conventions chosen in accordance with report naming conventions.
%%  Department of Electrical, Electronic and Computer Engineering.
%%  Date:
%%  Main cogeneration optimisation model m file.

%% Generate data file using prediction file and current data file.

clear;  %Clear workspace and variables.

%Load prediction file from prediction spread sheet.
PredData = xlsread('PredData','Prediction Data');
PredData = PredData(1:(end-1),:); %Ignore data last entry.
CurData = xlsread('DataBook');  %Read current data from data spread sheet.

%Generate and adjust data Time and Date information to Matlab reference.
CurFileDate = CurData(:,1);
CurFileDate = CurFileDate + datenum('30-Dec-1899 00:00:00');

%Determine size of current data file, number of entries is number of rows.
CurDataS = size(CurData);
CurEntries = CurDataS(1,1);

%Determine Date and Time of Interest variable which is the latest Date and time
entry from current data file.
DaToInt = CurFileDate(CurEntries,1);

%Determine number of days in current month using first date entry.
StartDaT = datevec(CurFileDate(1));
DaysInMonth = eomday(StartDaT(1,1),StartDaT(1,2));
RowEntries = (48*DaysInMonth) + 1;

%Final Data array is set to current data file up to current data point of
interest, and to appropriate prediction values for all future data points beyond
the current data point of interest.
for row = 1:RowEntries

    if row < (CurEntries + 1)
       Data(row,:)=[CurFileDate(row),CurData(row,2:end)];
    else
        DaToInt = DaToInt + (1/48); %Increment point of interest 30 min.
        %Determine row r in prediction file array to use.
        DaToIntVector = datevec(DaToInt);
        r = 2*DaToIntVector(1,4) + 1;

        if DaToIntVector(1,5) == 30
            r = r + 1;
        end

        Data(row,:)=[DaToInt,PredData(r,:)]; %Final working Data array.
    end
end
```

```
%% Read time and date from raw data spread sheet DataBook into Matlab array,
generate date array FDateVector(Y, M, D, h, m).

Date = Data(:,1);  %Read time & date from data into Matlab.
DateVector = datevec(Date);  %Create date array (Y, M, D, h, m, s).

%Seconds column is not used and is omitted resulting in FDateVector.
FDateVector = DateVector(1:RowEntries,1:5);

%% Determine how many data point entries there are, different for different
months.

Entries = size(Date);  %Determines dimensions of Date array (row,column).
RowEntries = Entries(1,1);  %Row value is number of data point entries.

%% Calculate arrays i and j, number of days in the month, n, generate final
%% work array FWorkArray in the form [i, j, Y, M, D, h, m, DayNumber(1-7)].

n = max(FDateVector(:,3));
i = FDateVector(:,3);
j = ceil((2*FDateVector(:,4)) + (FDateVector(:,5)/30));
DayNumber = weekday(Date);  %Generate day number 1 - 7 (Sunday to Monday).

%j must be from 1 to 48. j formula above calculates values of 0 that should
%be 48. Therefore set all these 0 values to 48. i must be from 1 to n and
%the last data point for each day must be considered as part of the previous
%day due to the back-filling of data assumed. Therefore the final i value
%per day must also be adjusted.
for row = 1:RowEntries

    if j(row) == 0
        j(row) = 48;
        i(row) = i(row) - 1;

        %Shift DayNumber to account for backfilling property of data.
        DayNumber(row) = DayNumber(row) - 1;

        if DayNumber(row) == 0
            DayNumber(row) = 7;
        end

        if i(row) == 0
            i(row) = i(row) + n;
        end
    end
end

FWorkArray = [i j FDateVector DayNumber];  %Final work array.

%% Set SHigh flag. Set to 1 for high demand season and set to 0 for low
%% demand season.

switch FWorkArray(1,4)
    case{6,7,8}
        SHigh = 1;
    otherwise
        SHigh = 0;
end

%% Generate Day array and add to FWorkArray. Day = 1 (Mon-Fri), 2 (Sat) and
%% 3 (Sun).

for row = 1:RowEntries
```

```
    if FWorkArray(row,8) == 1  %Sunday
        Day(row,1) = 3;
    elseif FWorkArray(row,8) == 7  %Saturday
        Day(row,1) = 2;
    else
        Day(row,1) = 1; %Monday - Friday
    end
end

FWorkArray = [FWorkArray Day];  %Add Day array to FWorkArray.

%% Generate peak (P), standard (S) and off-peak (O) time-of-use flag arrays
%% according to MEGFLEX defined time-of-use periods. Add P, S and O flag
%% arrays to FWorkArray.

%Generate Pi,j array.
for row = 2:RowEntries
    if FWorkArray(row,9) == 1
        if (FWorkArray(row,2) >= 15 && FWorkArray(row,2) <= 20) || ...
                (FWorkArray(row,2) >= 37 && FWorkArray(row,2) <= 40)
            P(FWorkArray(row,1),FWorkArray(row,2)) = 1;
        end
    else
        P(FWorkArray(row,1),FWorkArray(row,2)) = 0;
    end
end

%Generate Si,j array.
for row = 2:RowEntries
    if FWorkArray(row,9) == 1
        if (FWorkArray(row,2) >= 13 && FWorkArray(row,2) <= 14) || ...
                (FWorkArray(row,2) >= 21 && FWorkArray(row,2) <= 36) || ...
                (FWorkArray(row,2) >= 41 && FWorkArray(row,2) <= 44)
            S(FWorkArray(row,1),FWorkArray(row,2)) = 1;
        end
    elseif FWorkArray(row,9) == 2
        if (FWorkArray(row,2) >= 15 && FWorkArray(row,2) <= 24) || ...
                (FWorkArray(row,2) >= 37 && FWorkArray(row,2) <= 40)
            S(FWorkArray(row,1),FWorkArray(row,2)) = 1;
        end
    else
            S(FWorkArray(row,1),FWorkArray(row,2)) = 0;
    end
end

%Generate Oi,j array.
for row = 2:RowEntries
    if FWorkArray(row,9) == 1
        if (FWorkArray(row,2) >= 1 && FWorkArray(row,2) <= 12) || ...
                (FWorkArray(row,2) >= 45 && FWorkArray(row,2) <= 48)
            O(FWorkArray(row,1),FWorkArray(row,2)) = 1;
        end
    elseif FWorkArray(row,9) == 2
        if (FWorkArray(row,2) >= 1 && FWorkArray(row,2) <= 14) || ...
                (FWorkArray(row,2) >= 25 && FWorkArray(row,2) <= 36) || ...
                (FWorkArray(row,2) >= 41 && FWorkArray(row,2) <= 48)
            O(FWorkArray(row,1),FWorkArray(row,2)) = 1;
        end
    elseif FWorkArray(row,9) == 3
        O(FWorkArray(row,1),FWorkArray(row,2)) = 1;
    else
        O(FWorkArray(row,1),FWorkArray(row,2)) = 0;
    end
```

```
end

%% Read F1-4 apparent and real load powers from raw data spread sheet
%% DataBook and generate all required furnace load i,j arrays.

%Read furnace data: F1MVA, F1MW, F2MVA, F2MW, F3MVA, F3MW, F4MVA, F4MW.
FPower = [Data(:,2),Data(:,3),Data(:,8),Data(:,9),Data(:,14),Data(:,15),...
    Data(:,20),Data(:,21)];

%Generate all furnace MVA and MW i,j arrays.
for row = 2:RowEntries
    F1MVA(FWorkArray(row,1),FWorkArray(row,2)) = FPower(row,1);
    F1MW(FWorkArray(row,1),FWorkArray(row,2)) = FPower(row,2);
    F2MVA(FWorkArray(row,1),FWorkArray(row,2)) = FPower(row,3);
    F2MW(FWorkArray(row,1),FWorkArray(row,2)) = FPower(row,4);
    F3MVA(FWorkArray(row,1),FWorkArray(row,2)) = FPower(row,5);
    F3MW(FWorkArray(row,1),FWorkArray(row,2)) = FPower(row,6);
    F4MVA(FWorkArray(row,1),FWorkArray(row,2)) = FPower(row,7);
    F4MW(FWorkArray(row,1),FWorkArray(row,2)) = FPower(row,8);
end

AbsSload = F1MVA + F2MVA + F3MVA + F4MVA;    %Calculate |Sload,i,j| array.
Pload = F1MW + F2MW + F3MW + F4MW;  %Calculate Pload,i,j array.

%% Read all required furnace and bagplant temperatures from raw data
%% spread sheet DataBook and generate all required temperature i,j arrays.

%Read F1-4 stack temperatures 1, 2 and 3, as well as bagplant 1-4 inlet
%temperatures
FTemp = [Data(:,4:7),Data(:,10:13),Data(:,16:19),Data(:,22:end)];

%Generate all furnace stack 1 - 3 and bagplant temperature i,j arrays.
for row = 2:RowEntries
    F1S1T(FWorkArray(row,1),FWorkArray(row,2)) = FTemp(row,1);
    F1S2T(FWorkArray(row,1),FWorkArray(row,2)) = FTemp(row,2);
    F1S3T(FWorkArray(row,1),FWorkArray(row,2)) = FTemp(row,3);
    B1T(FWorkArray(row,1),FWorkArray(row,2)) = FTemp(row,4);
    F2S1T(FWorkArray(row,1),FWorkArray(row,2)) = FTemp(row,5);
    F2S2T(FWorkArray(row,1),FWorkArray(row,2)) = FTemp(row,6);
    F2S3T(FWorkArray(row,1),FWorkArray(row,2)) = FTemp(row,7);
    B2T(FWorkArray(row,1),FWorkArray(row,2)) = FTemp(row,8);
    F3S1T(FWorkArray(row,1),FWorkArray(row,2)) = FTemp(row,9);
    F3S2T(FWorkArray(row,1),FWorkArray(row,2)) = FTemp(row,10);
    F3S3T(FWorkArray(row,1),FWorkArray(row,2)) = FTemp(row,11);
    B3T(FWorkArray(row,1),FWorkArray(row,2)) = FTemp(row,12);
    F4S1T(FWorkArray(row,1),FWorkArray(row,2)) = FTemp(row,13);
    F4S2T(FWorkArray(row,1),FWorkArray(row,2)) = FTemp(row,14);
    F4S3T(FWorkArray(row,1),FWorkArray(row,2)) = FTemp(row,15);
    B4T(FWorkArray(row,1),FWorkArray(row,2)) = FTemp(row,16);
end

%Calculate final F1-4 output temperature i,j arrays.
F1T = 1/3 * (F1S1T + F1S2T + F1S3T);
F2T = 1/3 * (F2S1T + F2S2T + F2S3T);
F3T = 1/3 * (F3S1T + F3S2T + F3S3T);
F4T = 1/3 * (F4S1T + F4S2T + F4S3T);

%% Find enthalpy values for each off gas constituent CO2, N2 and O2 for all
%% data point F1-4 and bagplant 1-4 temperatures using Find_Enthalpy
%% function which holds CO2, N2 and O2 enthalpy tables.

for row = 2:RowEntries
    %Furnace 1 outlet.
```

```
%Call Find_Enthalpy function to obtain enthalpy for each constituent at
%each furnace 1 outlet temperature.
[CO2,N2,O2] = Find_Enthalpy(F1T(FWorkArray(row,1),FWorkArray(row,2)));
%Generate constituent enthalpy arrays for furnace 1.
ECF1(FWorkArray(row,1),FWorkArray(row,2)) = CO2;
ENF1(FWorkArray(row,1),FWorkArray(row,2)) = N2;
EOF1(FWorkArray(row,1),FWorkArray(row,2)) = O2;

%Bagplant 1 inlet.
%Call Find_Enthalpy function to obtain enthalpy for each constituent at
%each bagplant 1 inlet temperature.
[CO2,N2,O2] = Find_Enthalpy(B1T(FWorkArray(row,1),FWorkArray(row,2)));
%Generate constituent enthalpy arrays for bagplant 1.
ECB1(FWorkArray(row,1),FWorkArray(row,2)) = CO2;
ENB1(FWorkArray(row,1),FWorkArray(row,2)) = N2;
EOB1(FWorkArray(row,1),FWorkArray(row,2)) = O2;

%Furnace 2 outlet.
%Call Find_Enthalpy function to obtain enthalpy for each constituent at
%each furnace 2 outlet temperature.
[CO2,N2,O2] = Find_Enthalpy(F2T(FWorkArray(row,1),FWorkArray(row,2)));
%Generate constituent enthalpy arrays for furnace 2.
ECF2(FWorkArray(row,1),FWorkArray(row,2)) = CO2;
ENF2(FWorkArray(row,1),FWorkArray(row,2)) = N2;
EOF2(FWorkArray(row,1),FWorkArray(row,2)) = O2;

%Bagplant 2 inlet.
%Call Find_Enthalpy function to obtain enthalpy for each constituent at
%each bagplant 2 inlet temperature.
[CO2,N2,O2] = Find_Enthalpy(B2T(FWorkArray(row,1),FWorkArray(row,2)));
%Generate constituent enthalpy arrays for bagplant 2.
ECB2(FWorkArray(row,1),FWorkArray(row,2)) = CO2;
ENB2(FWorkArray(row,1),FWorkArray(row,2)) = N2;
EOB2(FWorkArray(row,1),FWorkArray(row,2)) = O2;

%Furnace 3 outlet.
%Call Find_Enthalpy function to obtain enthalpy for each constituent at
%each furnace 3 outlet temperature.
[CO2,N2,O2] = Find_Enthalpy(F3T(FWorkArray(row,1),FWorkArray(row,2)));
%Generate constituent enthalpy arrays for furnace 3.
ECF3(FWorkArray(row,1),FWorkArray(row,2)) = CO2;
ENF3(FWorkArray(row,1),FWorkArray(row,2)) = N2;
EOF3(FWorkArray(row,1),FWorkArray(row,2)) = O2;

%Bagplant 3 inlet.
%Call Find_Enthalpy function to obtain enthalpy for each constituent at
%each bagplant 3 inlet temperature.
[CO2,N2,O2] = Find_Enthalpy(B3T(FWorkArray(row,1),FWorkArray(row,2)));
%Generate constituent enthalpy arrays for bagplant 3.
ECB3(FWorkArray(row,1),FWorkArray(row,2)) = CO2;
ENB3(FWorkArray(row,1),FWorkArray(row,2)) = N2;
EOB3(FWorkArray(row,1),FWorkArray(row,2)) = O2;

%Furnace 4 outlet.
%Call Find_Enthalpy function to obtain enthalpy for each constituent at
%each furnace 4 outlet temperature.
[CO2,N2,O2] = Find_Enthalpy(F4T(FWorkArray(row,1),FWorkArray(row,2)));
%Generate constituent enthalpy arrays for furnace 4.
ECF4(FWorkArray(row,1),FWorkArray(row,2)) = CO2;
ENF4(FWorkArray(row,1),FWorkArray(row,2)) = N2;
EOF4(FWorkArray(row,1),FWorkArray(row,2)) = O2;

%Bagplant 4 inlet.
```

```
    %Call Find_Enthalpy function to obtain enthalpy for each constituent at
    %each bagplant 4 inlet temperature.
    [CO2,N2,O2] = Find_Enthalpy(B4T(FWorkArray(row,1),FWorkArray(row,2)));
    %Generate constituent enthalpy arrays for bagplant 4.
    ECB4(FWorkArray(row,1),FWorkArray(row,2)) = CO2;
    ENB4(FWorkArray(row,1),FWorkArray(row,2)) = N2;
    EOB4(FWorkArray(row,1),FWorkArray(row,2)) = O2;
end

%% Initialise all model time independent constants using Time_Indep_Info
%% function.

[AMCO2, PercN2, PercO2, TotReqN2, TotReqO2, STPGasVol, ST, F1BpD, ...
    F2BpD, F3BpD, F4BpD, MWCO2, MWN2, MWO2, F1OGVol, F2OGVol, F3OGVol, ...
    F4OGVol, ID1, ID2, ID3, ID4, AD, gAD, ORCout, ORCcaptive, ThermalIn,...
    COP] = Time_Indep_Info();

%% Perform all required process chemical calculations in order to determine
%% overall available heat from combined furnace off gas recovery
%% cogeneration system and generate all furnace i,j available heat arrays.

%Calculate total off gas constituent mass flow rates in kg/s and generate
%appropriate mass flow rate i,j arrays.
for row = 2:RowEntries
    %Furnace 1.
    %Calculate m^3/h CO2.
    F1TotCO2(FWorkArray(row,1),FWorkArray(row,2)) = (AMCO2/MWCO2)*...
        (F1BpD/24) * STPGasVol * ((F1T(FWorkArray(row,1),...
        FWorkArray(row,2)) + ST)/ST);

    %Calculate m^3/h N2.
    F1N2(FWorkArray(row,1),FWorkArray(row,2)) = (TotReqN2/MWN2)*...
        (F1BpD/24) * STPGasVol * ((F1T(FWorkArray(row,1),...
        FWorkArray(row,2)) + ST)/ST);

    %Calculate m^3/h O2.
    F1O2(FWorkArray(row,1),FWorkArray(row,2)) = (TotReqO2/MWO2)*...
        (F1BpD/24) * STPGasVol * ((F1T(FWorkArray(row,1),...
        FWorkArray(row,2)) + ST)/ST);

    %Calculate excess N2.
    F1ExcN2(FWorkArray(row,1),FWorkArray(row,2)) = PercN2/100 * ...
        (F1OGVol - F1TotCO2(FWorkArray(row,1),FWorkArray(row,2))...
        - F1N2(FWorkArray(row,1),FWorkArray(row,2))...
        - F1O2(FWorkArray(row,1),FWorkArray(row,2)));

    %Calculate excess O2.
    F1ExcO2(FWorkArray(row,1),FWorkArray(row,2)) = PercO2/100 * ...
        (F1OGVol - F1TotCO2(FWorkArray(row,1),FWorkArray(row,2))...
        - F1N2(FWorkArray(row,1),FWorkArray(row,2))...
        - F1O2(FWorkArray(row,1),FWorkArray(row,2)));

    %Calculate total extracted m^3/h N2 (required + excess).
    F1TotN2(FWorkArray(row,1),FWorkArray(row,2)) = ...
        F1N2(FWorkArray(row,1),FWorkArray(row,2)) + ...
        F1ExcN2(FWorkArray(row,1),FWorkArray(row,2));

    %Calculate total extracted m^3/h O2 (required + excess).
    F1TotO2(FWorkArray(row,1),FWorkArray(row,2)) = ...
        F1O2(FWorkArray(row,1),FWorkArray(row,2)) + ...
        F1ExcO2(FWorkArray(row,1),FWorkArray(row,2));

    %Calculate total extracted CO2 mass flow rate in kg/s.
```

```
F1CO2m(FWorkArray(row,1),FWorkArray(row,2)) = ...
    (F1TotCO2(FWorkArray(row,1),FWorkArray(row,2)) * MWCO2 * ...
    ST/(F1T(FWorkArray(row,1),FWorkArray(row,2)) + ST) * ...
    (1/STPGasVol))/3600;

%Calculate total extracted N2 mass flow rate in kg/s.
F1N2m(FWorkArray(row,1),FWorkArray(row,2)) = ...
    (F1TotN2(FWorkArray(row,1),FWorkArray(row,2)) * MWN2 * ...
    ST/(F1T(FWorkArray(row,1),FWorkArray(row,2)) + ST) * ...
    (1/STPGasVol))/3600;

%Calculate total extracted O2 mass flow rate in kg/s.
F1O2m(FWorkArray(row,1),FWorkArray(row,2)) = ...
    (F1TotO2(FWorkArray(row,1),FWorkArray(row,2)) * MWO2 * ...
    ST/(F1T(FWorkArray(row,1),FWorkArray(row,2)) + ST) * ...
    (1/STPGasVol))/3600;

%Furnace 2.
%Calculate m^3/h CO2.
F2TotCO2(FWorkArray(row,1),FWorkArray(row,2)) = (AMCO2/MWCO2)*...
    (F2BpD/24) * STPGasVol * ((F2T(FWorkArray(row,1),...
    FWorkArray(row,2)) + ST)/ST);

%Calculate m^3/h N2.
F2N2(FWorkArray(row,1),FWorkArray(row,2)) = (TotReqN2/MWN2)*...
    (F2BpD/24) * STPGasVol * ((F2T(FWorkArray(row,1),...
    FWorkArray(row,2)) + ST)/ST);

%Calculate m^3/h O2.
F2O2(FWorkArray(row,1),FWorkArray(row,2)) = (TotReqO2/MWO2)*...
    (F2BpD/24) * STPGasVol * ((F2T(FWorkArray(row,1),...
    FWorkArray(row,2)) + ST)/ST);

%Calculate excess N2.
F2ExcN2(FWorkArray(row,1),FWorkArray(row,2)) = PercN2/100 * ...
    (F2OGVol - F2TotCO2(FWorkArray(row,1),FWorkArray(row,2))...
    - F2N2(FWorkArray(row,1),FWorkArray(row,2))...
    - F2O2(FWorkArray(row,1),FWorkArray(row,2)));

%Calculate excess O2.
F2ExcO2(FWorkArray(row,1),FWorkArray(row,2)) = PercO2/100 * ...
    (F2OGVol - F2TotCO2(FWorkArray(row,1),FWorkArray(row,2))...
    - F2N2(FWorkArray(row,1),FWorkArray(row,2))...
    - F2O2(FWorkArray(row,1),FWorkArray(row,2)));

%Calculate total extracted m^3/h N2 (required + excess).
F2TotN2(FWorkArray(row,1),FWorkArray(row,2)) = ...
    F2N2(FWorkArray(row,1),FWorkArray(row,2)) + ...
    F2ExcN2(FWorkArray(row,1),FWorkArray(row,2));

%Calculate total extracted m^3/h O2 (required + excess).
F2TotO2(FWorkArray(row,1),FWorkArray(row,2)) = ...
    F2O2(FWorkArray(row,1),FWorkArray(row,2)) + ...
    F2ExcO2(FWorkArray(row,1),FWorkArray(row,2));

%Calculate total extracted CO2 mass flow rate in kg/s.
F2CO2m(FWorkArray(row,1),FWorkArray(row,2)) = ...
    (F2TotCO2(FWorkArray(row,1),FWorkArray(row,2)) * MWCO2 * ...
    ST/(F2T(FWorkArray(row,1),FWorkArray(row,2)) + ST) * ...
    (1/STPGasVol))/3600;

%Calculate total extracted N2 mass flow rate in kg/s.
F2N2m(FWorkArray(row,1),FWorkArray(row,2)) = ...
```

```
        (F2TotN2(FWorkArray(row,1),FWorkArray(row,2)) * MWN2 * ...
        ST/(F2T(FWorkArray(row,1),FWorkArray(row,2)) + ST) * ...
        (1/STPGasVol))/3600;

    %Calculate total extracted O2 mass flow rate in kg/s.
    F2O2m(FWorkArray(row,1),FWorkArray(row,2)) = ...
        (F2TotO2(FWorkArray(row,1),FWorkArray(row,2)) * MWO2 * ...
        ST/(F2T(FWorkArray(row,1),FWorkArray(row,2)) + ST) * ...
        (1/STPGasVol))/3600;

    %Furnace 3
    %Calculate m^3/h CO2.
    F3TotCO2(FWorkArray(row,1),FWorkArray(row,2)) = (AMCO2/MWCO2)*...
        (F3BpD/24) * STPGasVol * ((F3T(FWorkArray(row,1),...
        FWorkArray(row,2)) + ST)/ST);

    %Calculate m^3/h N2.
    F3N2(FWorkArray(row,1),FWorkArray(row,2)) = (TotReqN2/MWN2)*...
        (F3BpD/24) * STPGasVol * ((F3T(FWorkArray(row,1),...
        FWorkArray(row,2)) + ST)/ST);

    %Calculate m^3/h O2.
    F3O2(FWorkArray(row,1),FWorkArray(row,2)) = (TotReqO2/MWO2)*...
        (F3BpD/24) * STPGasVol * ((F3T(FWorkArray(row,1),...
        FWorkArray(row,2)) + ST)/ST);

    %Calculate excess N2.
    F3ExcN2(FWorkArray(row,1),FWorkArray(row,2)) = PercN2/100 * ...
        (F3OGVol - F3TotCO2(FWorkArray(row,1),FWorkArray(row,2))...
        - F3N2(FWorkArray(row,1),FWorkArray(row,2))...
        - F3O2(FWorkArray(row,1),FWorkArray(row,2)));

    %Calculate excess O2.
    F3ExcO2(FWorkArray(row,1),FWorkArray(row,2)) = PercO2/100 * ...
        (F3OGVol - F3TotCO2(FWorkArray(row,1),FWorkArray(row,2))...
        - F3N2(FWorkArray(row,1),FWorkArray(row,2))...
        - F3O2(FWorkArray(row,1),FWorkArray(row,2)));

    %Calculate total extracted m^3/h N2 (required + excess).
    F3TotN2(FWorkArray(row,1),FWorkArray(row,2)) = ...
        F3N2(FWorkArray(row,1),FWorkArray(row,2)) + ...
        F3ExcN2(FWorkArray(row,1),FWorkArray(row,2));

    %Calculate total extracted m^3/h O2 (required + excess).
    F3TotO2(FWorkArray(row,1),FWorkArray(row,2)) = ...
        F3O2(FWorkArray(row,1),FWorkArray(row,2)) + ...
        F3ExcO2(FWorkArray(row,1),FWorkArray(row,2));

    %Calculate total extracted CO2 mass flow rate in kg/s.
    F3CO2m(FWorkArray(row,1),FWorkArray(row,2)) = ...
        (F3TotCO2(FWorkArray(row,1),FWorkArray(row,2)) * MWCO2 * ...
        ST/(F3T(FWorkArray(row,1),FWorkArray(row,2)) + ST) * ...
        (1/STPGasVol))/3600;

    %Calculate total extracted N2 mass flow rate in kg/s.
    F3N2m(FWorkArray(row,1),FWorkArray(row,2)) = ...
        (F3TotN2(FWorkArray(row,1),FWorkArray(row,2)) * MWN2 * ...
        ST/(F3T(FWorkArray(row,1),FWorkArray(row,2)) + ST) * ...
        (1/STPGasVol))/3600;

    %Calculate total extracted O2 mass flow rate in kg/s.
    F3O2m(FWorkArray(row,1),FWorkArray(row,2)) = ...
        (F3TotO2(FWorkArray(row,1),FWorkArray(row,2)) * MWO2 * ...
```

```
        ST/(F3T(FWorkArray(row,1),FWorkArray(row,2)) + ST) * ...
        (1/STPGasVol))/3600;

    %Furnace 4
    %Calculate m^3/h CO2.
    F4TotCO2(FWorkArray(row,1),FWorkArray(row,2)) = (AMCO2/MWCO2)*...
        (F4BpD/24) * STPGasVol * ((F4T(FWorkArray(row,1),...
        FWorkArray(row,2)) + ST)/ST);

    %Calculate m^3/h N2.
    F4N2(FWorkArray(row,1),FWorkArray(row,2)) = (TotReqN2/MWN2)*...
        (F4BpD/24) * STPGasVol * ((F4T(FWorkArray(row,1),...
        FWorkArray(row,2)) + ST)/ST);

    %Calculate m^3/h O2.
    F4O2(FWorkArray(row,1),FWorkArray(row,2)) = (TotReqO2/MWO2)*...
        (F4BpD/24) * STPGasVol * ((F4T(FWorkArray(row,1),...
        FWorkArray(row,2)) + ST)/ST);

    %Calculate excess N2.
    F4ExcN2(FWorkArray(row,1),FWorkArray(row,2)) = PercN2/100 * ...
        (F4OGVol - F4TotCO2(FWorkArray(row,1),FWorkArray(row,2))...
        - F4N2(FWorkArray(row,1),FWorkArray(row,2))...
        - F4O2(FWorkArray(row,1),FWorkArray(row,2)));

    %Calculate excess O2.
    F4ExcO2(FWorkArray(row,1),FWorkArray(row,2)) = PercO2/100 * ...
        (F4OGVol - F4TotCO2(FWorkArray(row,1),FWorkArray(row,2))...
        - F4N2(FWorkArray(row,1),FWorkArray(row,2))...
        - F4O2(FWorkArray(row,1),FWorkArray(row,2)));

    %Calculate total extracted m^3/h N2 (required + excess).
    F4TotN2(FWorkArray(row,1),FWorkArray(row,2)) = ...
        F4N2(FWorkArray(row,1),FWorkArray(row,2)) + ...
        F4ExcN2(FWorkArray(row,1),FWorkArray(row,2));

    %Calculate total extracted m^3/h O2 (required + excess).
    F4TotO2(FWorkArray(row,1),FWorkArray(row,2)) = ...
        F4O2(FWorkArray(row,1),FWorkArray(row,2)) + ...
        F4ExcO2(FWorkArray(row,1),FWorkArray(row,2));

    %Calculate total extracted CO2 mass flow rate in kg/s.
    F4CO2m(FWorkArray(row,1),FWorkArray(row,2)) = ...
        (F4TotCO2(FWorkArray(row,1),FWorkArray(row,2)) * MWCO2 * ...
        ST/(F4T(FWorkArray(row,1),FWorkArray(row,2)) + ST) * ...
        (1/STPGasVol))/3600;

    %Calculate total extracted N2 mass flow rate in kg/s.
    F4N2m(FWorkArray(row,1),FWorkArray(row,2)) = ...
        (F4TotN2(FWorkArray(row,1),FWorkArray(row,2)) * MWN2 * ...
        ST/(F4T(FWorkArray(row,1),FWorkArray(row,2)) + ST) * ...
        (1/STPGasVol))/3600;

    %Calculate total extracted O2 mass flow rate in kg/s.
    F4O2m(FWorkArray(row,1),FWorkArray(row,2)) = ...
        (F4TotO2(FWorkArray(row,1),FWorkArray(row,2)) * MWO2 * ...
        ST/(F4T(FWorkArray(row,1),FWorkArray(row,2)) + ST) * ...
        (1/STPGasVol))/3600;
end

%Calculate all furnace available heat i,j arrays. If instantaneous furnace
%outlet temperature < 200 deg C or bagplant inlet temperature greater than
%furnace outlet temperature, cogeneration and heat recovery system assumed
```

```
%to be off for that furnace during that instantaneous time period.
for row = 2:RowEntries
  %Furnace 1.
  %Check if furnace instantaneous outlet temp less than 200 deg C.
  if F1T(FWorkArray(row,1),FWorkArray(row,2)) < 200
      F1Q(FWorkArray(row,1),FWorkArray(row,2)) = 0; %Heat recovery is off.
      mID1(FWorkArray(row,1),FWorkArray(row,2)) = 0; %ID fan is off.
  %Check if bagplant inlet temp greater than furnace outlet temp.
  elseif F1T(FWorkArray(row,1),FWorkArray(row,2)) <...
          B1T(FWorkArray(row,1),FWorkArray(row,2))
      F1Q(FWorkArray(row,1),FWorkArray(row,2)) = 0; %Heat recovery is off.
      mID1(FWorkArray(row,1),FWorkArray(row,2)) = 0; %ID fan is off.
  else
      %Calculate furnace available heat in MW using constituent mass flow
      %i,j arrays and constituent enthalpy values at all data point temps.
      F1Q(FWorkArray(row,1),FWorkArray(row,2)) = ...
          F1CO2m(FWorkArray(row,1),FWorkArray(row,2)) * MWCO2 * ...
          (ECF1(FWorkArray(row,1),FWorkArray(row,2)) - ...
          ECB1(FWorkArray(row,1),FWorkArray(row,2))) + ...
          F1N2m(FWorkArray(row,1),FWorkArray(row,2)) * MWN2 * ...
          (ENF1(FWorkArray(row,1),FWorkArray(row,2)) - ...
          ENB1(FWorkArray(row,1),FWorkArray(row,2))) + ...
          F1O2m(FWorkArray(row,1),FWorkArray(row,2)) * MWO2 * ...
          (EOF1(FWorkArray(row,1),FWorkArray(row,2)) - ...
          EOB1(FWorkArray(row,1),FWorkArray(row,2)));
      %ID fan is on and the ID fan load in MW must be considered.
      mID1(FWorkArray(row,1),FWorkArray(row,2)) = ID1;
  end

  %Furnace 2.
  %Check if furnace instantaneous outlet temp less than 200 deg C.
  if F2T(FWorkArray(row,1),FWorkArray(row,2)) < 200
      F2Q(FWorkArray(row,1),FWorkArray(row,2)) = 0; %Heat recovery is off.
      mID2(FWorkArray(row,1),FWorkArray(row,2)) = 0; %ID fan is off.
  %Check if bagplant inlet temp greater than furnace outlet temp.
  elseif F2T(FWorkArray(row,1),FWorkArray(row,2)) <...
          B2T(FWorkArray(row,1),FWorkArray(row,2))
      F2Q(FWorkArray(row,1),FWorkArray(row,2)) = 0; %Heat recovery is off.
      mID2(FWorkArray(row,1),FWorkArray(row,2)) = 0; %ID fan is off.
  else
      %Calculate furnace available heat in MW using constituent mass flow
      %i,j arrays and constituent enthalpy values at all data point temps.
      F2Q(FWorkArray(row,1),FWorkArray(row,2)) = ...
          F2CO2m(FWorkArray(row,1),FWorkArray(row,2)) * MWCO2 * ...
          (ECF2(FWorkArray(row,1),FWorkArray(row,2)) - ...
          ECB2(FWorkArray(row,1),FWorkArray(row,2))) + ...
          F2N2m(FWorkArray(row,1),FWorkArray(row,2)) * MWN2 * ...
          (ENF2(FWorkArray(row,1),FWorkArray(row,2)) - ...
          ENB2(FWorkArray(row,1),FWorkArray(row,2))) + ...
          F2O2m(FWorkArray(row,1),FWorkArray(row,2)) * MWO2 * ...
          (EOF2(FWorkArray(row,1),FWorkArray(row,2)) - ...
          EOB2(FWorkArray(row,1),FWorkArray(row,2)));
      %ID fan is on and the ID fan load in MW must be considered.
      mID2(FWorkArray(row,1),FWorkArray(row,2)) = ID2;
  end

  %Furnace 3.
  %Check if furnace instantaneous outlet temp less than 200 deg C.
  if F3T(FWorkArray(row,1),FWorkArray(row,2)) < 200
      F3Q(FWorkArray(row,1),FWorkArray(row,2)) = 0; %Heat recovery is off.
      mID3(FWorkArray(row,1),FWorkArray(row,2)) = 0; %ID fan is off.
  %Check if bagplant inlet temp is greater than furnace outlet temp.
  elseif F3T(FWorkArray(row,1),FWorkArray(row,2)) <...
```

```
            B3T(FWorkArray(row,1),FWorkArray(row,2))
        F3Q(FWorkArray(row,1),FWorkArray(row,2)) = 0; %Heat recovery is off.
        mID3(FWorkArray(row,1),FWorkArray(row,2)) = 0; %ID fan is off.
    else
        %Calculate furnace available heat in MW using constituent mass flow
        %i,j arrays and constituent enthalpy values at all data point temps.
        F3Q(FWorkArray(row,1),FWorkArray(row,2)) = ...
            F3CO2m(FWorkArray(row,1),FWorkArray(row,2)) * MWCO2 * ...
            (ECF3(FWorkArray(row,1),FWorkArray(row,2)) - ...
            ECB3(FWorkArray(row,1),FWorkArray(row,2))) + ...
            F3N2m(FWorkArray(row,1),FWorkArray(row,2)) * MWN2 * ...
            (ENF3(FWorkArray(row,1),FWorkArray(row,2)) - ...
            ENB3(FWorkArray(row,1),FWorkArray(row,2))) + ...
            F3O2m(FWorkArray(row,1),FWorkArray(row,2)) * MWO2 * ...
            (EOF3(FWorkArray(row,1),FWorkArray(row,2)) - ...
            EOB3(FWorkArray(row,1),FWorkArray(row,2)));
        %ID fan is on and the ID fan load in MW must be considered.
        mID3(FWorkArray(row,1),FWorkArray(row,2)) = ID3;
    end

    %Furnace 4.
    %Check if furnace instantaneous outlet temp less than 200 deg C.
    if F4T(FWorkArray(row,1),FWorkArray(row,2)) < 200
        F4Q(FWorkArray(row,1),FWorkArray(row,2)) = 0; %Heat recovery is off.
        mID4(FWorkArray(row,1),FWorkArray(row,2)) = 0; %ID fan is off.
    %Check if bagplant inlet temp greater than furnace outlet temp.
    elseif F4T(FWorkArray(row,1),FWorkArray(row,2)) <...
            B4T(FWorkArray(row,1),FWorkArray(row,2))
        F4Q(FWorkArray(row,1),FWorkArray(row,2)) = 0; %Heat recovery is off.
        mID4(FWorkArray(row,1),FWorkArray(row,2)) = 0; %ID fan is off.
    else
        %Calculate furnace available heat in MW using constituent mass flow
        %i,j arrays and constituent enthalpy values at all data point temps.
        F4Q(FWorkArray(row,1),FWorkArray(row,2)) = ...
            F4CO2m(FWorkArray(row,1),FWorkArray(row,2)) * MWCO2 * ...
            (ECF4(FWorkArray(row,1),FWorkArray(row,2)) - ...
            ECB4(FWorkArray(row,1),FWorkArray(row,2))) + ...
            F4N2m(FWorkArray(row,1),FWorkArray(row,2)) * MWN2 * ...
            (ENF4(FWorkArray(row,1),FWorkArray(row,2)) - ...
            ENB4(FWorkArray(row,1),FWorkArray(row,2))) + ...
            F4O2m(FWorkArray(row,1),FWorkArray(row,2)) * MWO2 * ...
            (EOF4(FWorkArray(row,1),FWorkArray(row,2)) - ...
            EOB4(FWorkArray(row,1),FWorkArray(row,2)));
        %ID fan is on and the ID fan load in MW must be considered.
        mID4(FWorkArray(row,1),FWorkArray(row,2)) = ID4;
    end
end

%Calculate and generate combined overall heat available in MW i,j array.
QTotal = F1Q + F2Q + F3Q + F4Q;
QMWTotal = QTotal/1000;

%% Calculate overall recovered and available electrical power in MW from
%% considered ORC heat recovery and power generation system.

nElec = ((ORCout - ORCcaptive)/ThermalIn)*100; %Net electrical efficiency.

%Apply 2% reduction in nElec due to alteration of condenser output water
%temperature to usable range for cooling system.
nElec = nElec - 2;

%Wt is electrical power that will be optimally dispatched between furnace
%loads and utility grid.
```

```
Wt = nElec/100 * QMWTotal;

%% Calculate overall and available theoretical cooling power in MW.

%Calculate thermal power available to cooling system.
QMWlow = (100 - nElec - 2)/100 * QMWTotal;
QMWcold = COP * QMWlow; %Calculate available cooling power in MW.

%% Obtain user and facility defined facility category and connection
%% characteristics for appropriate tariff structure consideration.

%Determine facility consumption and generation transmission zones.
disp('Please specify Consumption Transmission Zone(1-4)');
disp('Zone 1: <= 300 km');
disp('Zone 2: > 300 km & <= 600 km');
disp('Zone 3: > 600 km & <= 900 km');
disp('Zone 4: > 900 km');
ZoneC = input('Zone = ');   %User supplied zone input.

disp('Please specify Generation Transmission Zone(1-3)');
disp('Zone 1: <= 300 km');
disp('Zone 2: > 300 km & <= 600 km');
disp('Zone 3: > 600 km & <= 900 km');
ZoneG = input('Zone = ');   %User supplied zone input.

%Determine facility consumption and generation voltage levels.
disp('Please specify Consumption Supply Voltage Level(1-4)');
disp('Level 1: < 500 V');
disp('Level 2: >= 500 V & < 66 kV');
disp('Level 3: >= 66 kV & <= 132 kV');
disp('Level 4: > 132 kV');
VoltageC = input('Voltage Level = ');   %User supplied voltage input.

disp('Please specify Generation Supply Voltage Level(1-3)');
disp('Level 1: < 500 V');
disp('Level 2: >= 500 V & < 66 kV');
disp('Level 3: >= 66 kV & <= 132 kV');
VoltageG = input('Voltage Level = ');   %User supplied voltage input.

%Determine consumption customer category.
disp('Please specify Consumption Customer Category(0 or 1)');
disp('Category 0: > 1 MVA');
disp('Category 1: Key Customer');
KeyCustomer = input('Category = ');   %User supplied category input.

%Determine generation customer category.
disp('Please specify Maximum Generation Export Capacity (1 - 5)');
disp('Category 1: <= 100 kVA/kW');
disp('Category 2: > 100 kVA/kW & <= 500 kVA/kW');
disp('Category 3: > 500 kVA/kW & <= 1 MVA/MW');
disp('Category 4: > 1 MVA/MW');
disp('Category 5: Transmission Connected');
MaxExport = input('Category = ');   %User supplied category input.

%% Generate consumption & generation tariff structure arrays based on user
%% supplied inputs and high or low demand season flag.

%Generate consumption tariff array in the following format:
%[HDP,HDS,HDO,LDP,LDS,LDO,TNC,NAC,NDC,ULVSC,RSC,SC,AC,ERNSC,REC].
[CTariff] = Determine_Cons_Charges(ZoneC,VoltageC,SHigh,KeyCustomer);

%Generate generation tariff array in the following format:
%[TLF,gNAC,DLF,gRSC,WEPSPr,WEPSSr,WEPSOr,gSC,gAC]
```

```
[GTariff] = Determine_Gen_Charges(ZoneG,VoltageG,SHigh,MaxExport);

%% Generate reactive energy charge i,j flag array using REC_Test_Condition
%% function.

[RECTest,Qload] = REC_Test_Condition(AbsSload,Pload,FWorkArray,RowEntries);

%% Calculate total ID fan load in MW

Pid = mID1 + mID2 + mID3 + mID4;

%% Generate all cost function calculation constant and i,j arrays.

%Set High and Low values for appropriate tariff consideration and array
%generation purposes.
if SHigh == 1
    High = 1;
    Low = 0;
else
    High = 0;
    Low = 1;
end

%Calculate all required cost function i,j arrays: A,B,D,E,F,G,H and T.
for row = 2:RowEntries
    A(FWorkArray(row,1),FWorkArray(row,2))=(AbsSload(FWorkArray(row,1),...
        FWorkArray(row,2)) * (P(FWorkArray(row,1),FWorkArray(row,2)) + ...
        S(FWorkArray(row,1),FWorkArray(row,2))))*1000 * CTariff(1,9);

    B(FWorkArray(row,1),FWorkArray(row,2))=(AbsSload(FWorkArray(row,1),...
        FWorkArray(row,2)) * (P(FWorkArray(row,1),FWorkArray(row,2)) + ...
        S(FWorkArray(row,1),FWorkArray(row,2))))*1000 * ...
        (1/(Pload(FWorkArray(row,1),FWorkArray(row,2)) + ...
        Pid(FWorkArray(row,1),FWorkArray(row,2)))) * CTariff(1,9);

    D(FWorkArray(row,1),FWorkArray(row,2)) = Pload(FWorkArray(row,1),...
        FWorkArray(row,2)) + Pid(FWorkArray(row,1),FWorkArray(row,2));

    E(FWorkArray(row,1),FWorkArray(row,2)) = 1000 * (((...
        P(FWorkArray(row,1),FWorkArray(row,2)) * (((High*CTariff(1,1)) +...
        (Low*CTariff(1,4))) + (CTariff(1,14))))/100) + ...
        ((S(FWorkArray(row,1),FWorkArray(row,2)) * (((High*CTariff(1,2))...
        + (Low*CTariff(1,5))) + (CTariff(1,14))))/100) + ((O(FWorkArray...
        (row,1),FWorkArray(row,2))*(((High*CTariff(1,3)) + (Low*...
        CTariff(1,6))) + (CTariff(1,14))))/100));

    F(FWorkArray(row,1),FWorkArray(row,2)) = Wt(FWorkArray(row,1),...
        FWorkArray(row,2));

    G(FWorkArray(row,1),FWorkArray(row,2)) = 1000 * (((...
        P(FWorkArray(row,1),FWorkArray(row,2)) * GTariff(1,5))/100) + ...
        ((S(FWorkArray(row,1),FWorkArray(row,2)) * GTariff(1,6))/100) + ...
        ((O(FWorkArray(row,1),FWorkArray(row,2)) * GTariff(1,7))/100));

    H(FWorkArray(row,1),FWorkArray(row,2)) = 1000 * (sqrt((...
        AbsSload(FWorkArray(row,1),FWorkArray(row,2))/(...
        Pload(FWorkArray(row,1),FWorkArray(row,2)) + ...
        Pid(FWorkArray(row,1),FWorkArray(row,2))))^2 - 1)-0.3) * ...
        (P(FWorkArray(row,1),FWorkArray(row,2)) + S(FWorkArray(row,1),...
        FWorkArray(row,2)))*RECTest(FWorkArray(row,1),FWorkArray(row,2))...
        * ((CTariff(1,15))/100);

    T(FWorkArray(row,1),FWorkArray(row,2)) = 1000*...
```

```
        (P(FWorkArray(row,1),FWorkArray(row,2)) + ...
        S(FWorkArray(row,1),FWorkArray(row,2)) + ...
        O(FWorkArray(row,1),FWorkArray(row,2)));
end

%Calculate all required cost function constant arrays: K,L,M,N,Q,R and U.
K = n*(CTariff(1,13) + CTariff(1,12) + GTariff(1,9) + GTariff(1,8));

L = AD*1000*CTariff(1,8);

M = gAD*1000*GTariff(1,2);

N = (GTariff(1,3) * GTariff(1,1)) - 1;

Q = AD*1000*(CTariff(1,7) + CTariff(1,10));

R = 0.25 * CTariff(1,11)/100;

U = 0.25 * GTariff(1,4)/100;

%% Cost function and optimisation.

%Call model cost function with array x set as the optimisation variables.
Cost = @(x)Cost_Function(FWorkArray,RowEntries,...
A,B,D,E,F,G,H,K,L,M,N,Q,R,T,U,x);

%Set optimisation model lower and upper bounds and initial starting point.
for row = 2:RowEntries

    lb(FWorkArray(row,1),FWorkArray(row,2)) = 0;
    ub(FWorkArray(row,1),FWorkArray(row,2)) = ...
        Wt(FWorkArray(row,1),FWorkArray(row,2));
    x0(FWorkArray(row,1),FWorkArray(row,2)) = ...
        (0.5*Wt(FWorkArray(row,1),FWorkArray(row,2)));
end

%Set optimisation options: Maximum function evaluations and optimisation
%algorithm.
options = optimset('MaxFunEvals',1000000,'Algorithm','sqp');

%Perform optimisation and calculate optimisation variable array x and
%minimised overall cost.
[x ,fval] = fmincon(Cost,x0,[],[],[],[],lb,ub,[],options);

%Generate arrays for export to output and analysis spread sheet.
for l = 2:RowEntries

    %T.O.U period.
    if P(FWorkArray(l,1),FWorkArray(l,2)) == 1
        TOU(l-1,1) = 'P';
    elseif S(FWorkArray(l,1),FWorkArray(l,2)) == 1
        TOU(l-1,1) = 'S';
    else
        TOU(l-1,1) = 'O';
    end

    %Combined furnace operating apparent power.
    COAbsSload(l-1,1) = AbsSload(FWorkArray(l,1),FWorkArray(l,2));
    %Combined furnace operating real power.
    COPload(l-1,1) = Pload(FWorkArray(l,1),FWorkArray(l,2));
    %Cogeneration recovered heat in MW.
    COheat(l-1,1) = QMWTotal(FWorkArray(l,1),FWorkArray(l,2));
    %Cogeneration generated power in MW.
```

```
    COWt(l-1,1) = Wt(FWorkArray(l,1),FWorkArray(l,2));
    %Power in MW dispatched to furnace loads.
    COx(l-1,1) = x(FWorkArray(l,1),FWorkArray(l,2));
    %Power in MW dispatched to utility grid.
    COEskom(l-1,1) = Wt(FWorkArray(l,1),FWorkArray(l,2)) - ...
        x(FWorkArray(l,1),FWorkArray(l,2));
    %Cooling power in MW available for facility use.
    COcold(l-1,1) = QMWcold(FWorkArray(l,1),FWorkArray(l,2));
end

%% Determine initial system cost without cogeneration system and waste heat
%% recovery using model cost function.

x(:,:) = 0; %Set optimisation variables array to 0;
F(:,:) = 0; %Set cogeneration generated power to 0;
%Call cost function, calculate initial cost due to setting of x and F to 0.
ICost = Cost_Function(FWorkArray,RowEntries,...
A,B,D,E,F,G,H,K,L,M,N,Q,R,T,U,x);

%% Determine overall energy cost savings from final & initial system costs
%% and write model resulting data to a cogeneration output spread sheet.

FCost = fval;   %System cost after energy saving method implementation.
TotalSavings = ICost - FCost;   %System implementation energy cost savings.

filename = 'CogenOutput.xlsx'; %Result cogeneration output file.
%Write i and j data stamp to file.
xlswrite(filename,FWorkArray(2:end,1:2),1,'A3');
%Write T.O.U period to file.
xlswrite(filename,TOU,1,'C3');
%Write combined furnace operation apparent power to file.
xlswrite(filename,COAbsSload,1,'D3');
%Write combined furnace operation real power to file.
xlswrite(filename,COPload,1,'E3');
%Write cogeneration recovered heat to file.
xlswrite(filename,COheat,1,'F3');
%Write cogeneration generated power to file.
xlswrite(filename,COWt,1,'G3');
%Write power dispatched to furnace loads to file.
xlswrite(filename,COx,1,'H3');
%Write power dispatched to utility grid to file.
xlswrite(filename,COEskom,1,'I3');
xlswrite(filename,COcold,1,'J3'); %Write cooling power available to file.
xlswrite(filename,ICost,1,'L1'); %Write initial cost to file.
xlswrite(filename,FCost,1,'L2'); %Write final cost to file.
xlswrite(filename,TotalSavings,1,'L3'); %Write energy savings to file.
```

A.2 EPD MODEL FUNCTION: FIND_ENTHALPY

```
%%  Author: Michael Chennells
%%  Naming conventions chosen in accordance with report naming conventions.
%%  Department of Electrical, Electronic and Computer Engineering.
%%  Date:
%%  Enthalpy table development m file.

%% Generate enthalpy value for CO2, N2 and O2 at pre-specified temperature.

function [ECO2,EN2,EO2] = Find_Enthalpy(Temp)

%Generate CO2 enthalpy lookup table.
CO2x = [25,100,200,300,400,500,600,700,800,900,1000];
CO2y = [0,2.963,7.276,11.848,16.604,21.508,26.539,31.687,36.944,42.305,...
    47.768];

%Generate N2 enthalpy lookup table.
N2x = [25,100,200,300,400,500,600,700,800,900,1000];
N2y = [0,2.197,5.164,8.174,11.227,14.322,17.46,20.64,23.863,27.129,30.438];

%Generate O2 enthalpy lookup table.
O2x = [25,100,200,300,400,500,600,700,800,900,1000];
O2y = [0,2.239,5.317,8.47,11.683,14.949,18.264,21.627,25.034,28.487,...
    31.983];

%Perform linear interpolation for each off gas constituent and calculate
%enthalpy value for each at pre-specified temperature.
xdt = 'double';
xscale = 1;
ydt = 'double';
yscale = 1;
rndmeth = 'Nearest';

ECO2 = fixpt_interp1(CO2x,CO2y,Temp,xdt,xscale,ydt,yscale,rndmeth);
EN2 = fixpt_interp1(N2x,N2y,Temp,xdt,xscale,ydt,yscale,rndmeth);
EO2 = fixpt_interp1(O2x,O2y,Temp,xdt,xscale,ydt,yscale,rndmeth);

end
```

A.3 EPD MODEL FUNCTION: TIME_INDEP_INFO

```
%%  Author: Michael Chennells
%%  Naming conventions chosen in accordance with report naming conventions.
%%  Department of Electrical, Electronic and Computer Engineering.
%%  Date:
%%  Time independent information and constant initialisation m file.

%% Function sets and returns all required time independent data and
%% constants for use in calculation of overall available heat and
%% electrical power.

function [AMCO2, PercN2, PercO2, TotReqN2, TotReqO2, STPGasVol, ST, ...
    F1BpD, F2BpD, F3BpD, F4BpD, MWCO2, MWN2, MWO2, F1OGVol, F2OGVol, ...
    F3OGVol, F4OGVol, ID1, ID2, ID3, ID4, AD, gAD, ORCout, ORCcaptive, ...
    ThermalIn, COP] = Time_Indep_Info()

%Batch size, recipe and %required raw materials from each feed bin.
%Bin 7.
PercMoistB7 = 4.6;
PercFeOB7 = 25.8;
PercCr2O3B7 = 40.6;
PercReqB7 = 30;

%Bin 10.
PercMoistB10 = 4.6;
PercFeOB10 = 25.8;
PercCr2O3B10 = 40.6;
PercReqB10 = 30;

%Bin 12.
PercMoistB12 = 4.6;
PercFeOB12 = 25.8;
PercCr2O3B12 = 40.6;
PercReqB12 = 20;

%Bin 1.
PercMoistB1 = 0.4;
PercFeOB1 = 23.6;
PercCr2O3B1 = 40.3;
PercReqB1 = 20;

BatchMass = 4000;

%Calculate total mass of feed required from each bin.
TotMB7 = PercReqB7/100 * BatchMass;
TotMB10 = PercReqB10/100 * BatchMass;
TotMB12 = PercReqB12/100 * BatchMass;
TotMB1 = PercReqB1/100 * BatchMass;

%Calculate total amount of moisture in feed.
TotMoist = (PercMoistB7/100 * TotMB7) + (PercMoistB10/100 * TotMB10) + ...
    (PercMoistB12/100 * TotMB12) + (PercMoistB1/100 * TotMB1);

%Calculate actual dry sample batch feed raw material masses.
AMFeOB7 = PercFeOB7/100 * (TotMB7 - (PercMoistB7/100 * TotMB7));
AMCr2O3B7 = PercCr2O3B7/100 * (TotMB7 - (PercMoistB7/100 * TotMB7));

AMFeOB10 = PercFeOB10/100 * (TotMB10 - (PercMoistB10/100 * TotMB10));
AMCr2O3B10 = PercCr2O3B10/100 * (TotMB10 - (PercMoistB10/100 * TotMB10));

AMFeOB12 = PercFeOB12/100 * (TotMB12 - (PercMoistB12/100 * TotMB12));
AMCr2O3B12 = PercCr2O3B12/100 * (TotMB12 - (PercMoistB12/100 * TotMB12));
```

```
AMFeOB1 = PercFeOB1/100 * (TotMB1 - (PercMoistB1/100 * TotMB1));
AMCr2O3B1 = PercCr2O3B1/100 * (TotMB1 - (PercMoistB1/100 * TotMB1));

%Calculate final masses of important feed metals FeO and Cr2O3.
TotMFeO = AMFeOB7 + AMFeOB10 + AMFeOB12 + AMFeOB1;
TotMCr2O3 = AMCr2O3B7 + AMCr2O3B10 + AMCr2O3B12 + AMCr2O3B1;

%Important feed metal molecular weights and assumed air composition %.
MWFeO = 72;
MWCr2O3 = 152;
MWCO = 28;
PercN2 = 77;
PercO2 = 23;

%Calculate amount of CO gas from each internal process chemical reaction
%and total obtained process CO gas.
CO_FeO = TotMFeO/MWFeO * MWCO;
CO_Cr2O3 = TotMCr2O3/MWCr2O3 * 3 * MWCO;
TotCO = CO_FeO + CO_Cr2O3;

%Off gas constituent molecular weights.
MWCO2 = 44;
MWO2 = 32;
MWN2 = 28;

%Calculate total mass of CO2 and O2 from the smelting balanced chemical
%reactions, calculate total air and therefore N2 required.
TotCO2 = TotCO/(2 * MWCO) * 2 * MWCO2;
AMCO2 = TotCO2;

TotO2 = TotCO/(2 * MWCO) * MWO2;
TotReqO2 = TotO2;

TotAir = TotO2/(PercO2/100);
TotN2 = PercN2/100 * TotAir;
TotReqN2 = TotN2;

%Furnace 4 ID fan off gas extraction capacity in m^3/h.
F4OGVol = 155492;

%Furnace raw material feed rates in batches/day.
F1BpD = 110;
F2BpD = 110;
F3BpD = 110;
F4BpD = 160;

%%Calculate furnace 1-3 ID fan off gas extraction capacities in m^3/h
%according to a constant ratio between furnace feed rates and extracted off
%gas capacities in m^3/h.
F1OGVol = F4OGVol/F4BpD * F1BpD;
F2OGVol = F4OGVol/F4BpD * F2BpD;
F3OGVol = F4OGVol/F4BpD * F3BpD;

%STP gas volume and temperature to be used for overall available heat
%calculations.
STPGasVol = 22.414;
ST = 273.15;

%ID fan sizes in MW.
ID1 = 1.1;
ID2 = 1.1;
ID3 = 1.1;
```

```
ID4 = 1.5;

%Total installed capacity for transmission network charges and network
%access charges.
AD = 190;

%Maximum generation capacity for generation network access charge.
gAD = 10;

%Turboden design ORC power generation electrical output and thermal input
%power values, and system captive consumption of power in MW.
ORCout = 4.13;
ThermalIn = 17.06;
ORCcaptive = 0.195;

%Cooling system coefficient of performance.
COP = 0.7;

end
```

A.4 EPD MODEL FUNCTION: DETERMINE_CONS_CHARGES

```
%%  Author: Michael Chennells
%%  Naming conventions chosen in accordance with report naming conventions.
%%  Department of Electrical, Electronic and Computer Engineering.
%%  Date:
%%  Consumption tariff structure development m file.

%% Generate Megaflex Local Authority consumption tariff structure table in
%% the form of an array.

function [CTariff] = Determine_Cons_Charges(Zone,Voltage,SHigh,KeyCustomer)

%Check facility zone (1, 2, 3 or 4), generate TariffArray1 with tariffs for
%all 4 supply voltage levels.
%TariffArray1 elements: HDPC,HDSC,HDOC,LDPC,LDSC,LDOC,TNC.
switch Zone
    case 1
        TariffArray1 = [209.42,63.72,34.78,68.57,47.32,30.16,5.83;...
            206.12,62.45,33.91,67.24,46.28,29.36,5.32;199.61,...
            60.47,32.83,65.11,44.82,28.43,5.18;188.13,56.99,30.95,...
            61.37,42.24,26.8,6.55];
    case 2
        TariffArray1 = [211.12,63.96,34.73,68.88,47.41,30.08,5.87;...
            208.18,63.07,34.25,67.92,46.74,29.65,5.38;201.56,...
            61.06,33.15,65.75,45.25,28.7,5.22;190,57.56,31.25,...
            61.97,42.66,27.06,6.62];
    case 3
        TariffArray1 = [213.23,64.59,35.07,69.55,47.87,30.37,5.94;...
            210.27,63.70,34.59,68.6,47.2,29.95,5.42;203.62,...
            61.68,33.49,66.41,45.71,28.99,5.27;191.91,58.14,31.57,...
            62.61,43.09,27.34,6.71];
    case 4
        TariffArray1 = [215.37,65.25,35.43,70.26,48.35,30.68,5.97;...
            212.37,64.33,34.93,69.27,47.67,30.24,5.48;205.66,...
            62.3,33.83,67.08,46.17,29.29,5.3;193.8,58.74,31.92,...
            63.25,43.54,27.64,6.76];
end

%Generate TariffArray2 for 4 supply voltage levels.
%TariffArray: NAC,NDC,ULVSC,RSC.
TariffArray2 = [11.63,22.05,0,0.27;10.67,20.23,0,0.26;3.81,7.05,...
    9.39,0.25;0,0,9.39,0.23];

%Combine TariffArray1 and TariffArray2 into single FTariffArray.
FTariffArray = [TariffArray1,TariffArray2];

%Determine REC depending on low or high demand season.
if SHigh == 1
    REC = 9.35;
else
    REC = 0;
end

%Determine SC & AC depending on whether facility is > 1MVA or key customer.
if KeyCustomer == 1
    SC = 2603.95;
    AC = 83.16;
else
    SC = 132.88;
    AC = 59.89;
end
```

```
%Set ERNSC.
ERNSC = 5.17;

%Generate final consumption tariff array with elements:
%FTariffArray,SC,AC,ERNSC,REC, depending on supply voltage level..
switch Voltage
    case 1
        CTariff = [FTariffArray(1,:),SC,AC,ERNSC,REC];
    case 2
        CTariff = [FTariffArray(2,:),SC,AC,ERNSC,REC];
    case 3
        CTariff = [FTariffArray(3,:),SC,AC,ERNSC,REC];
    case 4
        CTariff = [FTariffArray(4,:),SC,AC,ERNSC,REC];
%Final consumption tariff array CTariff elements:
%HDP,HDS,HDO,LDP,LDS,LDO,TNC,NAC,NDC,ULVSC,RSC,SC,AC,ERNSC,REC.
end

end
```

A.5 EPD MODEL FUNCTION: DETERMINE_GEN_CHARGES

```
%%  Author: Michael Chennells
%%  Naming conventions chosen in accordance with report naming conventions.
%%  Department of Electrical, Electronic and Computer Engineering.
%%  Date:
%%  Generation tariff structure development m file.

%% Generate Megaflex Local Authority based generation tariff structure
%% table in the form of an array.

function [GTariff] = Determine_Gen_Charges(Zone,Voltage,SHigh,MaxExport)

%Check facility zone (1, 2, 3 or 4), generate GTariffArray1 with tariff
%info concerning Transmission Loss factors.
%GTariffArray1 elements: TLF.
switch Zone
    case 1
        GTariffArray1 = [1.0107];
    case 2
        GTariffArray1 = [1.0208];
    case 3
        GTariffArray1 = [1.0310];
    case 4
        GTariffArray1 = [1.0413];
end

%Generate GTariffArray2 for 3 supply levels (1, 2 and 3).
%GTariffArray2 elements: gNAC,DLF,gRSC.
switch Voltage
    case 1
        GTariffArray2 = [0,1.1111,0.27];
    case 2
        GTariffArray2 = [0,1.0957,0.26];
    case 3
        GTariffArray2 = [9.4,1.0611,0.25];
end

%Determine WEPS Peak, Standard and Off peak rates depending on low or high
%demand season.
if SHigh == 1
    GWEPSTariff = [211.06,68,01,39.21];
else
    GWEPSTariff = [72.56,51.58,34.66];
end

%Determine gSC and gAC depending on max export category (1, 2, 3, 4 or 5),
%generate GTariffArray3.
%GTariffArray3 elements: gSC,gAC.
switch MaxExport
    case 1
        GTariffArray3 = [9.49,2.08];
    case 2
        GTariffArray3 = [43.38,12.16];
    case 3
        GTariffArray3 = [133.5,24.17];
    case 4
        GTariffArray3 = [133.5,60.17];
    case 5
        GTariffArray3 = [2616.06,83.55];
end

%Generate final generation tariff array GTariff.
```

```
%GTariff elements: GTariffArray1, GTariffArray2,GWEPSTariff,GTariffArray3.
GTariff = [GTariffArray1,GTariffArray2,GWEPSTariff,GTariffArray3];

%%Final generation tariff array GTariff elements:
%TLF,gNAC,DLF,gRSC,WEPSPr,WEPSSr,WEPSOr,gSC,gAC.

end
```

A.6 EPD MODEL FUNCTION: REC_TEST_CONDITION

```
%%  Author: Michael Chennells
%%  Naming conventions chosen in accordance with report naming conventions.
%%  Department of Electrical, Electronic and Computer Engineering.
%%  Date:
%%  Excess reactive energy consumption test m file.

%% Test if final reactive energy obtained from Eskom exceeds 30% of
%% final real energy obtained from Eskom, generate REC_Test_Condition flag
%% i,j array that is 1 only if the 30% exceedance criteria applies to time
%% interval data point.

function [RECTest,Qload] =
REC_Test_Condition(AbsSload,Pload,FWorkArray,RowEntries)

for row = 2:RowEntries
    %Generate reactive load i,j array.
    Qload(FWorkArray(row,1),FWorkArray(row,2)) = ...
        sqrt((AbsSload(FWorkArray(row,1),FWorkArray(row,2)))^2 -...
        (Pload(FWorkArray(row,1),FWorkArray(row,2)))^2);

    %Test whether reactive load exceeds 30% of real load.
    CritTest = Qload(FWorkArray(row,1),FWorkArray(row,2)) - 0.3*...
        (Pload(FWorkArray(row,1),FWorkArray(row,2)));

    %If 30% criteria exceeded, set RECTest i,j array element to 1.
    if CritTest > 0
        RECTest(FWorkArray(row,1),FWorkArray(row,2)) = 1;
    else
        RECTest(FWorkArray(row,1),FWorkArray(row,2)) = 0;
    end

end

end
```

A.7 EPD MODEL FUNCTION: COST_FUNCTION

```
%%  Author: Michael Chennells
%%  Naming conventions chosen in accordance with report naming conventions.
%%  Department of Electrical, Electronic and Computer Engineering.
%%  Date:
%%  Optimisation model cost function m file.

function [Cost] = Cost_Function(FWorkArray,RowEntries,...
    A,B,D,E,F,G,H,K,L,M,N,Q,R,T,U,x)

%% Maximum demand charge calculation.

%Calculate l1 i,j array components for max demand charge calculation.
for r = 2:RowEntries
    l1(FWorkArray(r,1),FWorkArray(r,2)) = ...
        A(FWorkArray(r,1),FWorkArray(r,2)) - ...
        (B(FWorkArray(r,1),FWorkArray(r,2)) * ...
        x(FWorkArray(r,1),FWorkArray(r,2)));
end

%Calculate lambda 1 = maximum demand charge.
lamda1 = max(max(l1));

%% Combined consumption and generation network access charge calculation.

%Calculate generation access demand charge rebate i,j array components for
%combined consumption and generation network access charge calculation.
m_hold = 0;

for r = 2:RowEntries

    m_hold = m_hold + (G(FWorkArray(r,1),FWorkArray(r,2)) * ...
        (F(FWorkArray(r,1),FWorkArray(r,2)) - ...
        x(FWorkArray(r,1),FWorkArray(r,2))));
end

%Calculate lambda 2 = combined consumption and generation network access
%charge including potential rebate.
lamda2 = max(L,(M - 0.5*N*(m_hold)));

%% Combined consumption and generation network reliability service charge
%% calculation.

%Calculate i,j array components of power consumed from and dispatched to
%utility for combined consumption and generation network reliability
%service charge calculation.
r_hold = 0;
u_hold = 0;

for r = 2:RowEntries

    %Consumed from utility.
    r_hold = r_hold + (T(FWorkArray(r,1),FWorkArray(r,2)) * ...
        (D(FWorkArray(r,1),FWorkArray(r,2)) - ...
        x(FWorkArray(r,1),FWorkArray(r,2))));
    %Dispatched to utility.
    u_hold = u_hold + (T(FWorkArray(r,1),FWorkArray(r,2)) * ...
        (F(FWorkArray(r,1),FWorkArray(r,2)) - ...
        x(FWorkArray(r,1),FWorkArray(r,2))));
end

%Calculate lamda3 = combined consumption and generation network reliability
```

```
%service charge.
lamda3 = max((R*r_hold),(U*u_hold));

%% Calculate incentive for power dispatched to utility and all costs
%% associated with power consumed from utility: Active energy charges,
%% electrification and rural subsidy charge and reactive energy charge.
g_hold = 0;
z_hold = 0;

for r = 2:RowEntries

    %Incentive from generation.
    g_hold = g_hold + (G(FWorkArray(r,1),FWorkArray(r,2)) * ...
        (F(FWorkArray(r,1),FWorkArray(r,2)) - ...
        x(FWorkArray(r,1),FWorkArray(r,2))));

    %Charges for consumption.
    z_hold = z_hold + ((E(FWorkArray(r,1),FWorkArray(r,2)) + ...
       H(FWorkArray(r,1),FWorkArray(r,2))) * ...
        (D(FWorkArray(r,1),FWorkArray(r,2)) - ...
        x(FWorkArray(r,1),FWorkArray(r,2))));
end

%% Calculate final cost from all charges and incentives above. Also include
%% combined service and administration charges, transmission network
%% charges and urban low voltage subsidy charges.

Cost = lamda1 + lamda2 + lamda3 + (0.5*(z_hold)) - (0.5*(g_hold)) ...
    + K + Q;

end
```

ADDENDUM B TABLES OF RESULTS AND CONSTANTS FOR TIME INDEPENDENT CALCULATIONS

Table B.1: Actual dry sample batch recipe

Ores	Feed Type and Bin	TM_s (kg)	FeO (kg)	% FeO	Cr_2O_3 (kg)	% Cr_2O_3
ORE CR PEL OUT ME	TSWELOPELE Bin 7	55.2	295.36	24.61	464.79	38.73
ORE CR PEL OUT ME	TSWELOPELE Bin 10	55.2	295.36	24.61	464.79	38.73
ORE CR PEL OUT ME	TSWELOPELE Bin 12	36.8	196.91	24.61	309.86	38.73
ORE CR LUMPY UG	KD LUMPY Bin 1	3.2	188.04	23.51	321.11	40.14
	Batch Totals	150.40	975.67	24.39	1560.55	39.01

Table B.2: Process chemical reactions and constituent masses

Fe Chemical Reaction			
Reaction Components	Molecular Weight	Actual Mass (kg)	MR
FeO	72	975.67	13.55
C	12	162.61	13.55
Fe	56	758.85	13.55
CO	28	379.43	13.55
Cr Chemical Reaction			
Reaction Components	Molecular Weight	Actual Mass (kg)	MR
Cr_2O_3	152	1560.55	10.27
3C	36	369.6	10.27
2Cr	104	1067.74	10.27
3CO	84	862.41	10.27
CO-CO_2 Chemical Reaction			
Reaction Components	Molecular Weight	Actual Mass (kg)	MR
2CO	56	1241.83	22.18
O_2	32	709.62	22.18
$2CO_2$	88	1951.45	22.18

Table B.3: Off gas air requirements and constituent masses

Off Gas Air Requirements		
Air Constituent	Constituent Percentage	Constituent Mass (kg)
N_2	77	2375.68
O_2	23	709.62
Total Air	100	3085.30

Table B.4: Additional time independent model constants

Constant	Value
Gas Volume at STP (m^3)	22.414
ST (K)	273.15
SP (atm)	1
F1 batch feed rate (batches/day)	110
F2 batch feed rate (batches/day)	110
F3 batch feed rate (batches/day)	110
F4 batch feed rate (batches/day)	160
F1 off gas volumetric flow rate (m^3/h)	106900.8
F2 off gas volumetric flow rate (m^3/h)	106900.8
F3 off gas volumetric flow rate (m^3/h)	106900.8
F4 off gas volumetric flow rate (m^3/h)	155492
MW (CO_2)	44
MW (N_2)	28
MW (O_2)	32
F1 ID fan size (MW)	1.1
F2 ID fan size (MW)	1.1
F3 ID fan size (MW)	1.1
F4 ID fan size (MW)	1.5

ADDENDUM C GENERATED EPD MODEL SCHEDULES

Table C.1: EPD model generated schedule segment for winter month August 2014, time period 2014/08/18 10:00 to 2014/08/19 00:00

i	j	T.O.U Period	$\lvert\mathbf{S}_{i,j}^{load}\rvert$ (MVA)	$P_{i,j}^{load}$ (MW)	$Q_{i,j}^{h,total}$ (MW)	$\dot{W}_{i,j}^{T}$ (MW)	$C_{i,j}$ (MW)	$\dot{W}_{i,j}^{T} - C_{i,j}$ (MW)	$QM\dot{W}_{cold}$ (MW)
..	..	..	..	..	..	..	..	..	..
18	20	P	85.54	79.00	12.22	2.57	2.32	0.25	6.58
18	21	S	84.40	77.00	11.42	2.40	0.00	2.40	6.15
18	22	S	80.32	73.00	10.95	2.31	0.00	2.31	5.90
18	23	S	78.94	73.00	11.37	2.40	0.00	2.40	6.12
18	24	S	93.67	86.00	12.46	2.62	0.00	2.62	6.71
18	25	S	91.50	85.00	12.87	2.71	0.00	2.71	6.93
18	26	S	83.70	78.00	12.23	2.58	0.00	2.58	6.59
18	27	S	92.69	85.00	12.97	2.73	0.00	2.73	6.99
18	28	S	94.40	85.00	12.97	2.73	2.73	0.00	6.99
18	29	S	90.87	86.00	12.92	2.72	0.00	2.72	6.96
18	30	S	96.25	91.00	14.04	2.96	0.00	2.96	7.56
18	31	S	103.87	95.00	13.74	2.90	1.49	1.40	7.40
18	32	S	104.03	95.00	13.06	2.75	2.75	0.00	7.04
18	33	S	98.14	89.00	13.59	2.86	2.86	0.00	7.32
18	34	S	100.51	91.00	13.68	2.88	2.88	0.00	7.37
18	35	S	94.72	85.00	13.62	2.87	2.87	0.00	7.33
18	36	S	100.63	92.00	13.62	2.87	0.84	2.03	7.33
18	37	P	100.22	89.00	13.04	2.75	2.75	0.00	7.02
18	38	P	88.88	79.00	12.19	2.57	2.57	0.00	6.56
18	39	P	96.74	87.00	13.26	2.79	2.79	0.00	7.14
18	40	P	110.63	98.00	13.13	2.77	2.77	0.00	7.07
18	41	S	94.11	85.00	13.10	2.76	2.76	0.00	7.05
18	42	S	99.16	92.00	13.78	2.90	0.00	2.90	7.42
18	43	S	104.38	96.00	13.32	2.81	0.00	2.81	7.17
18	44	S	105.31	94.00	13.27	2.80	2.80	0.00	7.15
18	45	O	94.12	86.00	13.71	2.89	2.89	0.00	7.38
18	46	O	94.90	84.00	13.74	2.89	2.89	0.00	7.40
18	47	O	83.12	78.19	12.39	2.61	2.61	0.00	6.67
18	48	O	101.10	95.00	12.29	2.59	2.59	0.00	6.62
..	..	..	..	..	..	..	..	..	..

Table C.2: EPD model generated schedule segment for summer month October 2014, time period 2014/10/10 17:00 to 2014/10/11 07:00

i	j	T.O.U Period	$\lvert\mathbf{S}_{i,j}^{load}\rvert$ (MVA)	$P_{i,j}^{load}$ (MW)	$Q_{i,j}^{h,total}$ (MW)	$\dot{W}_{i,j}^{T}$ (MW)	$C_{i,j}$ (MW)	$\dot{W}_{i,j}^{T} - C_{i,j}$ (MW)	$QM\dot{W}_{cold}$ (MW)
..	..	..	..	..	..	..	..	..	..
10	34	S	92.47	86.48	11.64	2.45	2.23	0.23	6.27
10	35	S	99.16	91.78	11.89	2.50	1.32	1.19	6.40
10	36	S	97.60	91.91	11.41	2.40	2.21	0.20	6.15
10	37	P	119.06	110.08	11.50	2.42	1.21	1.21	6.19
10	38	P	124.94	114.41	13.44	2.83	1.42	1.42	7.24
10	39	P	126.92	115.78	13.71	2.89	1.39	1.50	7.39
10	40	P	131.21	118.07	13.65	2.87	1.44	1.44	7.35
10	41	S	116.13	106.65	13.68	2.88	1.44	1.44	7.37
10	42	S	137.73	125.06	16.09	3.39	2.79	0.60	8.67
10	43	S	129.61	115.02	12.94	2.73	2.55	0.17	6.97
10	44	S	128.18	114.47	13.39	2.82	2.62	0.20	7.21
10	45	O	131.54	119.07	15.56	3.28	2.77	0.51	8.38
10	46	O	131.95	118.17	14.51	3.06	1.53	1.53	7.81
10	47	O	132.83	118.22	13.81	2.91	2.73	0.18	7.44
10	48	O	137.53	122.92	13.31	2.80	1.40	1.40	7.17
11	1	O	130.14	116.88	15.28	3.22	2.76	0.46	8.23
11	2	O	149.38	137.61	18.12	3.82	2.88	0.94	9.76
11	3	O	141.81	129.14	16.08	3.39	2.79	0.60	8.66
11	4	O	145.93	131.67	17.04	3.59	2.83	0.76	9.18
11	5	O	131.19	118.17	15.97	3.36	2.78	0.58	8.60
11	6	O	133.24	121.76	15.19	3.20	2.90	0.30	8.18
11	7	O	144.87	132.95	16.78	3.54	2.82	0.72	9.04
11	8	O	145.09	130.75	16.30	3.43	2.80	0.64	8.78
11	9	O	141.58	125.25	15.16	3.19	2.76	0.44	8.16
11	10	O	141.71	126.15	16.20	3.41	2.79	0.62	8.72
11	11	O	146.67	129.60	16.84	3.55	2.82	0.73	9.07
11	12	O	145.15	131.08	17.46	3.68	2.85	0.83	9.40
11	13	O	146.52	133.57	17.62	3.71	2.83	0.89	9.49
11	14	O	146.39	133.84	17.48	3.68	2.85	0.84	9.42
..	..	..	..	..	..	..	..	..	..